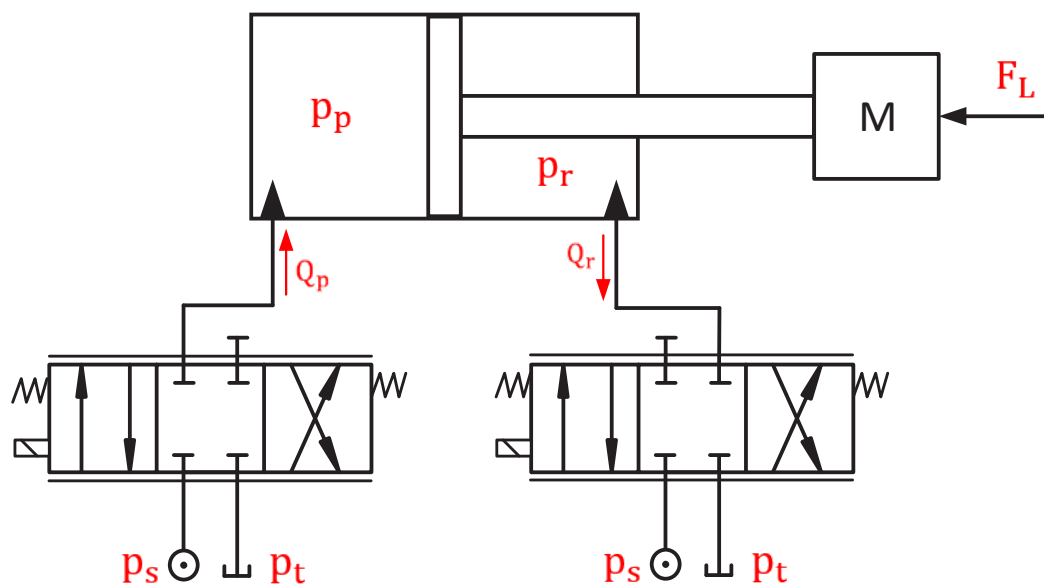




# Investigation of Separate Meter-In Separate Meter-Out Control Strategies



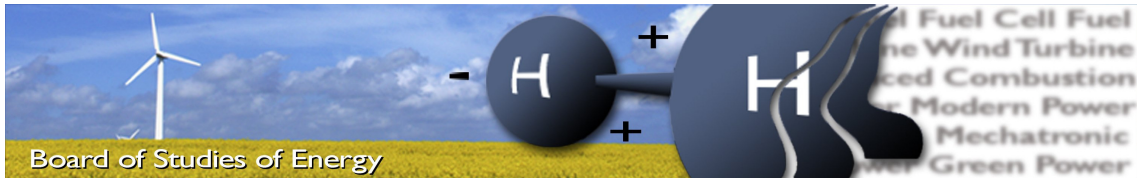
10th Semester - Master's Thesis

14th of October  
2019

Anders Berthing

Mechatronic Control Engineering - Department of Energy Technology





**Title:** Investigation of Separate Meter-In Separate Meter-Out Control Strategies  
**Semester:** 10th Semester  
**Semester theme:** Master's Thesis in Mechatronic Control Engineering  
**Project period:** 14.06.19 to 14.10.19  
**ECTS:** 30 ECTS  
**Supervisors:** Henrik C. Pedersen

#### SYNOPSIS:

The objective of this Master's Thesis is to investigate the concept of separate meter-in separate meter-out flow control and to design the best suitable control strategies for a hydraulic cylinder. The limits associated with separate meter-in separate meter-out control is investigated and results in the possibility of cavitation and excessive pressure build up. To avoid these scenarios suitable control strategies are considered. To find the most suitable control strategy a coupling analysis is conducted which indicates that the velocity together with the rod pressure would be the most convenient control method. The requirement for the designed PI-controllers is to ensure accurate velocity tracking. The system behavior when testing the controllers indicates that the system parameters varies significant when the reference velocity switches between positive and negative. The approach of improving the overall velocity tracking the gains of the designed controllers are required to be tuned for the negative velocity scenario. An improved velocity tracking introduces a control structure where the gains of the controllers switches accordingly to the velocity reference.

---

Anders Berthing

**Pages, total:** 109  
**Appendices:** 62

By accepting the request from the fellow students who uploads the study group's project report in Digital Exam System, you confirm that all group members have participated in the project work, and thereby all members are collectively liable for the contents of the report. Furthermore, all group members confirm that the report does not include plagiarism.



# Preface

This project is written in the time period from 14th of June to the 14th October of 2019, by a student on 10th semester from the Department of Energy Technology at Aalborg University.

The preconditions for reading this report is an understanding of mechanical physics and control theory.

The software used in this project is:

- *Microsoft Visio* - Illustrations and schematics.
- *MATLAB* - Data analysis and plotting.
- *Simulink* - Modelling and simulation of dynamic systems.

**Reader's Guide:** The literature used in this report encompasses textbooks, web pages, technical reports and note collections. A list of the literature is presented in the bibliography. Harvard Style of referencing has been applied when citing information sources - displaying the last name of the author(s) followed by publishing year. If a citation is presented after paragraphs and equations, it covers the section above. If a citation is presented within a sentence, it covers that sentence.

Figures, tables and equations are numbered according to the chapter in question followed by sequential numbers.

A nomenclature list of used symbols, acronyms and constants is presented. The list shows the descriptions and units of the symbols.

Appendices are included in this report, and are found after the bibliography.



# Summary

The objective for this Master's Thesis is to investigate and design controllers for the concept of separate meter-in separate meter-out control for a hydraulic cylinder. The separate meter-in separate meter-out concept is investigated under various operation conditions where the velocity of the cylinder is positive and negative, an overrunning and resistive load force is applied to the system and the result of the analysis is that the concept has some limitations regarding certain operating conditions. The limitations associated with the concept is that cavitation and excessive pressure build up could occur. Cavitation can occur when the velocity is positive, an overrunning load is present and meter-in flow rate control is being used, causing a restriction on the inlet flow, which results in insufficient supply flow to the piston chamber and eventually causes the hydraulic oil to cavitate. A similar scenario where cavitation can occur is when the velocity is negative, a resistive load is present and meter-in flow rate control is being used, which causes the inlet flow to be restricted and causes insufficient flow to the rod chamber which can lead to cavitation in the chamber. Another limit associated with the concept is excessive pressure build up which occur in the scenario where meter-out flow rate control is being used and the velocity of the cylinder is positive and an overrunning load is present and in the scenario where the velocity is negative and a resistive load is present. In these critical operating conditions the cavitation or excessive pressure can result in unwanted behavior for the system and to overcome these suitable control strategies are investigated.

The possible control strategies are compared and two chosen control strategies are seen suitable to control the system. The control strategies investigated further are a slave function control where one input signal is dependent on the other input signal which results in the system only being able to control one state. The other control strategy is where the two proportional valves are controlled independently which allowing more flexibility and better performance for the system. Due to the limits for the slave function control the chosen control strategy that is further investigated is when the two proportional valves are controlled independently.

When the proportional valves are controlled independently a coupling analysis is conducted to observe the input-output pairing when choosing the primary control state as the velocity and the secondary control state as either the piston or the rod pressure. The coupling analysis includes two analysis, the relative gain array and a singular value decomposition. The results of the coupling analysis shows the least input-output pairing between the velocity and the rod pressure. The control method where the velocity is controlled by input signal  $u_p$  and the rod pressure is controlled by the input signal  $u_r$  is further investigated with respect to designing controllers for the control method.

To decouple the system a pre-compensator is designed and implemented in order to treat

the system as two single-input single-output systems. One single-input single-output system where the velocity is controlled by the input signal  $u_p$  and is independent on the input signal  $u_r$  and another single-input single-out system where the rod pressure is entirely controlled by the input signal  $u_r$ . For this control strategy two PI-controllers are designed where the design procedure is that the pressure controller is a factor of 10 faster than the velocity controller to eliminate eventually controller interference. The controllers are implemented and firstly tested on the linear system where the performance for the velocity and rod pressure tracking is acceptable. The controllers are then tested on the non-linear model where the velocity tracking is seen to not be acceptable when the velocity reference is negative. The poorly performance for the velocity tracking in the non-linear model is due to changing model parameters when the velocity changes to negative. To overcome the varying model parameters and the poorly velocity tracking for a negative velocity reference, a set of new PI-controllers are designed based on a linear model conducted for negative velocities, which should be activated when the velocity reference is negative. This is implemented with a switch depending on the reference velocity which switches between the controllers designed for positive and negative velocity. Implementing this control structure improved the overall tracking results of the velocity and thereby it can be concluded that a control method for a separate meter-in separate meter-out setup can be designed.

# Nomenclature

## Acronyms

MIMO	<i>Multiple Input Multiple Output</i>
RG	<i>Relative Gain Array</i>
SISO	<i>Single Input Single Output</i>
SVD	<i>Singular Value Decomposition</i>

## Greek symbols

$\alpha$	Area	[-]
$\bar{\sigma}$	Maximum singular value	[-]
$\beta_e$	Effective bulk modulus	[Pa]
$\beta_p$	Piston side bulk modulus	[Pa]
$\beta_r$	Rod side bulk modulus	[Pa]
$\beta_{oil}$	Bulk modulus of oil	[Pa]
$\gamma$	Flow ratio	[-]
$\omega$	System frequency	[rad/s]
$\underline{\sigma}$	Minimum singular value	[-]
$\zeta$	Damping coefficient	[-]

## Latin symbols

$\dot{p}_p$	Piston side pressure gradient	[Pa/s]
$\dot{p}_{ref}$	Pressure reference	[Pa]
$\dot{p}_r$	Rod side pressure gradient	[Pa/s]
$\dot{x}$	Cylinder velocity	[m/s]
$\dot{x}_{ref}$	Cylinder velocity reference	[m/s]
<b>G</b>	System transfer function	[-]
<b>P<sub>work</sub></b>	Working pressure	[Pa]

$\mathbf{W}$	System pre compensator	[-]
$\mathbf{W}_{ijn}$	Pre compensator for negative reference velocity	[-]
$\mathbf{W}_{ij}$	Pre compensator for positive reference velocity	[-]
$K_I$	Controller integral gain	[-]
$K_P$	Controller proportional gain	[-]
$\dot{x}_0$	Linearisation constant for cylinder velocity	[m/s]
$A_p$	Piston side area	[m <sup>2</sup> ]
$A_r$	Rod side area	[m <sup>2</sup> ]
$B_v$	Viscous friction constant	[N · s/m <sup>2</sup> ]
$F_{L0}$	Linearisation constant for load force	[N]
$F_{cyl}$	Cylinder force	[N]
$F_c$	Coulomb friction	[N]
$F_{fric}$	Friction force	[N]
$F_L$	Load force	[N]
$G$	Gravitational force	[N]
$K_{qp_p}$	Linearisation constant for piston side pressure	[-]
$K_{qp_r}$	Linearisation constant for rod side pressure	[-]
$K_{qu_p}$	Linearisation constant for piston side valve	[-]
$K_{qu_r}$	Linearisation constant for rod side valve	[-]
$L_{stroke}$	Cylinder stroke length	[m]
$M$	Mass	[kg]
$p_{r0}$	Linearisation constant for rod side pressure	[Pa]
$p_{atm}$	Atmospheric pressure	[Pa]
$p_e$	Chamber pressure	[Pa]
$p_N$	Nominal pressure	[Pa]
$p_p$	Piston side pressure	[Pa]
$p_r$	Rod side pressure	[Pa]
$p_s$	Supply pressure	[Pa]
$p_t$	Tank pressure	[Pa]
$Q_N$	Rated flow	[m <sup>3</sup> /s]
$Q_p$	Piston side flow	[m <sup>3</sup> /s]

$Q_r$	Rod side flow	$[\text{m}^3/\text{s}]$
$u_p$	Control input for piston side valve	$[-]$
$u_r$	Control input for rod side valve	$[-]$
$V_{p,hose}$	Hose and dead volume for the piston side	$[\text{m}^3]$
$V_{p0}$	Linearisation constant for piston side volume	$[\text{m}^3]$
$V_p$	Piston side volume	$[\text{m}^3]$
$V_{r,hose}$	Hose and dead volume for the rod side	$[\text{m}^3]$
$V_{r0}$	Linearisation constant for rod side volume	$[\text{m}^3]$
$V_r$	Rod side volume	$[\text{m}^3]$
$x_0$	Linearisation constant for cylinder position	$[\text{m}]$
$x$	Cylinder position	$[\text{m}]$



# Contents

<b>1</b>	<b>Introduction</b>	<b>1</b>
1.1	Problem Statement . . . . .	2
<b>2</b>	<b>System Analysis</b>	<b>3</b>
2.1	Pressure Gradients . . . . .	4
2.2	Force Equation . . . . .	5
2.3	Steady State Analysis . . . . .	5
2.4	Analysis of Operation Situations . . . . .	6
2.5	Control Strategies . . . . .	8
2.6	Validation of Non-linear Model . . . . .	14
2.7	Summary . . . . .	17
<b>3</b>	<b>Linear Analysis</b>	<b>19</b>
3.1	Linear Model . . . . .	19
3.2	Validation of Linear Model . . . . .	20
3.3	Coupling Analysis . . . . .	24
<b>4</b>	<b>Design of Control Strategies</b>	<b>29</b>
4.1	Decoupled Control of the System . . . . .	29
4.2	Design of Velocity & Pressure Control . . . . .	31
4.3	Validation of Controllers . . . . .	34
4.4	Combined Control Structure . . . . .	37
4.5	Discussion of Control Strategies . . . . .	40
<b>5</b>	<b>Conclusion</b>	<b>41</b>
<b>6</b>	<b>Further Work</b>	<b>43</b>
6.1	Experimental Validation . . . . .	43
6.2	Bumpless Switching . . . . .	43
6.3	Gain Scheduling . . . . .	44
	<b>Bibliography</b>	<b>45</b>
	<b>Appendix A Steady State Load Force Scenarios</b>	<b>47</b>
	<b>Appendix B System Design</b>	<b>51</b>
	<b>Appendix C RGA Analysis</b>	<b>53</b>



# 1 | Introduction

Control of hydraulic systems is commonly used in large scaled applications due to its ability to apply high forces which is due to the large power to volume ratio [Yingjie Liu and Zeng, 2009]. The control of a hydraulic system can be challenging due to its highly non-linear characteristics. Parameter variation when controlling a hydraulic system such as flow leakages, friction, bulk modulus etc. is common difficulties which makes it challenging to achieve an accurate model of these and can thus make the tuning of the control parameters accordingly hard [Yingjie Liu and Zeng, 2002]. The traditional method of controlling a hydraulic system is typically controlled by a four-way directional valve where high performance of trajectory tracking is achievable, but lacks the ability to control the pressure levels. The lack of ability to control two state of the hydraulic cylinder is due to that the meter-in and meter-out orifices are mechanically linked together. One way to improve the traditional method of controlling a hydraulic system would be to decouple the mechanical link and be able to control the meter-in and meter-out separately, which opens the possibility to significantly reduce the energy consumption [Bin Yao, 2002]. In recent years, the focus on controlling hydraulic control systems has increased because of its high energy consumption and the ability to achieve more energy sufficient systems by implementing improved control strategies for the hydraulic control system. The concept of controlling the hydraulic system by independently controlling the meter-in and meter-out has the possibility improve the overall system performance with respect to functionality, better tracking ability and reduced energy consumption. The requirements for implementing Separate Meter-In Separate Meter-Out control is that pressure transducers are available on the hydraulic system [Henrik C. Pedersen, 2013].

The concept of separate meter-in separate meter-out valve control can be applied in varies control systems for separately controlling the meter-in and the meter-out flow rates. With one method two proportional valves are required, in order to separately control the meter-in and meter-out flow rates. A schematic illustrating the concept of separate meter-in separate meter-out control system is seen in Figure 1.1. The control system consist mainly of a hydraulic cylinder with an inertia load, two proportional values, a supply pressure and a tank pressure. [CHEN Guangrong, 2017]

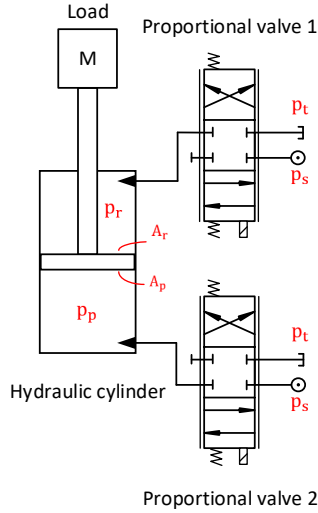


**Figure 1.1:** Concept of separate meter-in separate meter-out control system.

To achieve the desired motion trajectory for the hydraulic system the force generated by the cylinder is defined as  $F_{cyl} = A_p p_p - A_r p_r$  and should be controlled accordingly to the force produced by the load to achieve the desired trajectory motion. [CHEN Guangrong, 2017] Controlling the meter-in flow rate is performed when the velocity of the hydraulic cylinder is positive and the proportional valve 2 is controlling the inlet flow to the hydraulic cylinder. Controlling the meter-out flow rate is accomplished when the velocity is positive and proportional valve 1 controlling the outlet flow rate and thereby the rod side pressure. To avoid large pressure levels in the hydraulic cylinder it is suggested to keep the back pressure at a low value to avoid unnecessary pressure in the system. [Nielsen, 2005]

The objective for this Master's Thesis is to investigate a separate meter-in separate meter-out control system with respect to its operating conditions, limitations and suitable control methods which leads up the problem statement.

## 1.1 Problem Statement

*How can control strategies for a separate meter-in separate meter-out hydraulic system be designed?*

In order to answer the problem statement, a set of sub questions are set up.

- How does the separate meter-in separate meter-out control system work and what is the limits for separate control of the hydraulic cylinder?
- What are the consideration associated with chosen the most suitable control strategies for the hydraulic cylinder?
- What methods are sufficient for decoupling the separate meter-in separate meter-out hydraulic system?

## 2 | System Analysis

The analysis will be conducted for the hydraulic system illustrated in Figure 2.1 consisting of a single axis with a differential cylinder operated by two 4/3 proportional valves. The proportional valves each have three states, normally closed, position A and position B. When both valves are in position A the piston chamber is connected to the supply pressure and the rod chamber is connected to the tank pressure and reversed when both of the proportional valves are in position B. The purpose of the analysis is to obtain an understanding of the limitations associated with the different operating conditions regarding overrunning and resistive loads and the area and flow ratio. The problems encountered with separate control of the meter-in and meter-out flow rate is that it, in some cases, can be impossible to maintain the flow rate to the piston chamber when an overrunning load is present. Depending on the area and flow ratio it is possible to encounter both cavitation and excessive pressure build up, which can lead to undesired system behavior.

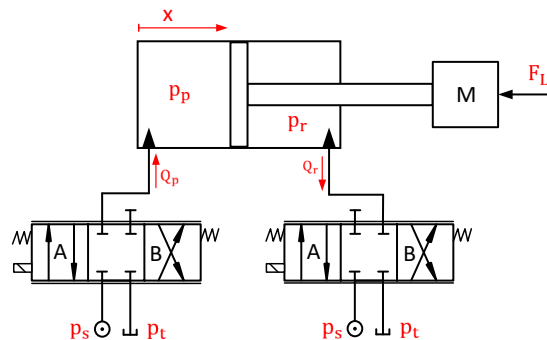


**Figure 2.1:** Hydraulic cylinder connected to two 4/3 proportional valves.

The foundation of the analysis is firstly to obtain a mathematical model for the hydraulic system. This is done in the following sections where the flow rates, pressures and force is analysed by deriving the relevant equations that describes the physical relation between each of these properties. Then an analysis of the operating conditions associated with cavitation and excessive pressure build up is conducted. In order to eliminate the occurrences of cavitation and excessive pressure build up, control strategies can be implemented that would adjust for any physical behavior that deviates from the desired performance of the system which leads to an analysis and comparison of the different control methods for the separate meter-in separate meter-out hydraulic system.

## 2.1 Pressure Gradients

The pressure gradients for the system can be described by utilizing the continuity equation for the two cylinders chambers, respectively. The model is assumed to be ideal and therefore no leakage flow is present. The continuity equations yields:

$$\dot{p}_p = \frac{\beta_p}{V_p}(Q_p - \dot{x}A_p) \quad (2.1)$$

$$\dot{p}_r = \frac{\beta_r}{V_r}(\dot{x}A_r - Q_r) \quad (2.2)$$

where  $Q_p$  is the piston side flow,  $Q_r$  is the rod side flow,  $A_p$  is the area of the piston side,  $A_r$  is the area of the rod side,  $V_p = V_{p,hose} + A_p x$  describes the volume in the piston side chamber and  $V_r = V_{r,hose} + (L_{stroke} - x)A_r$  describes the volume in the rod side chamber both dependent on the cylinder position  $x$ .  $\beta_e$  describes the effective bulk modulus for both chamber respectively and is expressed as:

$$\beta_e = \frac{1}{\frac{1}{\beta_{oil}} + \frac{\epsilon_{Air}}{1.4(p_{atm} + p_e)}} \quad , \quad \epsilon_{Air} = \frac{1}{\frac{1 - \epsilon_a}{\epsilon_a} \left( \frac{p_{atm}}{P_{atm} + p_e} \right)^{-1.4} + 1} \quad (2.3)$$

where  $\beta_{oil} = 16000$  bar is the bulk modulus for oil,  $\epsilon_a = 0.01$  is the percentage of air dissolved in the hydraulic oil,  $P_{atm}$  is atmospheric pressure and  $p_e$  is the pressure in the chamber respectively.

The piston area ratio  $\alpha$  and flow ratio  $\gamma$  is defined as:

$$\alpha = \frac{A_r}{A_p} \quad (2.4)$$

$$\gamma = \frac{Q_r}{Q_p} \quad (2.5)$$

Both the piston and rod sides cross-sectional areas are constants, furthermore because the piston side area is always greater or equal to the rod side area, the area ratio is limited as  $0 \leq \alpha \leq 1$ . The flow ratio, defined as the ratio between the inlet flow to the piston side chamber and outlet flow of the rod side chamber, is during steady state limited as  $0 < \gamma < \infty$ . However, during the transient behavior of the cylinder, no such limit exists, and the flow ratio can be between  $-\infty$  to  $\infty$  depending on the flows needed to obtain the wanted pressures in each chamber. For example when a negative flow ratio is needed is when both chamber pressures are required to be increased. If this is done by connecting both chambers to the supply pressure, the hydraulic oil will flow into both chambers until the desired pressures are reached, but because flow to the rod chamber is defined as positive when it is leaving the chamber, the ratio will be negative if the flow is going into both chambers.

The flow direction is determined by the position of the proportional valves and the definitions of state A and B is as:

$$\text{State A} = \begin{cases} Q_p = u_p Q_N \sqrt{\left| \frac{p_s - p_p}{p_N} \right|} \cdot \text{sign}(p_s - p_p) & \text{for } u_p \geq 0 \\ Q_r = u_r Q_N \sqrt{\left| \frac{p_r - p_t}{p_N} \right|} \cdot \text{sign}(p_r - p_t) & \text{for } u_r \geq 0 \end{cases} \quad (2.6)$$

$$\text{State B} = \begin{cases} Q_p = u_p Q_N \sqrt{\left| \frac{p_p - p_t}{p_N} \right|} \cdot \text{sign}(p_p - p_t) & \text{for } u_p < 0 \\ Q_r = u_r Q_N \sqrt{\left| \frac{p_s - p_r}{p_N} \right|} \cdot \text{sign}(p_s - p_r) & \text{for } u_r < 0 \end{cases} \quad (2.7)$$

where  $u_p$  and  $u_r$  are the proportional valves' control signals,  $Q_N$  is the rated flow and  $p_N$  is the rated pressure for the proportional valves.

## 2.2 Force Equation

There are three different forces that occur in conjunction with the movement of the piston. These are denoted as the cylinder force,  $F_{cyl}$ , which is generated by the difference between the piston and rod side pressures in the cylinder, the friction force,  $F_{fric}$ , which occurs due to the tension between the cylinder and piston. Lastly the force applied by the load,  $F_L$ . A free body diagram of the piston is illustrated in Figure 2.2.

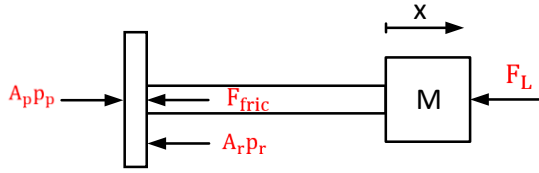


**Figure 2.2:** Free body diagram of the piston.

In order to produce a positive cylinder force it is required that  $A_p p_p > A_r p_r$  and vice versa if a negative cylinder force is needed. The equation for the cylinder force is described by Equation 2.8.

$$F_{cyl} = A_p p_p - A_r p_r - F_{fric} \quad (2.8)$$

where the friction model is described as a viscous friction coefficient  $B_v$  and Coulomb friction  $F_c$  and expressed in Equation 2.9.

$$F_{fric} = B_v \dot{x} + F_c \text{sign}(\dot{x}) \quad (2.9)$$

The mechanical model of the cylinder is described by Newton's second law of motion.

$$F_{cyl} = F_L + G + M\ddot{x} \quad (2.10)$$

where  $G$  is the gravitational force and  $M$  is the equivalent mass of the system. To achieve a constant velocity for the cylinder it is required that  $F_{cyl} = F_L$ . [Daniel Brusen Nielsen, 2016] The force equation for the system is defined as:

$$\ddot{x} = \frac{1}{M} (A_p p_p - A_r p_r - B_v \dot{x} - F_c \text{sign}(\dot{x}) - F_L - G) \quad (2.11)$$

## 2.3 Steady State Analysis

The model will be analyzed in steady state, by assuming constant pressures leading to the pressure gradients being zero,  $\dot{p}_p = 0$  and  $\dot{p}_r = 0$ . Assuming that the pressure gradients

are zero results in the velocities being constant from Equation 2.1 and 2.2.

$$\dot{x} = \frac{Q_p}{A_p} \quad (2.12)$$

$$\dot{x} = \frac{Q_r}{A_r} \quad (2.13)$$

In the steady state analysis, the acceleration is zero, which leads to force equation being simplified to:

$$\ddot{x} = \frac{1}{M}(A_p p_p - A_r p_r - F_L) \quad (2.14)$$

$$F_L = A_p p_p - A_r p_r \quad (2.15)$$

## 2.4 Analysis of Operation Situations

The purpose of the analysis is to interpret the behavior of the hydraulic cylinder in regards to cavitation and excessive pressure build up. Dependent on the different operating conditions these situations could occur. The operating condition is dependent on the proportional valves position either state A or state B, piston area ratio  $\alpha$ , flow ratio  $\gamma$ , and the direction of the load force. The direction of the load force can in some cases give clear indication of in which chamber the cavitation or excessive pressure build up will occur. The result of the different operating condition and the possible outcome is illustrated in Figure 2.3.

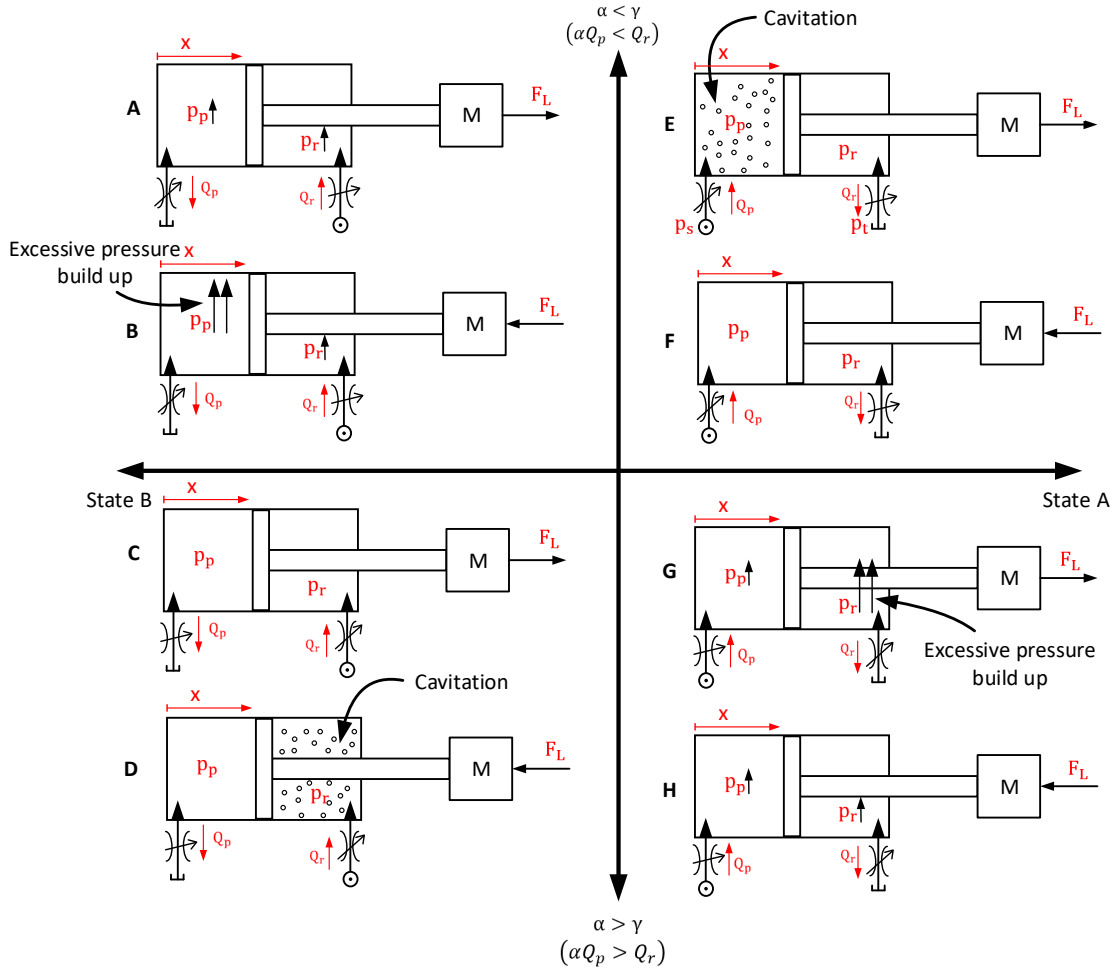


**Figure 2.3:** Different operating condition under variations of valve inputs, area and flow ratio and load force direction.

The figure illustrates the different operating conditions and possible behaviors the system could encounter. The idea is to achieve an overview of the operating conditions of the hydraulic system and predict the behavior of the system under every operating condition. The two unwanted situations are cavitation and excessive pressure build up. Cavitation occurs when the hydraulic fluid encounter relatively low pressure and small air bobbles are generated which in worst cases can cause damage to the system. Figure 2.3E and Figure 2.3D illustrates the two critical operating conditions where cavitation could occur. In Figure 2.3E the piston area ratio is larger than the flow ratio ( $\alpha > \gamma$ ), which is when the inlet flow is restricted relative to the outlet flow. In this case an overrunning load (negative load) is applied which causes the piston chamber side to eventually cavitate. This happens because the inlet flow is restricted and therefore unable to supply enough flow to the chamber to overcome the cavitation problem. Comparing Figure 2.3E with Figure 2.3G now the piston area ratio is smaller than the flow ratio ( $\alpha < \gamma$ ) and illustrated by a restriction on the outlet flow, same overrunning load, but cavitation is not the issue anymore. The restriction on the outlet flow is able to build and uphold pressure in the rod side chamber and withstand the overrunning load and therefore not causing low pressure in the piston chamber that leads to cavitation. The issue in Figure 2.3G is instead excessive pressure build up which happens in this case when the outlet flow is restricted and an overrunning load is applied. In this case the rod chamber pressure will keep increasing

depending on the magnitude of the overrunning load. The outcome of unnecessary pressure increase could possibly effect the performance together with the efficiency of the system. This phenomena also occur in Figure 2.3B. [Henrik C. Pedersen, 2015] [Kim Heybroek, 2008]

These phenomena can be eliminated with a suitable control strategy of the two proportional valves. The control strategy will withstand the possibility of the critical scenarios where the pressure becomes relatively low and the scenario where the pressure unnecessarily keeps increasing.

## 2.5 Control Strategies

Separate meter-in separate meter-out control systems can be used for flow control, pressure control, velocity control, velocity/pressure control etc. Different options of control strategies will be investigated and outlined in regards of benefits and limitations.

The hydraulic system consist of two separate controlled 4/3 proportional valves, one connected to the piston side chamber  $u_p$  and another connected to the rod side chamber  $u_r$ , which is illustrated in Figure 2.4. All of the possible control options such as the piston side flow, rod side flow, piston side pressure, rod side pressure, piston velocity and position and lastly a slave function are listed in Table 2.1. The slave function is defined as one of the valves operating as a function of the other valve signal. For example if the input signal for the rod side valve is a function of the piston side valve the control method is then applied by the relation  $u_r = \alpha u_p$ .

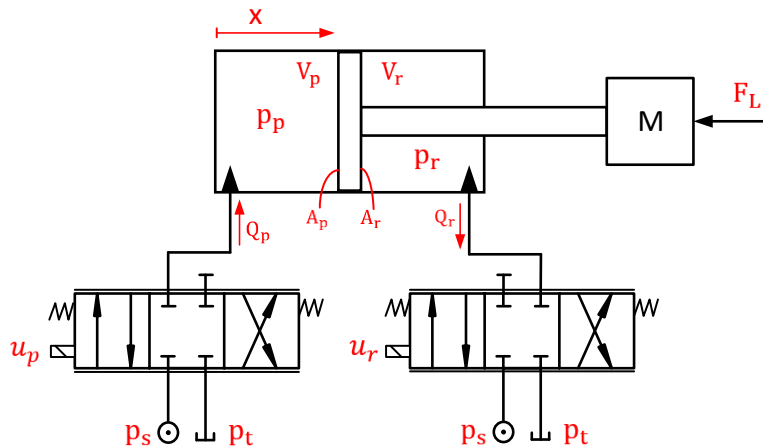


**Figure 2.4:** Hydraulic cylinder connected to two separate controlled 4/3 proportional valves.

The different combinations of control strategies for the hydraulic cylinder are listed in Table 2.1 and is divided into 3 different categories,  $\ominus$  which indicates that the control method is not suitable,  $\otimes$  is the control methods which are partly suitable and lastly  $\oplus$  which indicates that the control methods are highly suitable for control purposes. The method of evaluating the suitability of every control strategies is conducted by steady state analysis. The steady state analysis are conducted on the system described in Appendix B - System Design on page 51.

$u_p \backslash u_r$	$Q_p$	$Q_r$	$p_p$	$p_r$	$\dot{x}$	$x$	Slave
$Q_p$	1. $\ominus$	2. $\ominus$	7. $\circ$	7. $\circ$	4. $\ominus$	4. $\ominus$	8. $\circ$
$Q_r$	2. $\ominus$	1. $\ominus$	7. $\circ$	7. $\circ$	4. $\ominus$	4. $\ominus$	8. $\circ$
$p_p$	7. $\circ$	7. $\circ$	1. $\ominus$	3. $\ominus$	9. $\oplus$	9. $\oplus$	6. $\ominus$
$p_r$	7. $\circ$	7. $\circ$	3. $\ominus$	1. $\ominus$	9. $\oplus$	9. $\oplus$	6. $\ominus$
$\dot{x}$	4. $\ominus$	4. $\ominus$	9. $\oplus$	9. $\oplus$	1. $\ominus$	5. $\ominus$	10. $\oplus$
$x$	4. $\ominus$	4. $\ominus$	9. $\oplus$	9. $\oplus$	5. $\ominus$	1. $\ominus$	10. $\oplus$
Slave	8. $\circ$	8. $\circ$	6. $\ominus$	6. $\ominus$	10. $\oplus$	10. $\oplus$	1. $\ominus$

**Table 2.1:** Analysis of the different control strategies.

In the following subsections the case number refers to the number in Table 2.1. Each possibility will be discussed and analyzed accordingly.

**1.** The diagonals of the table are invalid control strategies, because it is impossible to control the same state with both control signals  $u_p$  and  $u_r$ . It is for example impossible to control the piston flow,  $Q_p$ , with both input signals. Therefore these control combinations are eliminated.

**2.** Controlling the inlet flow with  $u_p$  and the outlet flow with  $u_r$  is not suitable for control purposes, because of the flow ratio  $\gamma$  is required to match with the cylinder. If the two flows are to be controlled individually the possibility is that cavitation or pressure build up could occur. This is illustrated in Figure 2.3 where the flow ratio varies from  $\alpha > \gamma$  to  $\alpha < \gamma$  and depending on the load force direction and flow direction cavitation or pressure build up could occur.

**3.** Controlling both pressures result in  $\ddot{x} \neq 0$ . This will happen if the  $A_p p_p \neq A_r p_r$  and  $F = 0$ . In the case when  $A_p p_p > A_r p_r$  the acceleration will be positive and when  $A_p p_p < A_r p_r$  the acceleration will be negative. The system will be keep increasing its velocity and that is not suitable for control purpose.

$$\ddot{x} = \frac{1}{M}(A_p p_p - A_r p_r - F_L) \quad (2.16)$$

For example if the piston chamber pressure is set to 140 bar and the rod chamber pressure is set to 20 bar while no load force is applied the equation will result in:

$$\ddot{x} = \frac{1}{4000kg}(0.0031m^2 \cdot 140bar - 0.0015m^2 \cdot 20bar - 0N) = 10.91 \frac{m}{s^2} \quad (2.17)$$

Which clearly indicates that the acceleration for the cylinder is not zero  $\ddot{x} \neq 0$  and will result in the velocity either increasing or decreasing depending on the chamber pressures.

**4.** In these control strategies, one input signal is controlling the flow and the other is controlling the velocity of the cylinder. These control strategies can not be achieved, because of the steady state relation between the flow and the velocity. The relation is given for both chambers in the following equations:

$$Q_p = \dot{x} A_p \quad (2.18)$$

$$Q_r = \dot{x}A_r \quad (2.19)$$

For example if the piston side valve is to control the flow to be  $20l/min$ , the velocity of the cylinder is calculated in steady state as:

$$\dot{x} = \frac{Q_p}{A_p} = \frac{20 \frac{l}{min}}{0.0031 m^2} = 0.11 \frac{m}{s} \quad (2.20)$$

Which in steady state will result in a piston velocity of  $0.11 m/s$ . While the piston side valve is controlling the flow it is impossible for the rod side valve to control the velocity.

**5.** Controlling the velocity with one input signal and the position with another input signal is not possible as the relation between velocity and position is an integrator.

**6.** Operating in slave function where either  $u_p$  or  $u_r$  is operating as a function of the other valve when trying to control the pressure is difficult. To achieve a desired pressure level, change in the pressure gradient is required and is possible to obtain if the flows can be controlled and thereby making the flow ratio changeable. When operating in slave function the input signal given to the system affect both flows. The flows are dependent on the input signal and the pressure difference  $\Delta p$  as given by Equation 2.6 and 2.7. The flows are therefore controlled independently of each other by the pressure difference  $\Delta p$ , which can be complicated because it is explicit control of the flows.

**7.** Controlling the pressure with one input signal and controlling the flow with the other input signal is a possibility, but is not the most conventional control strategy. Controlling the piston chamber flow or the rod chamber flow is a durable control strategy, but due to flow sensors being expensive together with their variance of inaccuracy between 1-5% depending on the type of sensor it is not the most suitable control strategy when discussing control strategies for a hydraulic cylinder. Instead of an expensive inaccurate flow sensor a position/velocity sensor would be more suitable for control purposes. [Control, 2014]

**8.** It is possible to control the flow with one input signal and using the other input signal in slave function, but this is a limited control strategy compared to other options.

**9 & 10.** The two control strategies investigated in this project includes the ability to control the velocity of the cylinder. The first control strategy is by controlling the velocity with one input signal and controlling the pressure with the other input signal. The second control strategy is to operate one valve in slave function while controlling the velocity with the other input signal. These two control strategies are further investigated.

### 2.5.1 Velocity & Pressure Control

The purpose of controlling the pressure together with the velocity is to increase the efficiency for the system. The velocity can be controlled to track a velocity trajectory while the pressure in one chamber is kept at a minimum pressure level in order to uphold the stiffness in the system and to increase the energy efficiency of the system. A steady state analysis is conducted when the velocity is set to  $0.2 m/s$  and the rod pressure is set to  $20 bar$ . The purpose of the analysis is to evaluate the flows, pressures, input signals of the proportional valves and the effect on these in a load force scenario. In this example the input signal  $u_p$  is used to control the velocity and the input signal  $u_r$  is used to control

the rod pressure. In Figure 2.5 the hydraulic system is illustrated together with the valves control purposes.

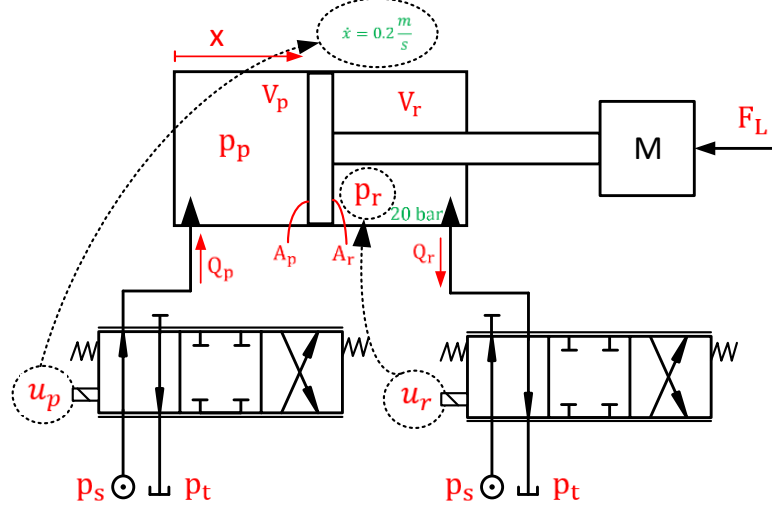


**Figure 2.5:** Basic idea of the multiple input multiple output control strategy.

The velocity of the piston is set to  $0.2 \text{ m/s}$  and it is then possible to calculate the steady state flow to the piston. The continuity equation for the piston chamber is shown in Equation 2.1. The continuity equation when in steady state is simplified to Equation 2.12 and reformulated as:

$$Q_p = \dot{x}A_p \quad (2.21)$$

$$Q_p = 0.2 \text{ m/s} \cdot 0.0031 \text{ m}^2 = 37.40 \text{ l/min} \quad (2.22)$$

Then it is possible to calculate the rod side steady state flow from Equation 2.13.

$$Q_r = \dot{x}A_r \quad (2.23)$$

$$Q_r = 0.2 \text{ m/s} \cdot 0.0015 \text{ m}^2 = 18.32 \text{ l/min} \quad (2.24)$$

The pressures in the chambers is then calculated in steady state by the force balance equation from Equation 2.10. In steady state the acceleration of the mass is assumed to be  $\ddot{x} = 0$ . In this example the rod pressure is set to  $20 \text{ bar}$  and the piston pressure is then calculated when no load force is applied. The effect of applying a load force will result in a change of the piston side pressure. The piston side pressure is calculated by:

$$\ddot{x} = \frac{1}{M}(A_p p_p - A_r p_r - F_L) \quad (2.25)$$

$$p_p = \frac{A_r p_r + F_L}{A_p} = \frac{0.0015 \text{ m}^2 \cdot 20 \text{ bar} - 0 \text{ N}}{0.0031 \text{ m}^2} = 9.8 \text{ bar} \quad (2.26)$$

If the rod side pressure is set to  $20 \text{ bar}$  the piston side pressure should be  $9.8 \text{ bar}$  when no load is present. If load force were applied the piston pressure will change in order to achieve the rod pressure of  $20 \text{ bar}$  and is shown in Table 2.2.

$p_r$ [bar]	$p_p$ [bar]	$F_L$ [N]
20	1	-2742
20	9.8	0
20	70	18766
20	100	28118
20	140	40587
20	210	62408

**Table 2.2:** Effect of applying load force when the rod pressure is set to 20 bar.

From the table it is seen that when the system encounter a load force the piston pressure changes accordingly to maintain the rod side pressure of 20 bar where the maximum overrunning load the system can handle, without reaching the system limitations, is  $\approx 2.7$  kN and the maximum retracting load force the system is able to handle is  $\approx 62.4$  kN.

The opening of the proportional valves is calculated using Equation 2.6 and 2.7. For this case Equation 2.6 is utilized because of the velocity being positive where the supply is connected to the piston side chamber and the tank is connected to the rod side chamber. The equation for calculating the valve position is shown below where  $Q_N$ ,  $p_N$ ,  $p_s$  and  $P_t$  are listed in Table B.1 on page 51.

$$Q_p = u_p Q_N \sqrt{\left| \frac{p_s - p_p}{p_N} \right|} \cdot \text{sign}(p_s - p_p) \quad (2.27)$$

$$Q_r = u_r Q_N \sqrt{\left| \frac{p_r - p_t}{p_N} \right|} \cdot \text{sign}(p_r - p_t) \quad (2.28)$$

In order to calculate the valve position these two equations are reformulated as:

$$u_p = \frac{Q_p}{\sqrt{\left| \frac{p_s - p_p}{p_N} \right|} Q_N} = \frac{37.40 \text{ l/min}}{\sqrt{\left| \frac{210 \text{ bar} - 9.8 \text{ bar}}{35 \text{ bar}} \right|} \cdot 40 \text{ l/min}} = 0.3909 \quad (2.29)$$

$$u_r = \frac{Q_r}{\sqrt{\left| \frac{p_r - p_t}{p_N} \right|} Q_N} = \frac{18.32 \text{ l/min}}{\sqrt{\left| \frac{20 \text{ bar} - 1 \text{ bar}}{35 \text{ bar}} \right|} \cdot 40 \text{ l/min}} = 0.6217 \quad (2.30)$$

To achieve a rod chamber pressure of 20 bar together with a piston chamber pressure of 9.8 bar the required valve positions is  $u_p = 0.39$  and  $u_r = 0.62$ . In the scenario where the system encounters a load force the behaviour of the system is described in Appendix A - Steady State Load Force Scenarios on page 47.

## 2.5.2 Velocity Control with Slave Function

The method where one valve is functioning as a slave valve of the other valve is a possibility when controlling the velocity. Some limitation is associated with only being able to control

the velocity when operating in slave mode. The limitation is that controlling the velocity excludes the possibility of controlling one of the pressure levels, because the system now only has one input signal.

In this control strategy the velocity is controlled by the input signal  $u_p$  while the input signal  $u_r$  is a function of  $u_p$  with the following relation:

$$u_r = \alpha u_p \quad (2.31)$$

In Figure 2.6 the hydraulic system is illustrated together with the control method.

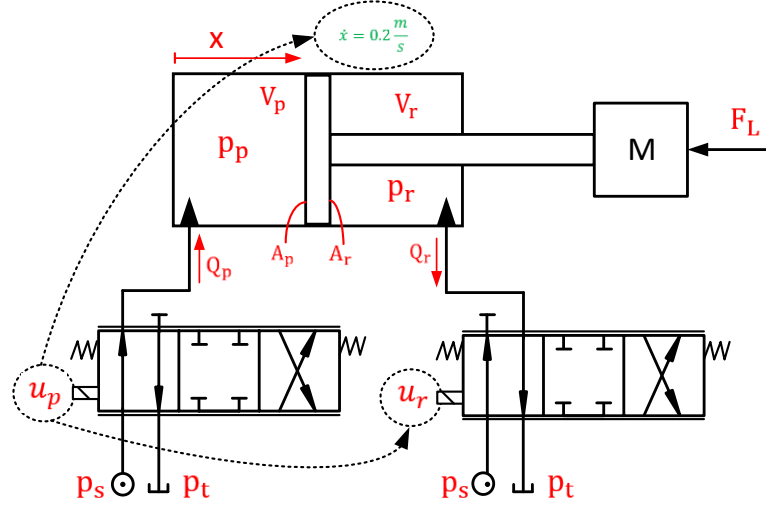


**Figure 2.6:** Basic idea of the velocity control operating in slave function.

In order to achieve a constant velocity of  $0.2 \text{ m/s}$  the piston and rod side flows are calculated similar as for the velocity/pressure control previously. The required piston flow is calculated to be  $37.40 \text{ l/min}$  and the rod side flow is required to be  $18.70 \text{ l/min}$  calculated by Equation 2.12 and 2.13. It is impossible to control any pressure levels for the slave function compared to the previous velocity and pressure control method. In order to solve the velocity control with slave function in a steady state it is required to solve two equation with two unknowns. The rod side flow is a function of the input signal  $u_p$  and is expressed by:

$$Q_r = u_r Q_N \sqrt{\left| \frac{p_r - p_t}{p_N} \right|} = \alpha u_p Q_N \sqrt{\left| \frac{p_r - p_t}{p_N} \right|} \quad (2.32)$$

where the rod side pressure can be isolate from Equation 2.15 and expressed as:

$$p_r = \frac{A_p p_p - F_L}{A_r} \quad (2.33)$$

The piston input for the slave function is defined by:

$$u_p = \frac{Q_p}{Q_N \sqrt{\left| \frac{p_s - p_p}{p_N} \right|}} \quad (2.34)$$

Combining the equations it is possible to calculate the piston pressure. The piston pressure when no load is present is calculated to be  $p_p = 69.38 \text{ bar}$ . In order to calculate the rod

side pressure Equation 2.33 is utilized and the rod side pressure is calculated to be 142.62 *bar*.

When the piston pressure is calculated the required input signal for the piston side valve is calculated from Equation 2.34.

$$u_p = \frac{37.40 \text{ l/min}}{40 \text{ l/min} \sqrt{\left| \frac{210 \text{ bar} - 69.38 \text{ bar}}{35 \text{ bar}} \right|}} = 0.4664 \quad (2.35)$$

To deliver the required piston flow of 37.40 *l/min* in order to maintain the piston velocity of 0.2 *m/s* when the piston chamber pressure is calculated to be 69.38 *bar* the input signal  $u_p$  should be 0.47. For the slave function the behavior of the system when a load force is applied to the system is also described in Appendix A - Steady State Load Force Scenarios on page 47.

## 2.6 Validation of Non-linear Model

The non-linear model is to be validated by comparing the simulation model with an estimate of the physical behavior of the system. In this validation no experimental data is conducted but to validate the non-linear model the idea is therefore to simulate the model in scenarios where the behavior of the physical system is known. For the comparison the hydraulic cylinder is placed vertically where the force acting on the cylinder is the gravitational force applied by the system mass. The initial position of the cylinder is in the middle,  $L_{stroke}/2$ , and dependent on the input signals of  $u_p$  and  $u_r$  the velocity is either zero (standstill), positive (upwards motion) or negative (downwards motion). In the simulations the Coulomb friction is neglected and the viscous friction coefficient  $B_v$  is set to 10000 N·s/m, which is estimate to contribute to the force balance, when the velocity is 0.1 *m/s*, with the force of 1000 N. The hydraulic cylinder placed in vertical position is seen in Figure 2.7.

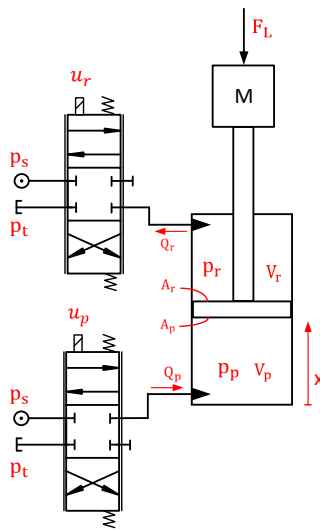


**Figure 2.7:** Basic idea of model validation when cylinder is in vertical position.

The simulation is given different input signals of  $u_p$  and  $u_r$  which connects the supply pressure or the tank pressure to the two chambers, separately. The velocity of the piston is dependent on which side is connected to the supply pressure and which is connected to the tank pressure. The simulation is given the input signals of  $u_p = u_r$  to evaluate the system when the input signals are equal. In the scenario where  $u_p = u_r = 0.3$ , the piston side is connected to the supply pressure and the rod side is connected to the tank pressure. In this scenario it is expected that the velocity of the piston is positive and result in the mass being lifted up. Regarding the pressures it is expected that the piston pressure is the highest and the rod pressure is close to the tank pressure. When the piston reaches the top of the cylinder it is expected that the piston pressure increases to supply pressure and the rod pressure decreases to tank pressure. The simulation of the model is illustrated in the figures below for the setup, position, velocity and the pressures.

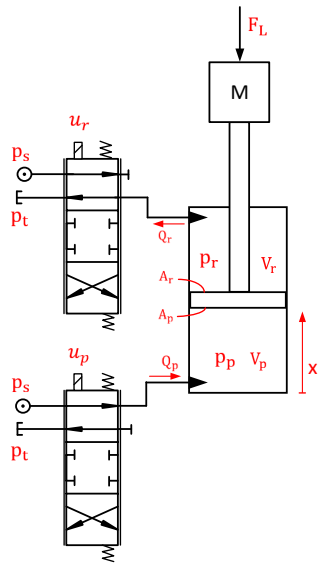


Figure 2.8: Input signals:  $u_p = u_r = 0.3$

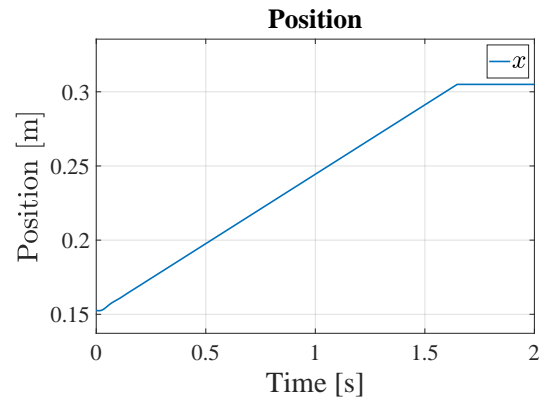


Figure 2.9: Position of the piston.

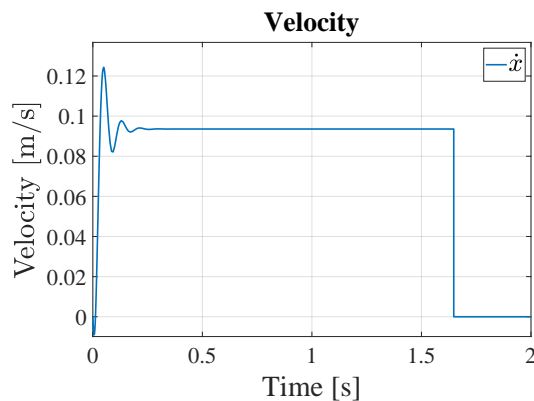


Figure 2.10: Velocity of the piston.

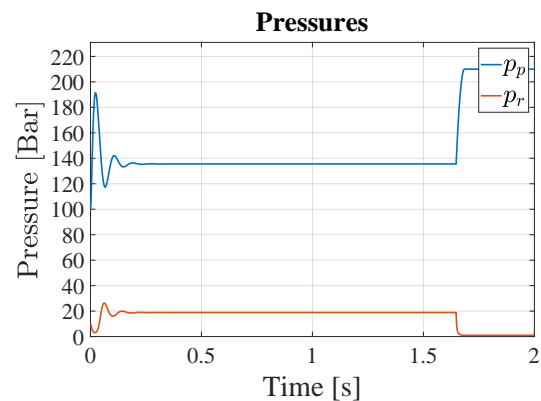


Figure 2.11: Piston and rod pressures.

From Figure 2.9 it is seen that when opening the piston side chamber to the supply pressure and the rod side to the tank pressure will result in the cylinder position increases from the middle to the top of the cylinder. At around 1.7 s the position reaches the top of the

cylinder and the velocity in Figure 2.10 drops to zero while the piston pressure increases to supply pressure and the rod side pressure decreases to tank pressure as expected. The velocity of the cylinder is  $\approx 0.1$  m/s when the cylinder is moving. The pressures in the chambers are seen in Figure 2.11 where the piston pressure settles to  $\approx 135$  bar and the rod pressure find a steady state pressure of  $\approx 20$  bar. The oscillations in the system for the pressures and the velocity are analysed and the damping of the system is calculated to be in the range of  $\zeta=0.27-0.33$  with a system frequency in the range of  $\omega=75-79$  rad/s.

The non-linear model is also to be validated when the velocity is negative and the cylinder starts from the middle of the cylinder and ends in the bottom. This is utilized when the input signals are given a negative value which connects the rod side chamber to the supply pressure and the piston side chamber to the tank pressure. In this scenario the inputs to the system is  $u_p=u_r=-0.2$  and it is expected that the velocity is negative and the piston pressure is higher than the rod pressure in order to satisfy the force balance equation. In the following figures, the system setup, position, velocity and the pressures are illustrated.

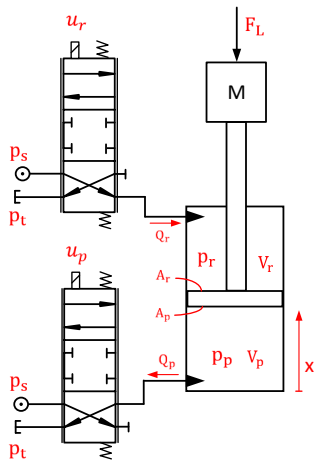


Figure 2.12: Input signals:  $u_p = u_r = -0.2$ .

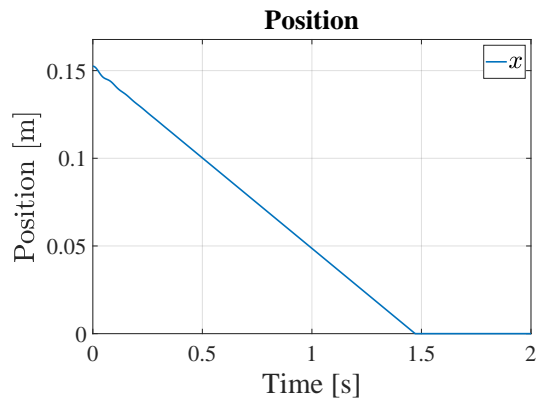


Figure 2.13: Position of the piston.

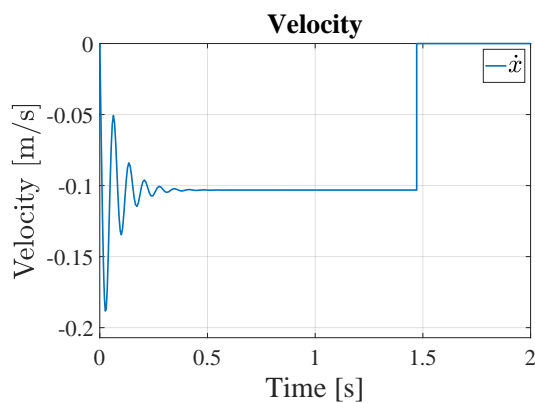


Figure 2.14: Velocity of the piston.

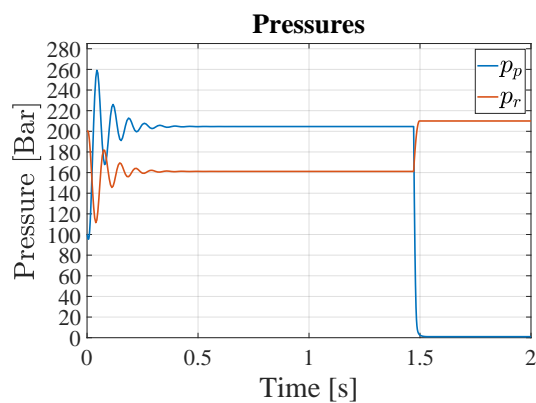


Figure 2.15: Piston and rod pressures.

From Figure 2.13 it is expected that the piston position will decrease until the piston is located at the bottom of the cylinder. The position starts in the middle of the cylinder and decreases to the bottom in around 1.5s. In Figure 2.14 the velocity gets a steady value

at around -0.1 m/s while the piston pressure is  $\approx 210$  bar and the rod pressure is  $\approx 160$  bar. When the cylinder reaches the bottom of the cylinder it is expected that the rod side pressure increases to supply pressure and the piston pressure decreases to tank pressure, which is illustrated in Figure 2.15. The damping of the system when having a negative velocity is calculated to be in the range of  $\zeta=0.17-0.25$  with a system frequency in the range of  $\omega=82-87$  rad/s. When the system has a negative velocity the damping ratio is lower than when the system having a positive velocity which is due to high non-linearity of the orifice equations. The high non-linearity of the orifice equations results in that the damping ratio increases with the magnitude of the input signals and almost decreases to zero damping when the input signals are close to zero. The highest damping for the non-linear model is present when the input signals are given fully positive or negative openings,  $u_p = \pm 1$  and  $u_r = \pm 1$ .

The non-linear model is validated to the extend of having no experimental data to compare with. The model is validated against the expected behavior the system would have had in certain scenarios. The model behaves as expected, when positive input signals are applied the cylinder velocity is positive and the cylinder moves upwards. When negative input signals are applied to the valves it was expected that the system achieved a negative velocity which is seen in the simulations.

## 2.7 Summary

The critical scenarios of the system operating conditions are where either cavitation or excessive pressure build up occur. There are two scenarios where cavitation may occur is firstly when the velocity is positive, an overrunning load is present and the inlet flow  $Q_p$  is restricted compared to the outlet flow  $Q_r$  and therefore not being able to supply enough hydraulic fluid to the piston chamber. The second scenario is when the velocity is negative, a resistive load is present and now the inlet flow  $Q_r$  is restricted compared to the outlet flow  $Q_p$  which may cause cavitation because the inlet flow  $Q_r$  can not be supplied sufficient enough.

The scenarios where excessive pressure build up occurs first is where the piston velocity is positive, an overrunning load is present and the outlet flow  $Q_r$  is restricted compared to the inlet flow  $Q_p$  and the rod side pressure will keep increasing. The same phenomena will occur when the piston velocity is negative, a resistive load is present and the outlet flow  $Q_p$  is restricted compared to the inlet flow  $Q_r$  and will result in the piston pressure will keep increasing.

In order to eliminate the occurrence of the critical scenarios suitable control strategies are outlined and the velocity together with pressure control and velocity control with the proportional valves operating in slave function have been chosen. Both control strategies indicates that it is possible to control the velocity but the difference between them is that the velocity control operating in slave function is limited to one input signal and therefore not able to control the pressure together with the velocity. Controlling the velocity together with the pressure by controlling the proportional valves independently and utilising both input signals achieves the possibility for more feasible and suitable control methods.

Both control methods are evaluated in a load force scenario where the effect on the system when applying a load force is observed. An open loop control method is utilised where the

input signals to the system is calculated with and without load force present and then the input signals are then changed accordingly to the change in load force.

The velocity control with slave function showed the possibility of controlling the velocity, but the control strategy is limited with respect to controlling the pressure and therefore other control strategies are further investigated. The simulations showed that both the piston side and rod side pressures changed significant when applying the load force.

In the velocity and pressure control the advantage of utilising the input signals independently is to be able to achieve more control options for the system. The more control possibilities that are investigated is primarily controlling the velocity with one input signal and investigate whatever the other input signal should control the piston or rod side pressure.

The non-linear model is validated to a satisfying level despite the lack experimental data. The non-linear model showed the behavior of the system as it was expected. If it was possibly to conduct experimental data the non-linear model where compared to the data and the viscous friction coefficient,  $B_v$ , the Coulomb friction,  $F_c$ , and potential leakage flow are used as fitting parameters in order to achieve higher degree of validation for the non-linear model.

## 3 | Linear Analysis

A linear model of the system is made to be able to design linear controllers for the system and to analyse the input-output parring. The linear model is a representation of the non-linear model regarding the orifice equations. These equations are linerised and the system is represented in state space form. The linear model is then validated against the non-linear model to compare system dynamics, steady state differences, system frequencies and damping. When the linear model is validated a coupling analysis is carried out consisting of a Relative Gain Array (RGA) analysis together with a Singular Value Decomposition (SVD) analysis. The purpose of the coupling analysis is to investigate the input-output parring and identify the most suitable control strategy for a given operating condition.

### 3.1 Linear Model

The linear system is conducted by firstly treating the volumes  $V_p$  and  $V_r$  as constants together with the effective bulk modules of the oil. Coulomb friction for the linear model has been disregarded and the viscous damping  $B_v$  it is set to a constant. The linear system is described as:

$$\ddot{x} = \frac{1}{M}(A_p p_p - A_r p_r - F_L - B_v \dot{x}) \quad (3.1)$$

$$\dot{p}_p = \frac{\beta_{p0}}{V_{p0}}(q_p - \dot{x}A_p) \quad (3.2)$$

$$\dot{p}_r = \frac{\beta_{r0}}{V_{r0}}(\dot{x}A_r - q_r) \quad (3.3)$$

where the linearised orifice equation  $q_p$  and  $q_r$  are applied by the following equations:

$$q_p = K_{qu_p}u_p - K_{qp_p}p_p \quad (3.4)$$

$$q_r = K_{qu_r}u_r + K_{qr_r}p_r \quad (3.5)$$

When deriving the constant  $K_{qp_p}$  it changes sign which leads to the negative contribution from  $p_p$  in Equation 3.4. The linearised constants are derived in Appendix C - RGA Analysis on page 53. A block diagram of the system is represented in Figure 3.1, where a positive input signal to  $u_p$  results in a positive piston pressure and a positive input signal to  $u_r$  results in a negative rod pressure, defined by the orifice equation on page 4. The three outputs in the block diagram are the velocity, the piston pressure and rod pressure. [Henrik C. Pedersen, 2013]

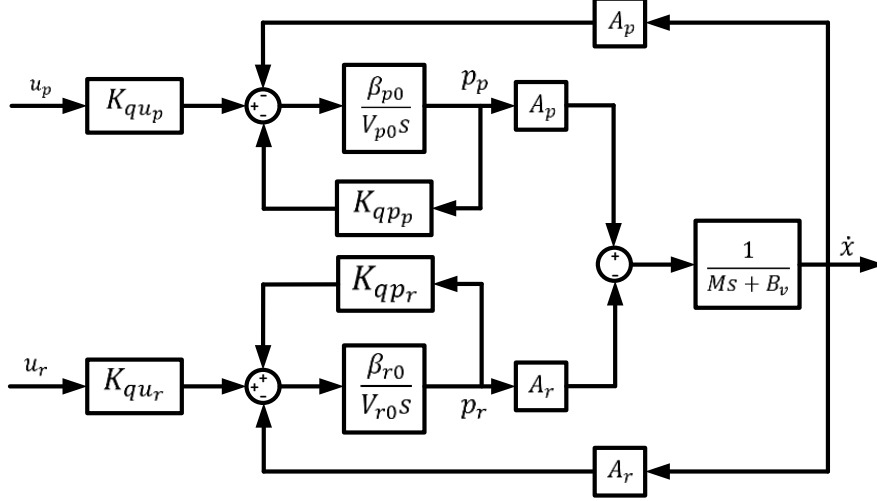


**Figure 3.1:** Linearised system in a block diagram.

The system is represented in state space form with the state vector  $\mathbf{x} = [\dot{x} \ p_p \ p_r]^T$ , the input vector  $\mathbf{u} = [u_p \ u_r]^T$ , the system matrix  $\mathbf{A}$  and the input matrix  $\mathbf{B}$  which is given as:

$$\mathbf{A} = \begin{bmatrix} -\frac{B_{eq}}{M_{eq}} & \frac{A_p}{M_{eq}} & -\frac{A_r}{M_{eq}} \\ \frac{\beta_{p0}K_{qu_p}}{V_{p0}} & -\frac{\beta_{p0}K_{qp_p}}{V_{p0}} & 0 \\ \frac{\beta_{r0}K_{qu_r}}{V_{r0}} & 0 & -\frac{\beta_{r0}K_{qp_r}}{V_{r0}} \end{bmatrix}, \quad \mathbf{B} = \begin{bmatrix} 0 & 0 \\ \frac{\beta_{p0}K_{qu_p}}{V_{p0}} & 0 \\ 0 & -\frac{\beta_{r0}K_{qu_r}}{V_{r0}} \end{bmatrix} \quad (3.6)$$

In the state space model the output matrix  $\mathbf{C}$  decides which pressure that is to be controlled as seen in Equation 3.7 and 3.8.

$$\mathbf{y} = [\dot{x} \ p_p]^T, \quad \mathbf{C} = \begin{bmatrix} 1 & 0 & 0 \\ 0 & 1 & 0 \end{bmatrix} \text{ (Controlling state } p_p) \quad (3.7)$$

$$\mathbf{y} = [\dot{x} \ p_r]^T, \quad \mathbf{C} = \begin{bmatrix} 1 & 0 & 0 \\ 0 & 0 & 1 \end{bmatrix} \text{ (Controlling state } p_r) \quad (3.8)$$

The transfer function for the system is found by:

$$\mathbf{G}(s) = \begin{bmatrix} G_{11}(s) & G_{12}(s) \\ G_{21}(s) & G_{22}(s) \end{bmatrix} = \mathbf{C} (s\mathbf{I} - \mathbf{A})^{-1} \mathbf{B} \quad (3.9)$$

## 3.2 Validation of Linear Model

The non-linear model is to be compared to the linear model derived above. In this validation the two models are given the same input signals and the position, velocity, piston

and rod pressures are compared. The comparison is conducted in the linearization point where the velocity is  $\dot{x}=0.1$  m/s, the cylinder position  $x_0=L_{stroke}/2$ , which will results in the volumes  $V_{p0}=0.67$  l and  $V_{r0}=0.43$  l, piston pressure  $p_{p0}=9.8$  bar, rod pressure  $p_{r0}=20$  bar and the bulk modulus for both chamber are set to 16000 bar. The input signals used to the comparison are the input signals  $u_{p0}=0.1955$  and  $u_{r0}=0.3109$ , which will results in the linearized velocity. The input signals are then step at 0.4 s in order to illustrate the behavior of the linear system compared to the non-linear system in another operating point than the linearization point. The input signals are shown in Figure 3.2.

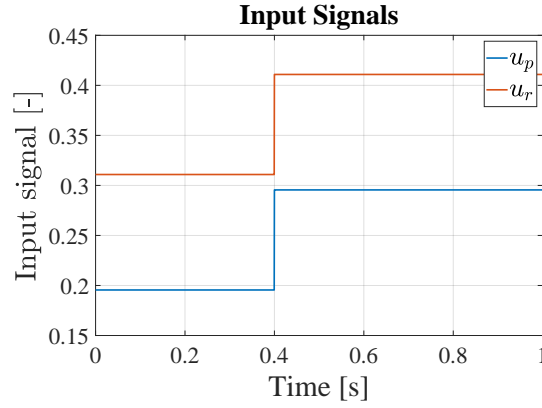


**Figure 3.2:** Input signals for the non-linear and linear model.

The position, velocity, piston and rod side pressures for the non-linear and linear system are illustrated in the figures below.

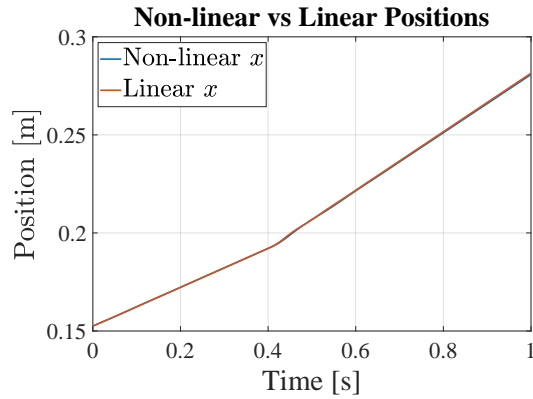


**Figure 3.3:** Position comparison.

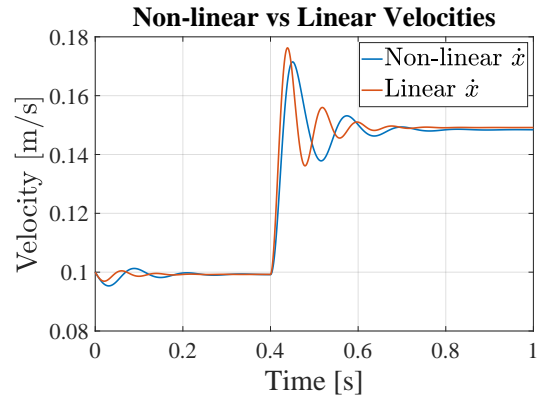


**Figure 3.4:** Velocity comparison.

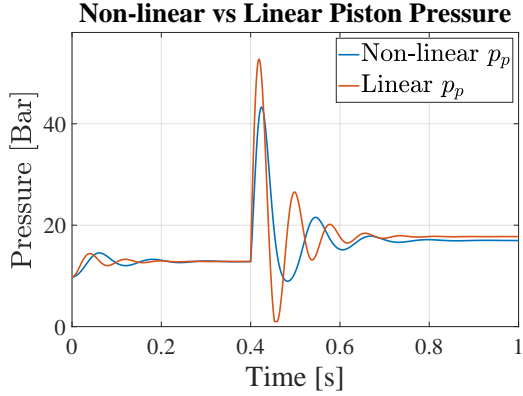


Figure 3.5: Piston pressure comparison.

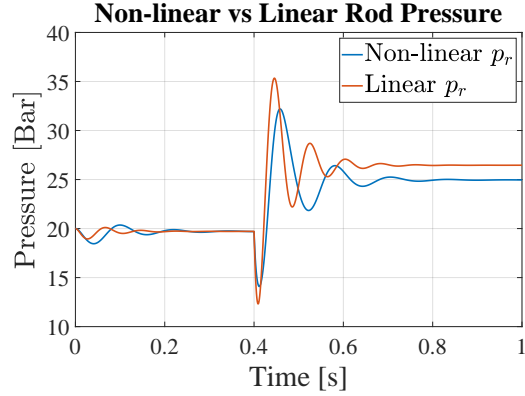


Figure 3.6: Rod pressure comparison.

From the figures it is seen that at the linearization point, when the systems reach steady state values, around 0.3 s to 0.4 s, the non-linear and linear system have identical values for the velocity, piston and rod pressure as expected. At the time of 0.4 s the system is given a step in the input signals to illustrate the difference between the non-linear and linear model when the systems are not operating in the linearization point. The oscillations for the velocities in Figure 3.4 have a slight difference in the frequency where the linear model is leading the non-linear model, which can be the result of a couple of factors such as: the linear model having constant volumes  $V_{p0}$  and  $V_{r0}$  while the volumes of the non-linear system varies with cylinder position. Another factor is that the bulk modulus of the linear model is constant at 16000 bar while the bulk modulus of the non-linear model varies with the pressures. A similar slightly difference in the frequency is seen in the pressure figures for the piston pressure in Figure 3.5 and the rod pressure in Figure 3.6. The frequency for the linear model is calculated to be 81.19 rad/s and the damping is 0.202.

To investigate if changing the bulk modulus for the linear model could impact the frequency difference between the non-linear and the linear model the varying bulk modulus for the non-linear system is firstly plotted in Figure 3.7.

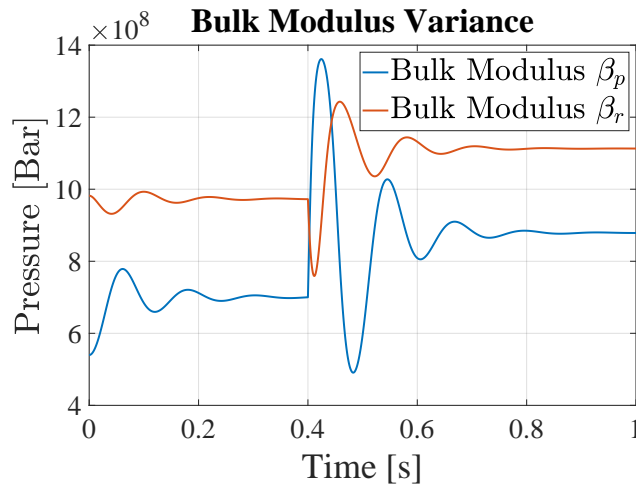
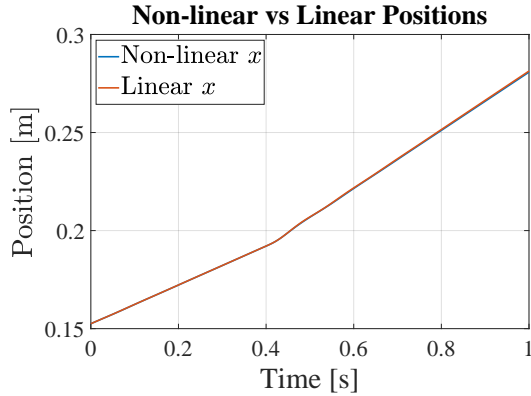


Figure 3.7: Bulk modulus for the non-linear model.

From inspecting the behavior of the varying bulk modulus in the non-linear model it is seen that setting both bulk modulus' to 16000 bar for the linear model is making the hydraulic oil of the linear model too stiff compared to the non-linear model. To adjust the linear model a simulation is conducted with changed values for the bulk modulus. From Figure 3.7 the piston side bulk modulus is set to a constant of  $\beta_p \approx 8000$  bar while the rod side bulk modulus is set to a constant of  $\beta_r \approx 10000$  bar.

The linear model with changed bulk modulus' is simulated and compared against the non-linear model again. The improved figures are seen below.



**Figure 3.8:** Position comparison.

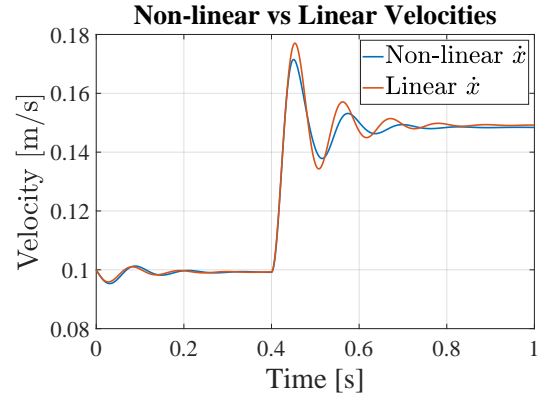


**Figure 3.9:** Velocity comparison.

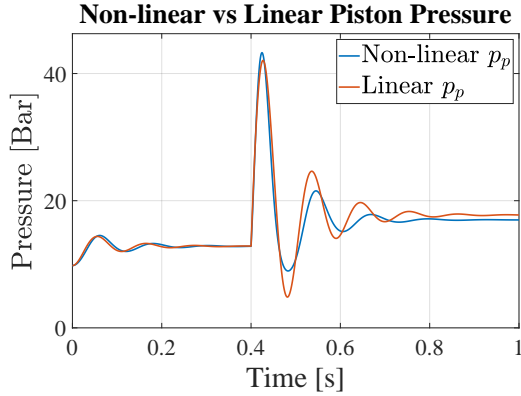


**Figure 3.10:** Piston pressure comparison.

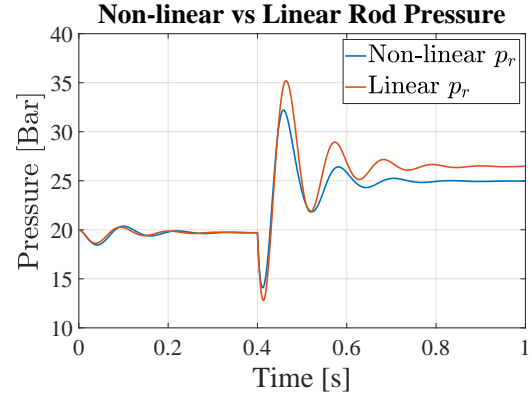


**Figure 3.11:** Rod pressure comparison.

Decreasing bulk modulus, which means decreasing the stiffness of the hydraulic oil, will result in the time constants for the two pressures will increase and make the system pressures slower. The effect of decreasing the bulk modulus in both chambers is seen in Figure 3.10 and Figure 3.11. The frequencies of the pressures compared in the non-linear and linear model are improved by the changed bulk modulus. The improvement is seen for the velocity as well where the non-linear and linear model are nearly identical with respect to the systems damping and frequency. The frequency for the linear model is 58.80 rad/s and the damping is 0.196. With the changed bulk modulus the linear model is then validated against the non-linear model for positive velocities.

Another similar linear model of the non-linear model when the cylinder velocity is negative

is conducted. In this scenario the supply pressure is connected to the rod side chamber and the tank pressure is connected to the piston side chamber. This results in the linearised orifice equations in Equation 3.4 and 3.5 are changed and new linearisation constants are derived. The simulation of the linear model with a negative velocity compared to the non-linear model showed a similar behavior as for the linear model with positive velocity shown in the above figures.

### 3.3 Coupling Analysis

A coupling analysis is to be carried out for the linear model to investigate the coupling between the inputs and outputs. The purpose of the coupling analysis is to achieve an understanding of the input-output pairing and find a control strategy that results in the least control effort when later designing controllers for the system. Two different coupling analysis are conducted which is the RGA analysis and the SVD analysis.

#### 3.3.1 Relative Gain Array

The relative gain array (RGA) analysis is conducted for a system with multiple inputs and outputs and the coupling between these is to be investigated. The RGA analysis is a measure of interaction between inputs and outputs and is widely used to determine the best input-output pairings for multivariable system. The RGA analysis consist of two measures that are used to determine the level of input-output pairing which is the RGA numbers and the RGA elements. The RGA analysis is conducted by Equation 3.10 where  $\mathbf{G}$  is a non-singular square complex matrix. [Skogestad and Postlethwaite, 2005]

$$RGA(\mathbf{G}) = \mathbf{G} \cdot * (\mathbf{G}^{-1})^T = \begin{bmatrix} \lambda_{11} & \lambda_{12} \\ \lambda_{21} & \lambda_{22} \end{bmatrix} \quad (3.10)$$

where  $\cdot *$  denotes the Schur product which is element-by-element multiplication. In the RGA matrix the rows and columns sums to 1 and the magnitudes are frequency dependent. The RGA matrix is the identity matrix if  $\mathbf{G}$  is upper or lower triangular. If the RGA matrix is the identity on the diagonal elements in Equation 3.10, output  $y_1$  is controlled by  $|\lambda_{11}| \cdot u_1$  and output  $y_2$  is controlled by  $|\lambda_{22}| \cdot u_2$ . If the RGA matrix shows that the off-diagonals is ones the control structure changes and the output  $y_1$  is controlled by  $|\lambda_{12}| \cdot u_2$  and output  $y_2$  is controlled by  $|\lambda_{21}| \cdot u_1$ . If the RGA matrix shows either of the two matrices the system is said to be decoupled and no cross-doubling is present.

The RGA analysis is dependent on the frequency, the chosen controlled pressure and the linearization point. The effect of choosing different linearization point regarding the RGA analysis is investigated in Appendix C - RGA Analysis on page 53, where the operating condition for the piston velocity  $\dot{x}$ , the load force  $F_L$ , the rod side pressure  $p_{r0}$  and the cylinder position  $x_0$  are varied independently. The RGA analysis is conducted to observe the interaction between the inputs and outputs when chosen the piston pressure or the rod pressure as the secondary control state. The purpose for investigating both the piston pressure and the rod pressure to be compare their RGA analysis' and obtain an understanding of which of the pressures that is easier to control.

From the different RGA analysis' conducted in Appendix C - RGA Analysis on page 53 some observations of the system frequency and damping in different operating condition can be listed as:

- **Cylinder position  $x_0$** : When changing the cylinder position from  $x_0 = 0$  to  $x_0 = L_{stroke}$  results in the volumes in the chambers changes and this effects the frequency and the damping of the system. When the velocity is positive it is seen that the system frequency and damping decreases as the cylinder position moves from the bottom to the top of the cylinder. The system frequency decreases from  $\approx 250$  rad/s to  $\approx 60$  rad/s when the cylinder position moves from bottom to the top position, which is associated with that the volume in the piston chamber is at its minimum when the piston is at the bottom and results in fast piston pressure response compared to when the cylinder position is at the top where the piston volume is at its maximum and results in a slower piston pressure response. See reference figures on page 54.
- **Load force  $F_{L,0}$** : Applying different load force to the system, varied from  $F_{L,0} = 0$  kN to  $F_{L,0} = 40$  kN, results in an increase in the piston pressure and causes the damping of the system to increase with increasing load force. The most undamped scenario is when no load is present and the cylinder position is at the top which results in the system have a damping coefficient of  $\zeta = 0.14$ . The highest damping coefficient is in the operation condition where the load force is at  $F_{L,0} = 40$  kN and the cylinder position is at the bottom which results in a damping coefficient of  $\zeta = 0.57$ . The effect of applying a positive load force to the system will results in the piston pressure increases when keeping a constant rod pressure and the increase in piston pressure will increase the required input signal  $u_p$ . Increasing the input signals and the piston pressure results in the linearization constants  $K_{qu_p}$  and  $K_{qp_p}$  increases and so does the damping ratio. See reference figures on page 54 for  $F_{L,0} = 0$ kN, page 60 for  $F_{L,0} = 20$ kN and page 69 for  $F_{L,0} = 40$ kN.
- **Rod side pressure  $p_{r,0}$** : The rod pressure is set to a constant pressure for the RGA analysis' and the effect of changing this value is seen to affect the damping ratio of the system. The rod pressure is varied as  $p_{r,0} = 10, 20$  and  $30$  bar. The highest damping found is  $\zeta = 0.26$  and is in the case where the rod pressure is set to  $30$  bar and the cylinder position is at the top position. Changing the rod pressure varies the damping ratio from  $\zeta = 0.14$  to  $\zeta = 0.26$ . See reference figures on page 54 for  $p_{r,0} = 10$  bar, page 63 for  $p_{r,0} = 20$  bar and page 66 for  $p_{r,0} = 30$  bar.
- **Velocity  $\dot{x}_0$** : The effect of changing the velocity for the system is found to change the the inputs significant. The input signals when  $\dot{x}_0$  is set to  $0.1$  m/s are  $u_{p,0} = 0.1932$  and  $u_{r,0} = 0.4517$  and when changing the  $\dot{x}_0$  to  $0.2$  m/s the input changes to  $u_{p,0} = 0.3863$  and  $u_{r,0} = 0.9035$ . The change in the input signals will again result in an increase in the damping of the system. The damping ratio, when the velocity is  $\dot{x}_0 = 0.1$  m/s, is found to vary between  $\zeta = 0.22$  to  $\zeta = 0.14$  while when the velocity is  $\dot{x}_0 = 0.2$  m/s the damping ratio varies between  $\zeta = 0.44$  to  $\zeta = 0.20$  depending on the cylinder position. See reference figures on page 54 for  $\dot{x}_0 = 0.1$  m/s and page 57 for  $\dot{x}_0 = 0.2$  m/s.

The two RGA analysis' illustrated below are conducted in the operating point where  $\dot{x}_0 = 0.1$  m/s,  $F_L = 0$  N,  $p_{r0} = 20$  bar and  $x_0 = 0$  m. The RGA analysis when the secondary control state is the piston pressure  $p_p$  is illustrated in Figure 3.12 from page 63 in RGA Analysis.

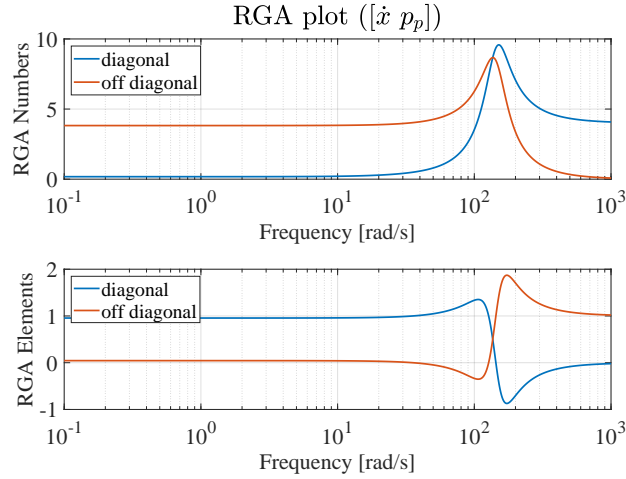


**Figure 3.12:** RGA analysis with  $p_p$  as secondary control state.

Selecting the secondary control state as the rod pressure results in the RGA analysis seen in Figure 3.13 from page 81 in RGA Analysis.

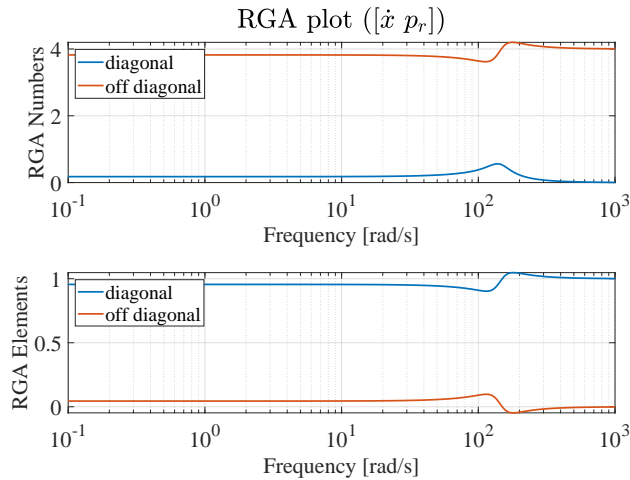


**Figure 3.13:** RGA analysis with  $p_r$  as secondary control state.

For a decoupled system the RGA number for the off-diagonal should be 4 while the diagonal is 0 or vice versa. If the RGA number is relatively large the system is said to be ill-conditioned which indicate that the system could be sensitive to uncertainties. When observing the RGA elements for complete decoupling the diagonal should be 1 and the off-diagonal should be 0 or vice versa. [Skogestad and Postlethwaite, 2005]

Observing the RGA plot in Figure 3.12 it can be seen that when choosing the secondary control state as the piston pressure results in strong coupling between the velocity and the piston pressure at the frequency range of 100-200 rad/s, which indicate that this method of controlling the system could be difficult. In the process of designing a control strategy for this scenario the control strategy could be frequency limited to around 50-100 rad/s so that the cross parring in the frequency range of 100-200 frequencies is cut off. The RGA

number for this case is relative large (between 5-10) which reveals that there is a large difference between the maximum and minimum singular values. Changing the secondary control state to the rod pressure in Figure 3.13 it is seen from the RGA elements that throughout the frequency range the diagonal is approximately kept at 1 while the off-diagonal is approximately kept at 0. This indicates that there is almost no coupling between the velocity and the rod pressure. The RGA number for this case is small and implies that the this method is not likely to be sensitive to uncertainties. The damping coefficient for the two scenarios is calculated to be  $\zeta = 0.23$  with a frequency of 144 rads/s. These RGA analysis' is conducted when the cylinder position is at  $x_0 = 0$ , which will result in the highest bandwidth for the system and when the cylinder position is changed  $x_0 = L_{stroke}$  the RGA analysis' changes as the volumes in the chamber changes from  $V_{p,0} = 0.2$  l and  $V_{r,0} = 0.67$  l to  $V_{p,0} = 1.15$  l and  $V_{r,0} = 0.2$  l. The impact of fully extending the cylinder position to  $x_0 = L_{stroke}$  is illustrated in Figure 3.14 from page 65 and 3.15 from page 83.

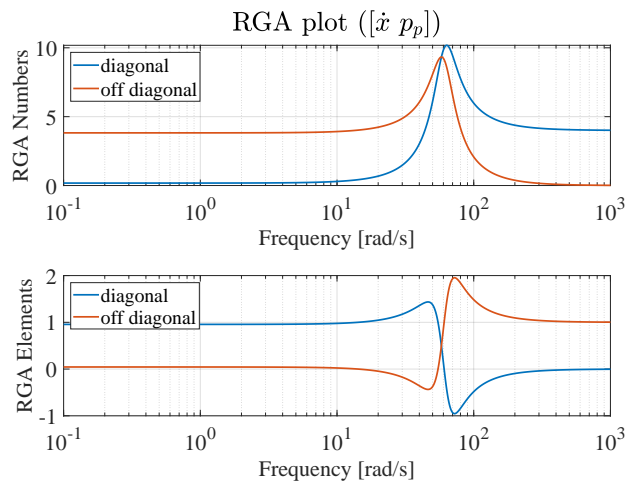


**Figure 3.14:** Changing the cylinder position to  $x_0 = L_{stroke}$ .

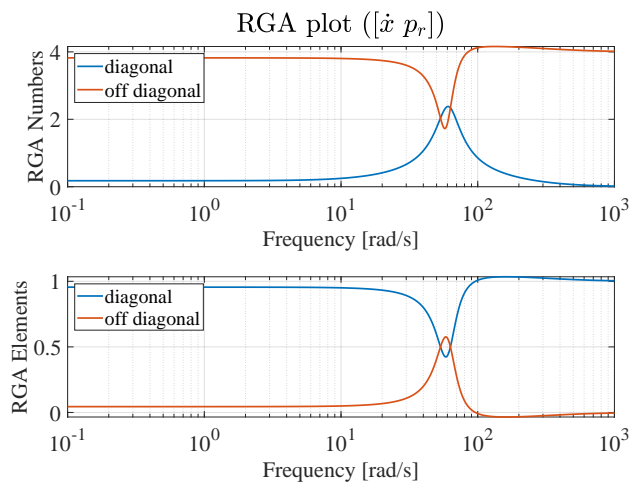


**Figure 3.15:** Changing the cylinder position to  $x_0 = L_{stroke}$ .

When the cylinder position have a positive velocity and moves from the bottom to the top of the cylinder the system frequency changed from 144 rad/s to 61 rad/s, which is seen to be the case in every scenarios. This indicates that as the cylinder position moves towards the top of the cylinder the system response becomes slower. The frequency of the system needs to be taking into consideration when designing controllers.

### 3.3.2 Singular Valve Decomposition

The system transfer function  $\mathbf{G}$  is decomposed into its Singular Value Decomposition (SVD) in order to observe the system gain dependent on the input direction. The SVD analysis is frequency dependent and gives an insight of the systems behavior accordingly to the input direction. The system performance is directly coupled to the SVD analysis in the sense of the difficulty of controlling the system. To achieve acceptable performance it is reasonable to have minimal gain variance for any input direction. The maximum and minimum system gain is calculated by Equation 3.11.

$$\bar{\sigma} = \sqrt{\lambda_{\max}(\mathbf{G}^H \mathbf{G})}, \quad \underline{\sigma} = \sqrt{\lambda_{\min}(\mathbf{G}^H \mathbf{G})} \quad (3.11)$$

where  $\mathbf{G}^H$  is the complex conjugate transpose. The Singular values is calculated throughout the frequency domain and illustrated in Figure 3.16.

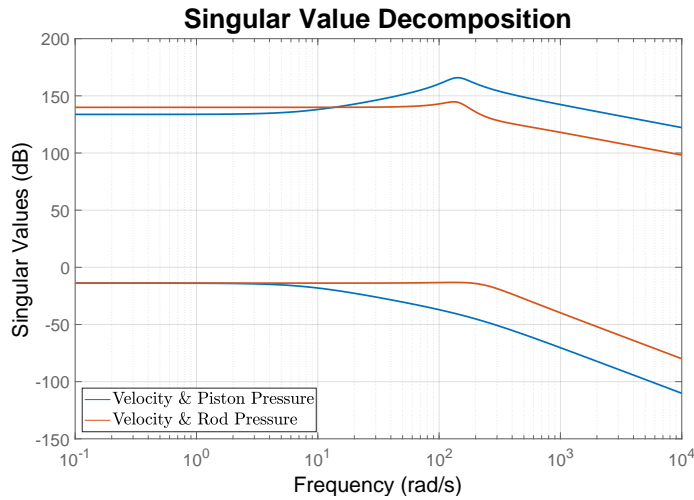


**Figure 3.16:** Singular Values Decomposition for system controlling velocity with different pressures.

From the figure it can be seen that there is a large difference between the minimum and maximum gain for both control methods. The large gain difference indicates that the input direction have a significant impact on the system gain and results in the system is difficult to control. Comparing the system gain difference when controlling the piston pressure and rod pressure it is seen that when controlling the position pressure the system gain is larger than when controlling the rod pressure. This also backs-up the RGA analysis about choosing the piston pressure as the secondary control state. This indicates that the system gain when controlling the piston pressure is more dependent on the input direction and resulting in the system being more difficult to control.

## 4 | Design of Control Strategies

In this chapter the control strategies for the MIMO system are considered. The purpose for the control strategies is to primarily control the velocity of the cylinder while the secondary control is to control one of the pressures in the chambers. The MIMO system is highly non-linear which makes using two separate SISO controllers difficult to control the system. In order to be able to consider the system as a SISO system two pre-compensators are required to eliminate the coupling effect in the system. The method of decoupling the system is by designing a static and a dynamic pre-compensator. When the pre-compensators are designed and implemented a decent performance of system with classic linear SISO controllers is achievable.

### 4.1 Decoupled Control of the System

The purpose of the pre-compensator is to decouple the system gain so that the system gain do not change with the input. The decoupling is done in order to be able to make the velocity dependent on only one input signal and the controlled pressure only dependent on the other input signal.

The implementation of the pre-compensators is illustrated in Figure 4.1 where the contribution from the pre-compensator is added to the control input from the controller and the compensated control input is then given to the plant. The purpose of the contribution from the pre-compensator is to manipulate the input to the plant so that the coupling effect is eliminated.

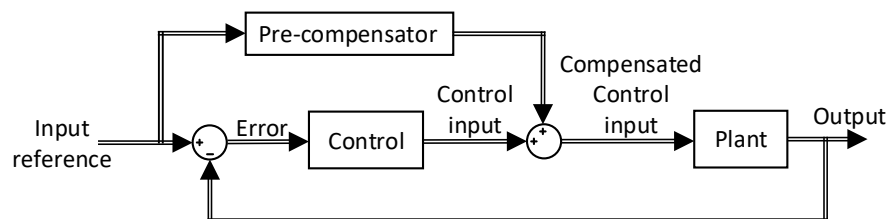


Figure 4.1: Block diagram of the pre-compensator design.

The static pre-compensator compensate the system gain at zero frequency and the dynamic pre-compensator compensate the system gain throughout the entire frequency range. The difference between the two pre-compensators is that the static pre-compensator only compensates the system at one frequency and the pre-compensator matrix does not change

throughout the frequency range while the pre-compensator matrix for the dynamic pre-compensator changes accordingly to the frequency. The static pre-compensator is found by taking the inverse of the plant and evaluate the pre-compensator matrix in the frequency  $\omega = 0$  rad/s seen in Equation 4.1.

$$\mathbf{W} = \mathbf{G}(0)^{-1} \quad (4.1)$$

The pre-compensator is found by the same method but evaluate throughout the frequency range and is found by Equation 4.2.

$$\mathbf{W} = \mathbf{G}(s)^{-1} \quad (4.2)$$

The advantage of utilizing the dynamic pre-compensator is to be sure that the system is decoupled throughout the frequency range. The system with a pre-compensator implemented is described by Equation 4.3 that ideally gives the identity matrix as the pre-compensators is the inverse of the plant.

$$\begin{bmatrix} y_1 \\ y_2 \end{bmatrix} = \mathbf{GW} \begin{bmatrix} u_1 \\ u_2 \end{bmatrix} = \mathbf{I} \begin{bmatrix} u_1 \\ u_2 \end{bmatrix} \quad (4.3)$$

The maximum and minimum singular values when the two pre-compensators is implemented to the plant is seen in Figure 4.2. A second order filter is implemented together with the pre-compensator in order to ensure that the system is strictly proper which results in elimination of high frequency signals. To ensure that the filter does not filter out any system dynamics the bandwidth of the filter is chosen to be higher than the bandwidth of the system.

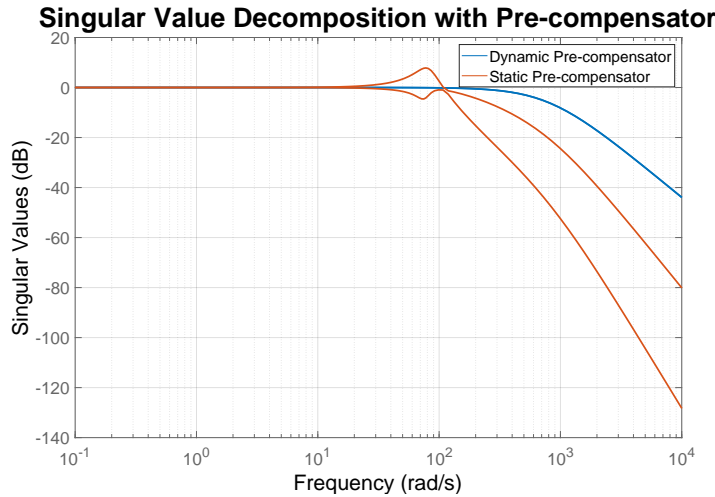
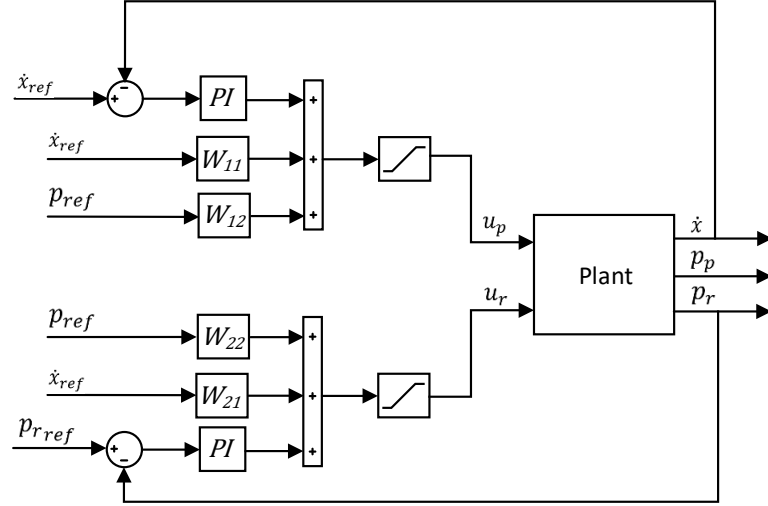


Figure 4.2: Singular value decomposition with pre-compensators.

From the figure it is seen that the maximum and minimum system gain for the dynamic pre-compensator is independent of the input direction throughout the frequency range. The static pre-compensator compensates the system gain at zero frequency which results in a difference between the maximum and minimum system gain at frequencies above 20 rad/s. Implementing the dynamic pre-compensator achieves that the system gain is independent on the input direction and indicates that the system can achieve decent performance with SISO controllers. The dynamic pre-compensator is therefore implemented to consider the

system as two SISO systems with two different designed controllers, one to control the velocity and another to control the rod pressure. The implementation of the dynamic pre-compensator together with the two PI-controllers is illustrated in a block diagram in Figure 4.3.



**Figure 4.3:** Block diagram of implementing the pre-compensator.

Where the inputs to the pre-compensators are the reference velocity and pressure. The output from the pre-compensator is then added to the output for the controller and the compensated output is then saturated to the input signal between 1 and -1.

## 4.2 Design of Velocity & Pressure Control

Two controllers are to be designed, one for the velocity and another for the rod pressure. The design of these controller is carried out for the linear model with a positive velocity. The control strategy is that the input signal  $u_p$  controllers the velocity and the input signal  $u_r$  controls the rod pressure. The method of designing the controls is based on classical feedback control from the Book [Skogestad and Postlethwaite, 2005]. The design criteria for the controllers are:

- The controllers are designed to be robust and stable in every operating condition.
- The controller for tracking the velocity is seen to have more importance than the controller tracking the rod pressure.
- The desired phase margin of the velocity controller is set to be  $45^\circ$ .
- The pressure control is to be designed so that the settling time for the pressure control is a factor of  $\approx 10$  faster than the velocity controller. This is done in order to reduce the controllers interference with each other where the velocity controller is effected by the pressure controller and working against each other.

The transfer function for the input signal  $u_p$  to the output as velocity and the input signal  $u_r$  to the output as the rod pressure is found by utilizing Equation 3.9 by converting the state space model into transfer functions. The bode diagram, pole-zero map and open

loop step response is illustrated below for the velocity transfer function and for the rod pressure transfer function.

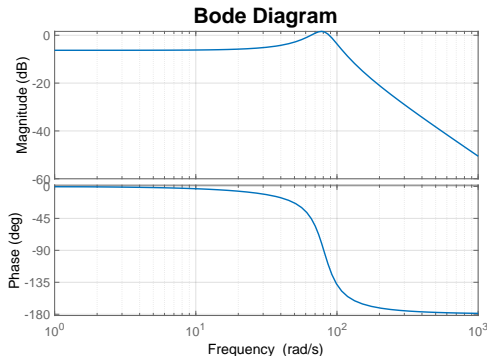


Figure 4.4: Velocity control by  $u_p$ .

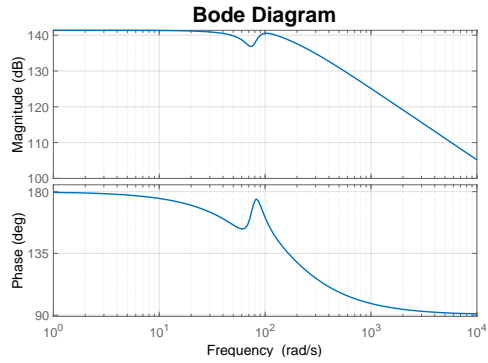


Figure 4.5: Rod pressure control by  $u_r$ .

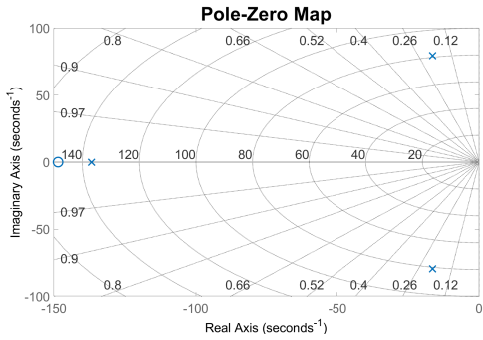


Figure 4.6: Pole-zero map for velocity.

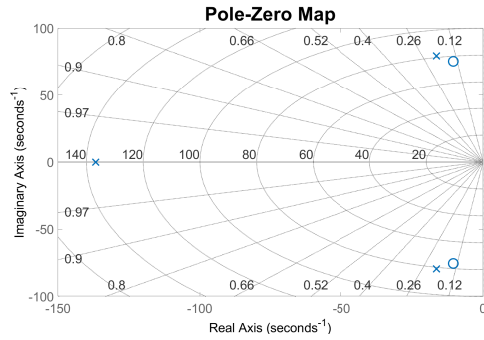


Figure 4.7: Pole-zero map for Rod pressure.

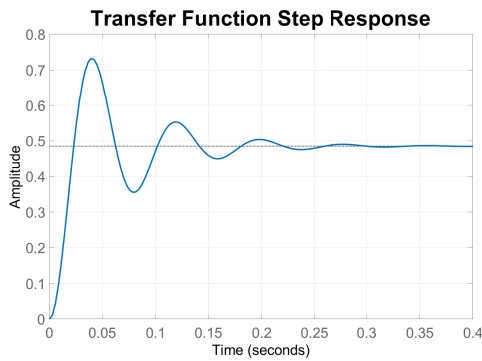


Figure 4.8: Open loop step response for  $\dot{x}$ .

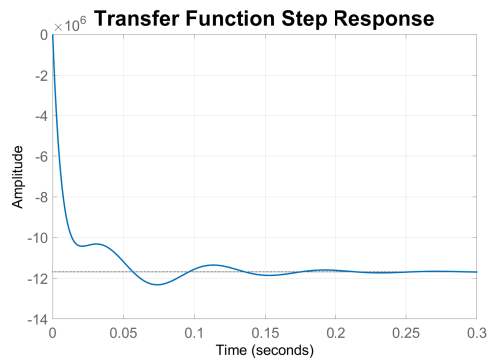


Figure 4.9: Open loop step response for  $p_r$ .

From Figure 4.4 it is seen that the bandwidth of the transfer function is 81 rad/s where the system have a resonance peak. The magnitude starts at -6.28 dB, which is equal to a gain of 0.4853 and is directly illustrated by the open loop step response in Figure 4.8. The system phase starts at  $0^\circ$  and ends in  $-180^\circ$ , which indicates that there are two more poles than there are zeros. In Figure 4.6 the system in illustrated in a pole-zero map where the system have one real zero at -148.53 and 3 poles, one real pole at -136.76 and two complex conjugate poles at  $-16.36 \pm j79.62$ .

For the rod pressure transfer function the bode diagram is seen in Figure 4.5 where the magnitude starts in 141 dB which equal to a gain of  $112.2 \cdot 10^5$  and the phase starts at  $+180^\circ$  which indicate that a positive input  $u_r$  to the system results in a negative rod pressure. This is the case because of the sign convention made for the proportional valves for the system. When the input  $u_r$  is given a positive input signal it results in the valve opening to the tank pressure and the pressure gradient becomes negative. Therefor it is seen in Figure 4.9 that the open loop step response for the rod pressure transfer function is settling at  $-112.2 \cdot 10^5$ . The chosen sign convention will results in, if an increase in the rod pressure is required by the controller the input signal  $u_p$  needs to be negative to connect the supply pressure to the rod side chamber and thereby increase the pressure. It is therefore expected that the gain for the pressure controller is negative.

The designed controllers are two PI-controller one for the velocity and other for the rod pressure. The PI-control structure is seen in Equation 4.4.

$$G_{PI}(s) = \frac{K_P s + K_I}{s} \quad (4.4)$$

The PI-controller adds a free integrator to the system in order to eliminate the steady state error. When adding a free integrator to the system the phase is changed by  $-90^\circ$ . The PI-controller also adds a zero to the system which is located at  $s = K_I/K_P$ . The zero adds positive phase to the system and makes it possible to manipulate the crossover frequency. To design the PI-controller a proportional gain and an integrator gain is to be calculated. The three steps for designing the PI-controllers are shown below.

$$\angle G(j\omega_1) = -180^\circ + \phi_m + 5^\circ \quad (4.5)$$

The first step is to find the frequency  $\omega_1$  and this is done by setting the phase margin  $\phi$  to  $45^\circ$  and then calculating the frequency  $\omega_1$  which should be the frequency required to make the phase margin  $45^\circ$ .

The proportional gain can then be calculated by Equation 4.6.

$$K_p = \frac{1}{|G(j\omega_1)|} \quad (4.6)$$

The proportional gain together with the frequency at which the phase margin is  $45^\circ$  is then used to calculate the integrator gain by Equation 4.7

$$K_I = 0.1 \cdot \omega_1 \cdot K_p \quad (4.7)$$

The velocity controller is designed by the classical feedback control while the pressure controller is designed based on the settling time for the velocity step response. To fulfil the design criteria the settling time for the pressure controller is required to be a factor of 10 lower than the velocity to avoid controller interference. This is done by first finding the settling time for the velocity controller, which is around 0.9 s and then designing the pressure controller so that its settling time is faster than 0.09 s. The proportional and integrator gains for the two controllers are seen in Equation 4.8.

$$G_{I\dot{x}}(s) = \frac{1.294s + 12.35}{s}, \quad G_{PIp_r}(s) = \frac{-1.848 \cdot 10^{-7}s - 3.851 \cdot 10^{-5}}{s} \quad (4.8)$$

The bode diagrams for the compensated system with the PI-controllers implemented are seen in Figure 4.10 for the velocity and in Figure 4.11 for the rod pressure. The close loop step response for the compensated system with the PI-controllers illustrated in Figure 4.12 for the velocity and in Figure 4.13 for the rod pressure.

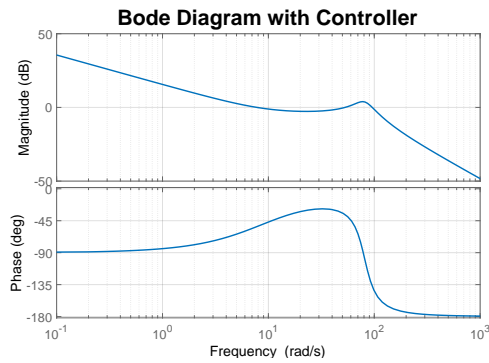


Figure 4.10: Velocity control by  $u_p$

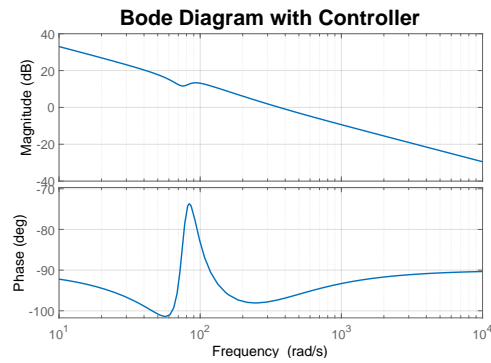


Figure 4.11: Rod pressure control by  $u_r$

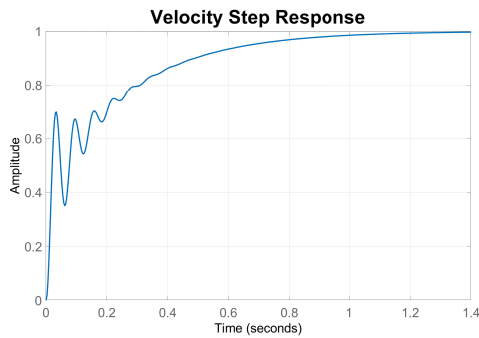


Figure 4.12: Step response for velocity.

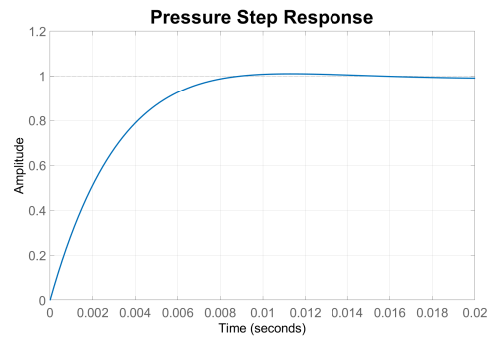
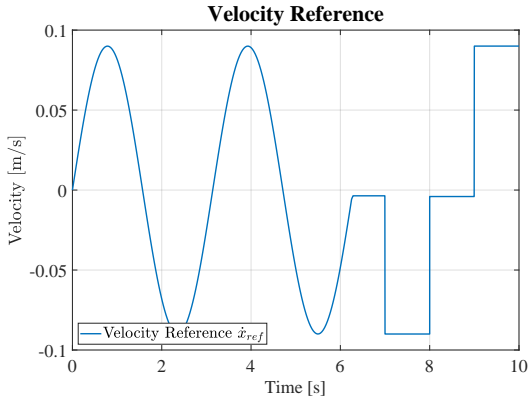


Figure 4.13: Step response for rod pressure.

From the step response for the velocity it is seen that the settling time is  $\approx 0.9$  s and for the rod pressure the settling time is 0.009s which actually makes the rod pressure control 100 times faster than the velocity controller. The location of the added zero for the velocity controller is at -190 and for the pressure controller the zero is added in -208.

### 4.3 Validation of Controllers

The system with with the designed controllers for the velocity and the rod pressure are to be validated and tested on the linear system. The controllers are designed based on a linear model conducted when the velocity reference is positive. The reference velocity and the load force disturbance is illustrated in Figure 4.14 and 4.15



**Figure 4.14:** Positive velocity reference.

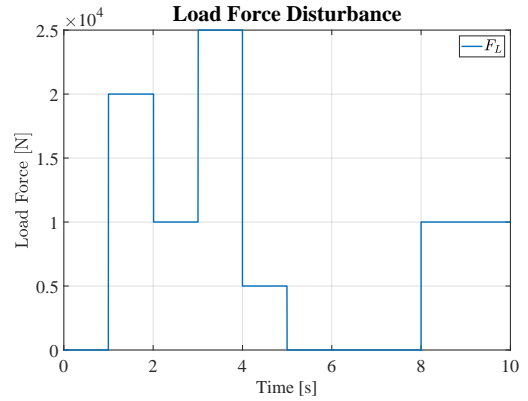


**Figure 4.15:** Load force input to the system.

The reference velocity is designed by a sinusoidal curve with an amplitude of 0.1 m/s and with a frequency of 2 rad/s so that two periods is present in the time interval from 0 s to 6.28 s. This is done to secure that the velocity controller can eliminate eventually steady state errors as the input velocity reference changes. From the sinusoidal curve the velocity reference changes to step inputs to observe the step response of the controllers. The load force the system is exposed to is seen in Figure 4.15, where the load force varies from 0 N to 25kN. The load force is applied when the velocity reference is the sinusoidal curve and applied again for one of the step inputs to observe if any difference in the step responses would occur when load force is applied.

In the four following figures, the velocity and rod pressure tracking ability together with the piston pressure and the input signals are illustrated.

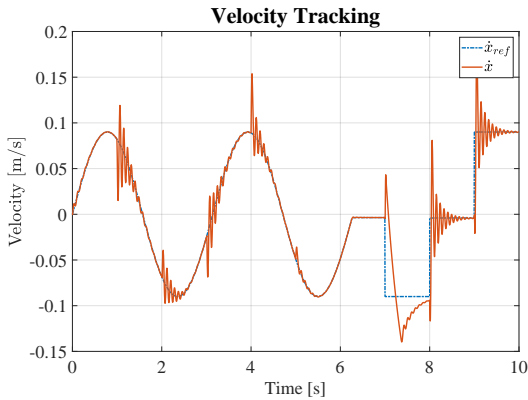


**Figure 4.16:** Velocity tracking.

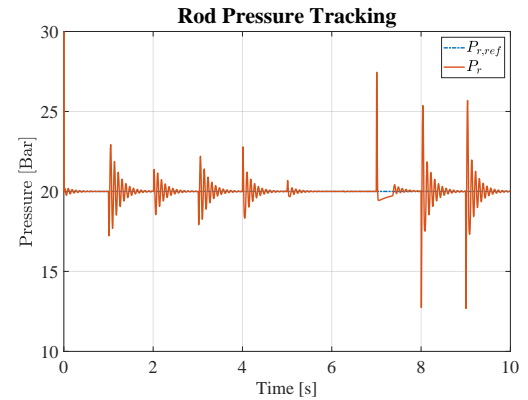


**Figure 4.17:** Rod pressure tracking.

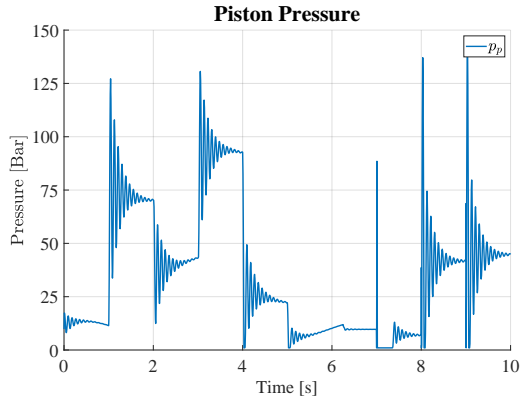


Figure 4.18: Piston pressure.

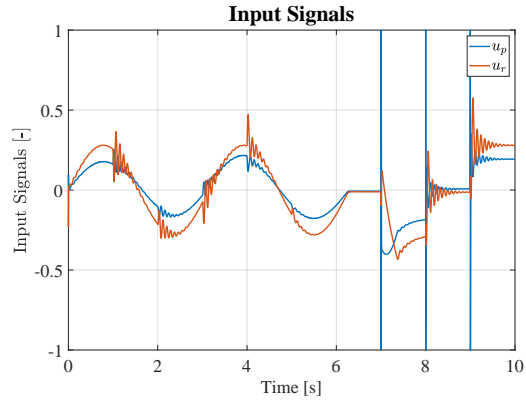


Figure 4.19: Input signals.

From Figure 4.16 it is seen that the performance for the velocity controller is descent, it is robust in regards to load force disturbances and step inputs. In Figure 4.17 the rod pressure is seen to maintain the desired back pressure of 20 bar. The rod pressure oscillates between approximately 15-25 bar and is seen to not be significant because the settling time for the rod pressure is approximately 1 s. The result of applying a load force to the system is that the controllers compensates for the force by changing the input signals which is seen in Figure 4.19 and the system response is that the piston pressure is increased seen in Figure 4.18. In the velocity tracking figure is it seen that when a step input is given to the system from 7 s to 8 s a velocity error occur because the velocity controller is suddenly limited. The limit is caused by the piston pressure reaching tank pressure in a short instant and making the velocity controller unable to perform as expected. An identical input step is given from 9 s to 10 s, but now a load force is present and causing the piston pressure to increase to around 60 bar, which results in a more expected behaviour for the step input.

### 4.3.1 Validation of Non-linear Model with Controllers

The expected behavior for the system with the designed controllers is seen for the linear system and the performance of the controllers is to be tested on the non-linear system. This is done to observe the performance of the linear designed controller on the non-linear system. The non-linear system is given the same velocity reference and load force profile. The velocity and rod pressure tracking together with the piston pressure and input signals is shown in the figures below.

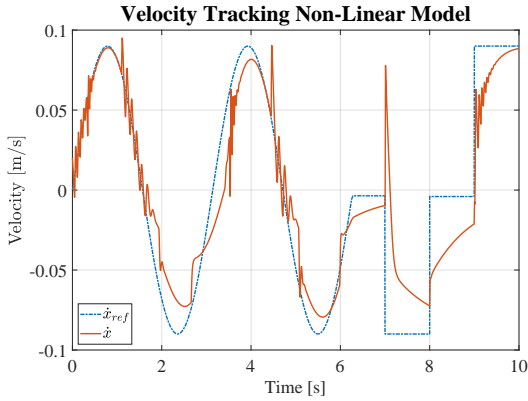


Figure 4.20: Velocity tracking.

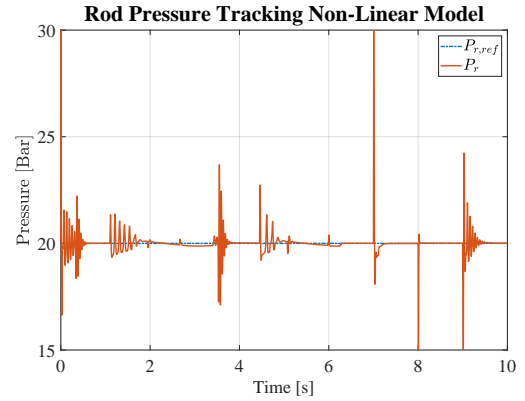


Figure 4.21: Rod pressure tracking.

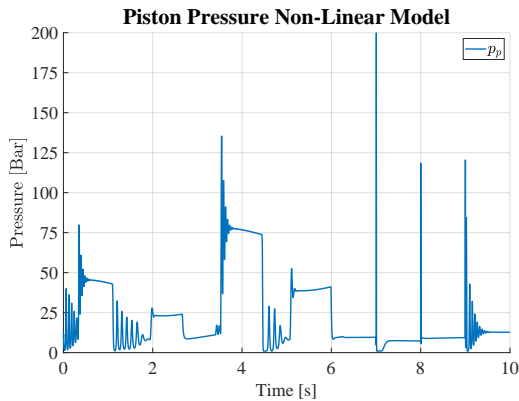


Figure 4.22: Piston pressure.

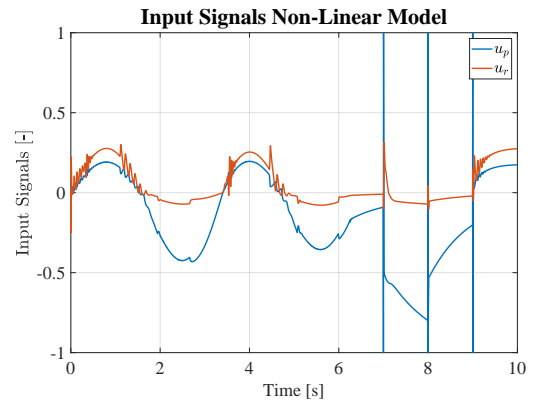


Figure 4.23: Input signals.

From Figure 4.20 it is seen that the velocity controller seems to encounter difficulties when the velocity reference is negative. This is associated with that the linear controllers are designed from a linear representation of the non-linear model when the velocity is positive. By observing the velocity tracking in the negative velocity regions it indicates that the behaviour of the non-linear system changes when the velocity is negative and results in the velocity controller being unable to track the velocity in the negative regions. The tracking of the rod pressure is seen in Figure 4.21 where the rod pressure controller is able to track the rod pressure reference. These observations indicates that the controllers designed by the linear model based on the velocity being positive only perform in the positive velocity regions and in order to track the velocity in the negative regions it seems that the gains of the controllers needs to be increased in order to track the velocity reference.

## 4.4 Combined Control Structure

The control difficulties encountered when the velocity reference is negative is investigated with respect to the linear model. The controllers are designed based on the linear model where the velocity is positive and is assumed to achieve a decent performance with the dynamic pre-compensator. The performance of the controllers on the non-linear model

when the velocity reference is negative showed that the system behavior changes and especially the velocity controller is not able to track a negative velocity reference. Therefore it is desired to design new controllers based on a linear model representing the non-linear model when the velocity is negative. Changing the velocity from positive to negative changes the linear representation of the non-linear model significantly. The idea for designing a new velocity and rod pressure controller when the velocity is negative is to be able to switch between the two sets of controllers, one set of controllers when the velocity is positive and another set of controllers when the velocity is negative. By doing this it should be possible to track the velocity reference even for negative references. The structure of the combined controllers with switching technique is illustrated in Figure 4.24.

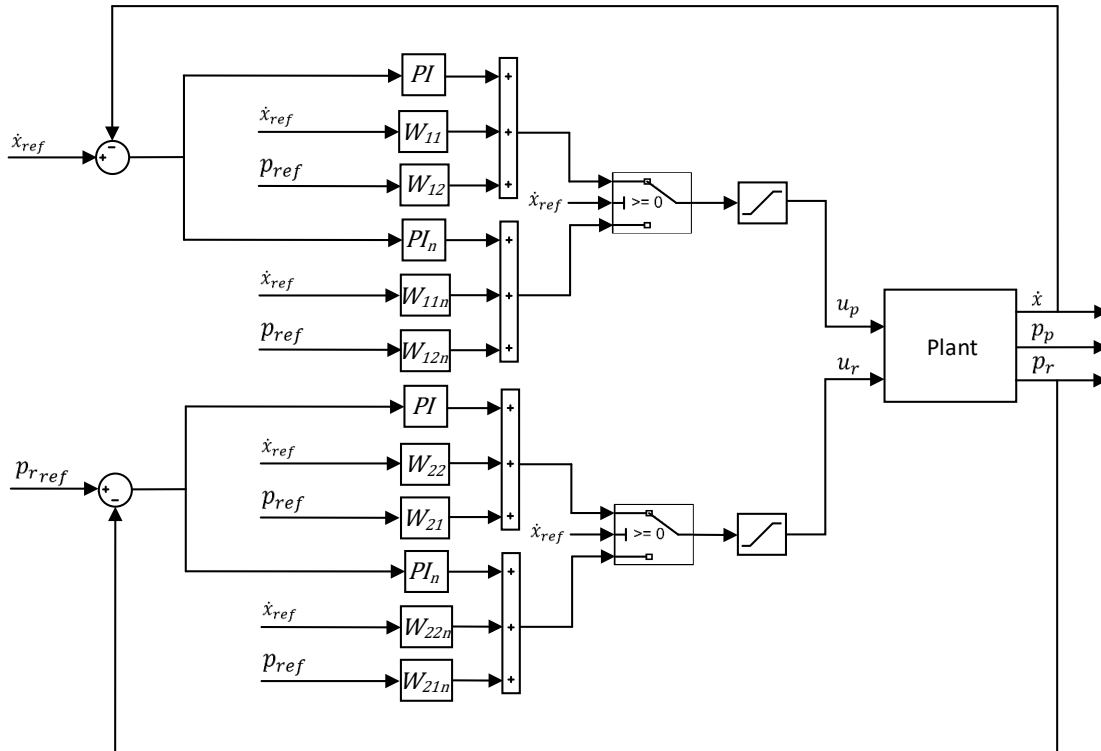


**Figure 4.24:** Block diagram of the control structure with switching controller gains.

In the block diagram the switching technique is applied so that when the velocity reference is positive ( $\dot{x}_{ref} > 0$ ) the controller gains designed with the linear model when the velocity is positive is utilized and when the ( $\dot{x}_{ref} < 0$ ) the controller gains designed for the linear model when the velocity is negative is applied. The PI-controllers activate when the velocity reference is negative and is denoted  $PI_n$  in conjunction with a designed pre-compensator based on the linear model when the velocity is negative and is denoted  $W_{ijn}$ . This control structure should ensure a decent and better performance for the non-linear model as in Section 4.3.1.

#### 4.4.1 Validation of Combined Control Structure

The combined control structure is to be tested for the non-linear model to investigate the behaviour of the system. The non-linear system is given the same velocity reference and

force load profile as in Section 4.3. The improved control structure tested on the non-linear system is illustrated for the velocity and rod pressure tracking together with the piston pressure and the input signals in the figures below.

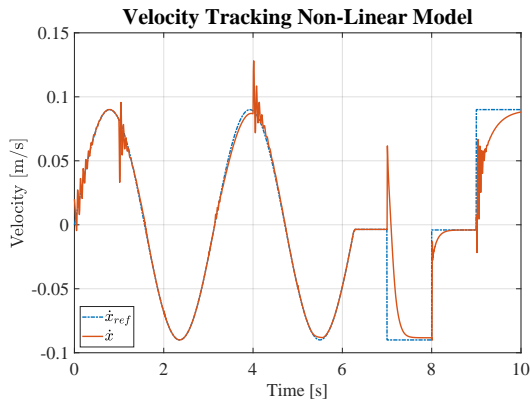


**Figure 4.25:** Piston pressure.

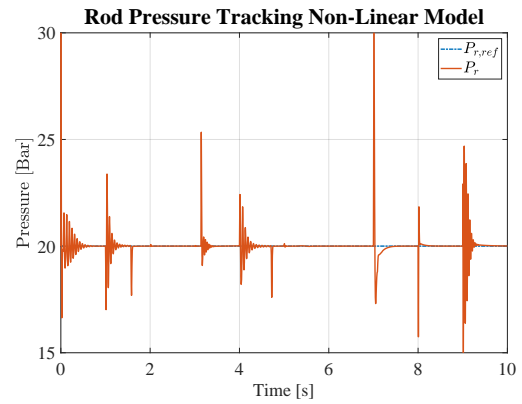


**Figure 4.26:** Input signals.

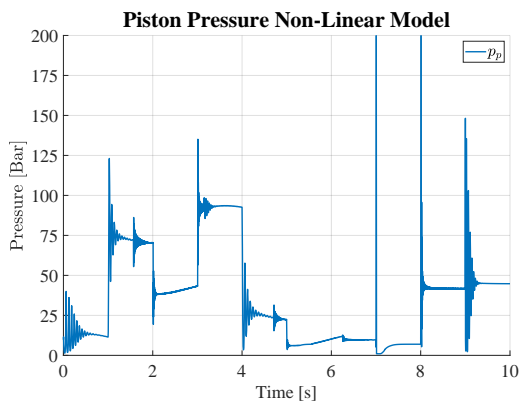


**Figure 4.27:** Piston pressure.

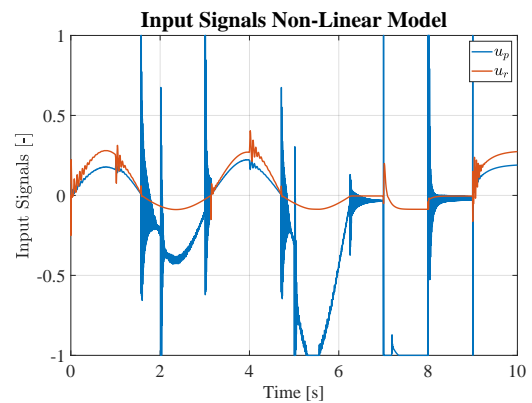


**Figure 4.28:** Input signals.

From figure 4.25 it can be seen that the velocity tracking is improved and able to track the velocity reference when a negative velocity is desired. The rod pressure seen in Figure 4.26 illustrates that the tracking of the rod pressure is achievable and when velocity reference is given a step input or a force force is applied to the system, the rod pressure seem to achieve a good performance with maintaining a constant rod pressure of 20 bar. When the load force is applied to the system an increase in the piston pressure is seen in Figure 4.27 where the piston pressure changes accordingly to the applied load force while remaining the rod pressure at 20 bar. Observing the input signals in Figure 4.28 it is seen that the input signal  $u_p$  is more aggressive when the velocity is negative than when the velocity reference is positive. This is associated with the different controller gains for the two velocity controllers. It is also notable that in the instant where the velocity changes from positive to negative it is seen that input signal  $u_p$  oscillates more and changes suddenly.

## 4.5 Discussion of Control Strategies

The requirement for the designed controllers through this chapter is to be able to track a given reference trajectory for the velocity while maintaining a constant rod pressure. The coupling analysis showed that there is a coupling between the velocity and the rod pressure which from a control sight indicated that a pre-compensator should be designed. To decouple the system two pre-compensators are designed, static and dynamic pre-compensators, where the dynamic pre-compensator showed the most decoupling for the system and were used in combination with classical SISO controllers for the velocity and the rod pressure. Two PI-controllers designed showed reasonable performance when implemented to the linear model, but showed a lack of tracking performance when the controllers were tested on the non-linear model. Considering the lack of performance with a negative velocity reference a suggesting is to change the controller gains as the velocity reference changes to negative. Therefore a switching control structure is conducted to improve the velocity tracking, which showed significantly improvement. The switching structure resulted in that the input signals behaved aggressively in the instant there the the velocity changed sign and the controllers were switched. To avoid a sudden change in the input signals a more smooth transition from one controller output to another controller output different techniques could have been applied but is reserved for further work.

## 5 | Conclusion

In this report the concept of controller a hydraulic cylinder with two separate controlled proportional valves with respect to velocity and pressure tracking has been investigated.

Under various operating conditions of the hydraulic cylinder an analysis with respect to the occurrence of two undesired phenomena, excessive pressure build up and cavitation, is outlined. An understanding of when the two undesired phenomena occurs is accomplished, where cavitation could occur when the cylinder has a positive velocity, an overrunning load is applied and in the scenario where meter-in is present, meaning the inlet is restricted. The other scenario causing cavitation is when the cylinder has a negative velocity, a resistive load is applied and meter-in on the rod side is present which restricts the flow to the rod side chamber and therefore making the system unable to supply enough flow to the rod chambers, which could cause cavitation.

The phenomena when the excessive pressure build up becomes an undesired behaviour is in the scenarios where meter-out is present and could occur when the cylinder velocity is positive and an overrunning load is present and in the case where the velocity is negative and a resistive load is present. To overcome these undesired behaviours suitable control methods are discussed, which resulted in two chosen control strategies, one where the input signals were controlled independently to be able to both control the velocity and the pressure. Another control strategy is the slave mode function where one valve is dependent on the other valve and therefore the system only has one input. The slave function is limited to one system input and the possibility of separate control of the two proportional valves is neglected. The method of controlling the velocity and the pressure with two independently proportional valves was therefore further investigated.

The non-linear model was theoretical validated where the cylinder was positioned in the center of the cylinder and depending on the sign of the input signals the non-linear system is either seen to reach the top or the bottom of the cylinder. When the input signals are positive the piston moves to the top of the cylinder and it moves to the bottom when the input signals are negative. The damping of the non-linear model with the tested input signals were found to be in the range of  $\zeta = 0.17-0.33$ . The damping of the non-linear model is highly dependent on the input signals, which is caused by the orifice equation.

A linear state space representation of the non-linear model was conducted to be able to design controllers for the system. The linear model was validated against the non-linear model and some corrections regarding the bulk modulus of the oil were conducted to adjust the linear model. The natural frequency and the damping of the non-linear and the linear model was seen to be similar around the linearization point and minor deviation occurred when operating away from the linearization point as expected.

A coupling analysis of the linear state space model was investigated where the relative gain array analysis together with the singular value decomposition was conducted. The relative gain array is used to determine the coupling between the inputs and the outputs. The input-output coupling was tested where the velocity were the primarily control state and the secondary control state either was the piston pressure or the rod pressure. The operating condition were the cylinder position, load force, rod side pressure and the velocity was seen to have a significant impact on the coupling of the inputs and output. It can be concluded from the coupling analysis that the coupling between the velocity and the rod pressure is almost ideal and this control method of the system was thus further investigated with a control perspective.

To control the hydraulic system classical linear controllers were designed and implemented together with a dynamic pre-compensator in order to decouple the system and being able to consider the system as two single-input single-output systems. With one system output being the velocity and another the rod pressure. Two PI-controllers were designed and tested on the linear model and the non-linear model. When the controllers were tested on the non-linear model it showed a reduced velocity tracking performance when the velocity reference was negative. This indicated that the system parameters varied significantly and therefore it was required to tune the controllers when the velocity was negative. Two new controllers were then designed for when the velocity was negative. This was implemented in a control structure that switched between the different controllers depending on the velocity reference. The simulation with the switching controller gains on the non-linear model showed improvement for the velocity tracking.

It can hereby be concluded that implementing a decoupling pre-compensator for the separate meter-in separate meter-out system decouples the hydraulic system to be able to consider the system as two single-input single-output which with classical linear controllers achieves a satisfying performance for the velocity and rod pressure tracking. The control strategy of controlling the velocity with the input signal  $u_p$  together with the input signal  $u_r$  controlling the rod pressure under different operating conditions, velocity trajectory and varied load forces, is concluded to be a suitable control strategy for the separate meter-in separate meter-out setup.

## 6 | Further Work

This chapter includes aspects of further development of potential design strategies and improvements of the designed controller in this project for the separate meter-in separate meter-out control system.

### 6.1 Experimental Validation

The non-linear model in this project is theoretical validated and the aspect of validating the non-linear model against experimental data would give the opportunity to achieve an understanding of the static friction, viscous damping, percentage of air in the oil and possibly investigate if leakage flow is present, which could be used as fitting parameters in the non-linear model. An extended validation of the non-linear model would be taking into account when designing controllers for the system. The possibility of validating the designed controllers against experimental data would change the approach for designing the controller where controller stability and robustness with respect to system noise and uncertainties could be taking into account and a conservative design approach would be considered for the specific system.

### 6.2 Bumpless Switching

In the project two sets of controllers were designed, one for a positive and another for a negative velocity reference, and a switch deciding which set of controllers should be used depending on the velocity reference. This control structure showed that in between one set of controllers being active to the other set of controllers being active, when the sign of the velocity reference switches, the controller output in this instant changes suddenly and results in a undesired bump for the control signals. The method of avoiding the suddenly changing controller output when switching from one set of controller gains to another is by implementing Bumpless switching where the previous control output is given to the new controller and that the new controller output is reset. [Arehart and Wolovich, 1996] [Cheong and Safonov, 2008]

## 6.3 Gain Scheduling

To improve the performance for the system could be to implement gain scheduling. Gain scheduling is a control method of which the control parameters changes accordingly to the operating condition for the system. The concept is based on achieving the optimal gains at each operating condition which would be an improvement compared to the classical controllers that is designed in the linearization point. The gain scheduling method would for every operating condition find the transfer function and change the gains accordingly to improve the performance of the system.

# Bibliography

- Arehart and Wolovich, 1996.** Alan B. Arehart and William A. Wolovich. *Bumpless Switching Controllers*. page 2, 1996.
- Bin Yao, 2002.** Song Liu Bin Yao. *Energy-Saving Control of Hydraulic Systems with Novel Programmable Valves*. page 5, 2002.
- Bosch Rexroth Group.** Bosch Rexroth Group. *Cylinder Catalog*.  
<https://www.coastalhydraulics.net/technical-library/Cylinder%20Interchange%20information/Rexroth%20Cyl.pdf>, page 76, Downloaded: 18/8/2019.
- CHEN Guangrong, 2017.** WANG Shoukun ZHAO Jiangbo SHEN Wei CHEN Guangrong, WANG Junzheng. *The Separate Meter in Separate Meter Out Control System Using Dual Servo Valves Based on Indirect Adaptive Robust Dynamic Surface Control*. page 20, 2017.
- Cheong and Safonov, 2008.** Shin-Young Cheong and Michael G. Safonov. *Bumpless Transfer for Adaptive Switching Controls*. page 6, 2008.
- Control, 2014.** Flow Control. *Flowmeter Accuracy Matters*, 2014.  
<https://www.flowcontrolnetwork.com/flowmeter-accuracy-matters/>,  
Downloaded: 20/8/2019.
- Daniel Brusen Nielsen, 2016.** Rasmus Lykke Lomholt Danjal Torgarg Alejandro Alonso García Daniel Brusen Nielsen, Kirsten Arnoldsen Juhl. *Hydraulic Impact Testing Machine*. page 154, 2016.
- Henrik C. Pedersen, 2013.** Tobias Skouboe Morten S. Jacobsen Henrik C. Pedersen, Torben O. Andersen. *Investigation and Comparison of Separate Meter-In Seperate Meter-Out Control Strategies*. page 10, 2013.
- Henrik C. Pedersen, 2015.** Torben O. Andersen Morten H. Brask Henrik C. Pedersen, Lasse Schmidt. *Investigation of New Servo Drive Concept Utilizing Two Fixed Displacement Units*. Servo Drive, Analysis, Efficiency, Simulation, Experimental, page 8, 2015.
- Kim Heybroek, 2008.** Jan-Ove Palmberg Kim Heybroek. *Applied Control Strategies for a Pump Controlled Open Circuit Solution*. page 14, 2008.
- MOOG, 2009.** MOOG. *Servoables - Direct Drive Servovalves D633/D634*, 2009.
- Nielsen, 2005.** Brian Nielsen. *Controller Development for a Separate Meter-In Separate Meter-Out Fluid Power Valve for Mobile Applications*. page 254, 2005.

**Skogestad and Postlethwaite, 2005.** S. Skogestad and I. Postlethwaite. *Multivariable Feedback Control - - Analysis and design*. JOHN WILEY and SONS, 2005.

**Yingjie Liu and Zeng, 2002.** Huayong Yang Yingjie Liu, Bing Xu and Dingrong Zeng. *Energy-Saving Control of Single-Rod Hydraulic Cylinders with Programmable Valves and Improved Working Mode Selection*. page 11, 2002.

**Yingjie Liu and Zeng, 2009.** Huayong Yang Yingjie Liu, Bing Xu and Dingrong Zeng. *Modeling of Separate Meter In and Separate Meter Out Control System*. page 6, 2009.

# A | Steady State Load Force Scenarios

In this appendix the two control strategies is investigated regarding a load force scenario. The idea is to, in steady state, calculate the input signals for the valves, when a load force is present, in order to remain the desired piston velocity and the chamber pressure. This is done in order to achieve an overview of how the system is to be controlled and the behaviour of the system when a load force is applied.

## Pressure & Velocity Control

To achieve steady state condition in the case where a load force is applied while keeping the rod pressure on 20 *bar* and the velocity of 0.2 *m/s* is utilized by changing the signal input for the piston side valve. When no load force is applied to the cylinder the rod pressure is 20 *bar* and the piston pressure is 9.8 *bar* when the valve positions is  $u_p = 0.39$  and  $u_r = 0.62$ . The effect of applying a load force of example 6500 *N* and maintaining the rod pressure and the velocity will result in a change of the input signal  $u_p$ . The piston side pressure with the load force is calculated as:

$$p_p = \frac{A_r p_r + F_L}{A_p} = \frac{0.0015 \text{ m}^2 \cdot 20 \text{ bar} + 6500 \text{ N}}{0.0031 \text{ m}^2} = 30.65 \text{ bar} \quad (\text{A.1})$$

In order to achieve a piston side pressure of 30 *bar* it is required to change the input signal  $u_p$ . The input signal with load force applied is calculated as:

$$u_p = \frac{Q_p}{\sqrt{\left| \frac{p_s - p_p}{p_N} \right|} Q_N} = \frac{37.40 \text{ l/min}}{\sqrt{\left| \frac{210 \text{ bar} - 30.65 \text{ bar}}{35 \text{ bar}} \right|} \cdot 40 \text{ l/min}} = 0.4130 \quad (\text{A.2})$$

The input signal for  $u_p$  is calculated to be 0.41 when the load force is applied. In order to validate the statement of maintaining the rod pressure of 20 *bar* and a velocity of 0.2 *m/s* a simulation is conducted where the simulation is without load force from 0-1 seconds and from 1-3 seconds the load force of 6500 *N* is applied together with a change in the input signal  $u_p$ . In the first 0-1 seconds the input signal is  $u_p = 0.39$  and the piston side pressure is 9.8 *bar*. From 1-3 seconds the load force of 6500 *N* is applied and the input signal  $u_p$  is change to 0.41 together with the piston side pressure being adjusted to 30 *bar*.

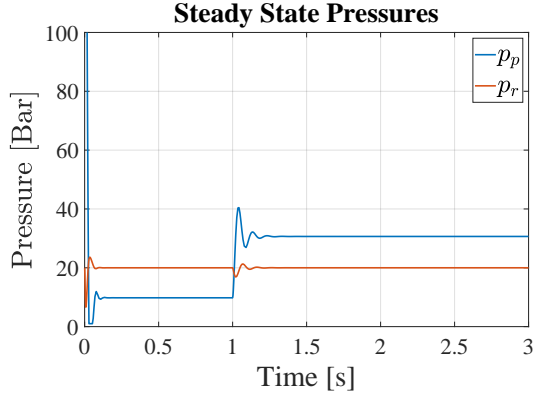


Figure A.1: Piston and rod chamber pressures.

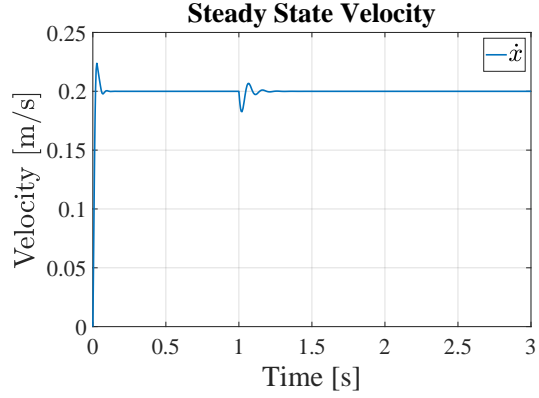


Figure A.2: Velocity of the piston.

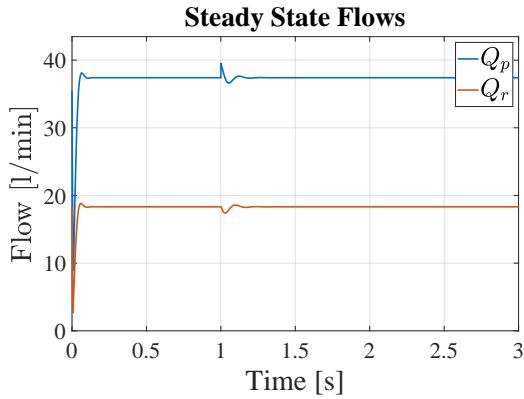


Figure A.3: Piston and rod side flows.

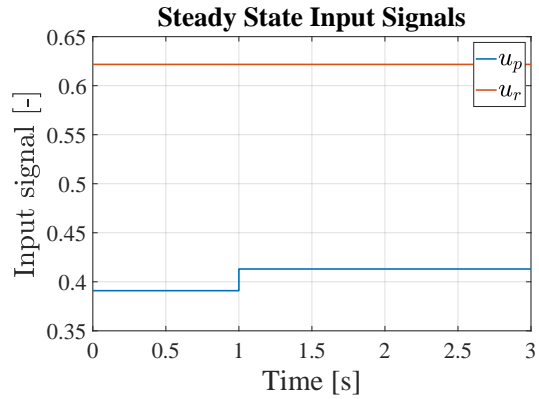


Figure A.4: Input signals for the two valves.

As the focus is on the steady state response when a load force is applied, the transient phase is disregarded. The focus is to illustrate the effect on the system in steady state when a load force is applied. In Figure A.1 the pressure is illustrated where the rod pressure is kept to be 20 *bar* while the piston side pressure without the load force of 6500 N applied is 9.8 *bar* and when the load force is applied the piston side pressure increases to 30 *bar* as calculated in Equation A.1. In Figure A.2 the velocity is illustrated and kept at 0.2 *m/s* with and without load force applied. In the figure the velocity oscillates when the load force is applied and the input signal  $u_p$  is stepped up which is due to the transient phase of the flows seen in Figure A.3 by the flow spikes.

## Velocity Control in Slave Function

In the scenario where a load force of 6500 *N* is applied the piston side pressure is calculated to be 83.37 *bar* and the rod side pressure is calculated to be 127.62 *bar*. When the piston pressure is calculated the input signal  $u_p$  is calculated as:

$$u_p = \frac{37.40 \text{ l/min}}{40 \text{ l/min} \sqrt{\left| \frac{210 \text{ bar} - 83.37 \text{ bar}}{35 \text{ bar}} \right|}} = 0.4915 \quad (\text{A.3})$$

To maintain the velocity of  $0.2 \text{ m/s}$  when a load force of  $6500 \text{ N}$  is applied it is required that the input signal  $u_p$  is  $0.49$ . To validate the statement of not being able to control the chamber pressures while focusing on controlling the velocity a simulation is conducted similar to the previous load force scenario where the no load scenario is present from 0-1 second and from 1-3 seconds the load force scenario is applied together with a change in the input signal  $u_p$ . In the no load scenario the input signal  $u_p$  is calculated to be  $0.47$  with the pressures  $p_p = 69.38 \text{ bar}$  and  $p_r = 141.62 \text{ bar}$ , but in the load force scenario the input signal  $u_p$  is changed to  $0.49$  in order to maintain the velocity of  $0.2 \text{ m/s}$  and the pressures changes to  $p_p = 83.37 \text{ bar}$  and  $p_r = 127.62 \text{ bar}$ . This simulation is illustrated in the figures below where the pressures, velocity, flows and input signals is presented.

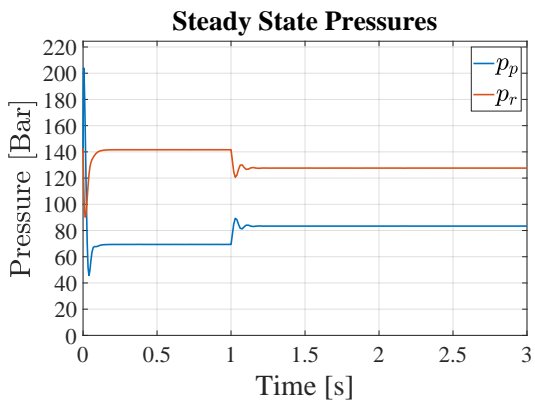


Figure A.5: Piston and rod chamber pressures.

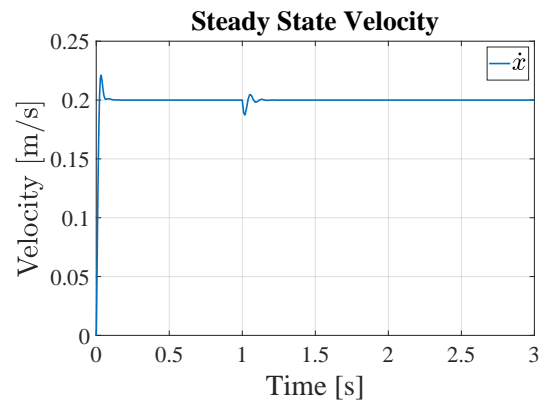


Figure A.6: Velocity of the piston.

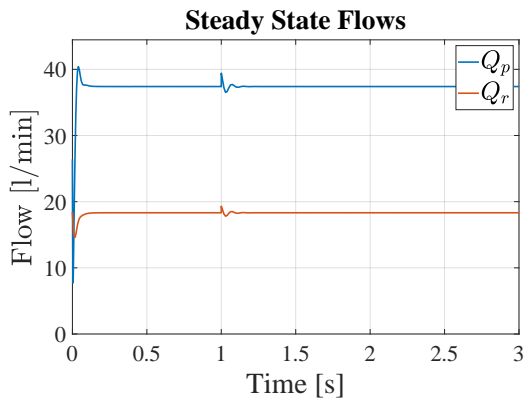


Figure A.7: Piston and rod side flows.

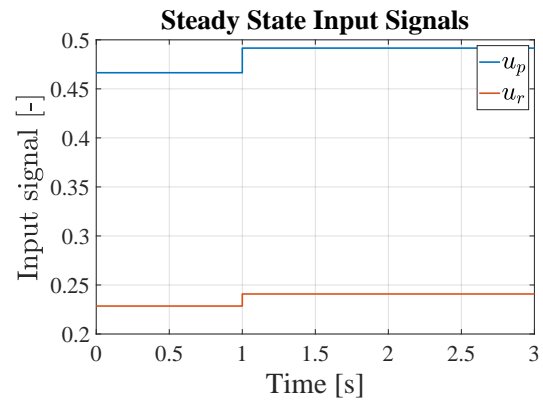


Figure A.8: Input signals for the two valves.

In this simulation the transient phase is not the focus. The focus is to illustrate the effect on the system in steady state when a load force is applied. In Figure A.6 it is seen that the velocity of  $0.2 \text{ m/s}$  is kept even when the load force is applied. To compensate for the load force and maintain the desired velocity the input signal  $u_p$  is changed from  $0.47$  to  $0.49$  which is seen in Figure A.8. The effect of not being able to control the pressures is seen in Figure A.5 where both the piston and rod side pressures changes simultaneously when the load force is applied. This is the limitation when operating in a slave mode and trying to control the velocity.



## B | System Design

The data for the system used for the steady state analysis is the two identically proportional valves which are the MOOG D633 valve with a rated flow of 40 *l/min* and a rated pressure of 35 *bar* MOOG [2009]. For the system in steady state it is desired that at rated flow of 40 *l/min* the piston velocity should be around 0.2 *m/s*. This is achieved by calculating the required piston side area.

$$A_p = \frac{Q_N}{\dot{x}} = \frac{40 \text{ l/min}}{0.2 \text{ m/s}} \approx 33 \text{ cm}^2 \quad (\text{B.1})$$

The piston area for the cylinder is calculated to be 33 *cm*<sup>2</sup>, which correspond to a diameter of  $\approx \text{Ø}65\text{mm}$ . The cylinder used for this analysis is found in the data sheet from Bosch Rexroth Cylinder Data Log with the specification closest to the required specification calculated in Equation B.1. The cylinder selected has a piston area of 31.17 *cm*<sup>2</sup> with a diameter of  $\text{Ø}63\text{mm}$ , which is reasonable close to the calculated diameter of  $\text{Ø}65$  required. The rod side area of the cylinder is 15.27 *cm*<sup>2</sup> with a diameter of  $\text{Ø}44$ , which results in an area ratio of 0.49. The maximum stroke length of the cylinder is  $L_{stroke} = 305 \text{ mm}$ . [Bosch Rexroth Group] The initial volumes in the chambers is calculated by applying the initial position for the piston as  $x_0 = 0$ , meaning that the piston is located all the way to the left in Figure C.16. This results in  $V_{p0}$  being at its minimum volume and  $V_{r0}$  being at its maximum volume. It is assumed that some volume is present in the hose and connections and is assumed to be 0.2 *l* for both sides. The initial volumes is calculated by:

$$V_{p0} = 0.2 \text{ l} + A_p x_0 \quad (\text{B.2})$$

$$V_{r0} = 0.2 \text{ l} + A_r(L_{stroke} - x_0) \quad (\text{B.3})$$

The initial volumes when the piston is at  $x_0 = 0$  are calculated to be  $V_{p0} = 0.2 \text{ l}$  and  $V_{r0} = 0.67 \text{ l}$ .

For the mechanical system the mass for the system is to be determined. In the scenario where the mass is acting vertically on the piston it applies the maximum gravitational force on the piston. In this scenario it is desired to have a working pressure on the piston side of  $p_{work} = 140 \text{ bar}$  when no back pressure is present. It is then possible to calculate the desired mass for the system.

$$M = \frac{p_{work} A_p}{g} = \frac{140 \text{ bar} \cdot 0.0033 \text{ m}^2}{9.82 \frac{\text{m}}{\text{s}^2}} = 4444 \text{ kg} \quad (\text{B.4})$$

When the working pressure is set to 140 *bar* with a piston area of  $\text{Ø}63\text{mm}$ , the mass is calculate to be 4444 *kg* in order to achieve force balance. To be in the range of 120-140 *bar* for the working pressure the mass is set to 4000 *kg*.

The supply pressure for the system is set to 210 *bar* which is determined by the working pressure that is 2/3 of the supply pressure. The tank pressure is assumed to be at atmospheric pressure with approximately  $p_t = 1 \text{ bar}$ . All the specifications is listed in Table B.1.

Cylinder	$\text{Ø}63/\text{Ø}44/305 \text{ mm}$ $A_p = 0.0031 \text{ m}^2, A_r = 0.0015 \text{ m}^2, \alpha = 0.49$
Valves	MOOG D633 $Q_N = 40 \text{ l/min}, P_N = 35 \text{ bar}$
Mechanical system	$M = 4000 \text{ kg}$
Volumes	$V_{p,0} = 0.2 \text{ l}, V_{r,0} = 0.67 \text{ l}$
Pressures	$P_s = 210 \text{ bar}, P_t = 1 \text{ bar}$

**Table B.1:** Data for the system to be analyzed.

## C | RGA Analysis

The relatively gain array analysis is conducted to investigate the input-output pairing for the system. To conduct the RGA analysis the linearization constants for the system plant needs to be calculated. The linearization constants are based on the velocity  $\dot{x}$ , the load force  $F_L$ , the rod side pressure  $p_{r0}$  and the cylinder position  $x_0$ . With these constants it is possible to calculate the piston pressure  $p_{p0}$ , opening of the proportional valves  $u_{p0}$  and  $u_{r0}$ , the constant volumes  $V_{p0}$  and  $V_{r0}$  and lastly the linearization constants used in the state space representation is calculated and the derived linearization constants is seen below.

$$K_{qu_p} = \left. \frac{\partial Q_p}{\partial u_p} \right|_{p_{p0}} = Q_N \sqrt{\frac{p_s - p_{p0}}{p_N}} \quad (C.1)$$

$$K_{qp_p} = \left. \frac{\partial Q_p}{\partial p_p} \right|_{u_{p0}} = -Q_N u_{p0} \frac{1}{2p_N \sqrt{\frac{p_s - p_{p0}}{p_N}}} \quad (C.2)$$

$$K_{qu_r} = \left. \frac{\partial Q_r}{\partial u_r} \right|_{p_{r0}} = Q_N \sqrt{\frac{p_{r0} - p_t}{p_N}} \quad (C.3)$$

$$K_{qp_r} = \left. \frac{\partial Q_r}{\partial p_r} \right|_{u_{r0}} = Q_N u_{r0} \frac{1}{2p_N \sqrt{\frac{p_{r0} - p_t}{p_N}}} \quad (C.4)$$

## C Matrix Controlling $p_p$

$$\left. \begin{array}{l} \dot{x}_0 = 0.1 \text{ m/s} \\ F_{L,0} = 0 \text{ kN} \\ p_{r,0} = 10 \text{ bar} \\ x_0 = 0 \text{ m} \end{array} \right\} \begin{cases} p_{p,0} = 4.9 \text{ bar} \\ u_{p,0} = 0.1932 \\ u_{r,0} = 0.4517 \\ K_{qu_p} = 1.61 \cdot 10^{-3} \\ K_{qp_p} = 7.60 \cdot 10^{-12} \\ K_{qu_r} = 3.38 \cdot 10^{-4} \\ K_{qp_r} = 8.48 \cdot 10^{-11} \\ V_{p,0} = 0.2 \text{ l} \\ V_{r,0} = 0.67 \text{ l} \end{cases} \quad (\text{C.5})$$

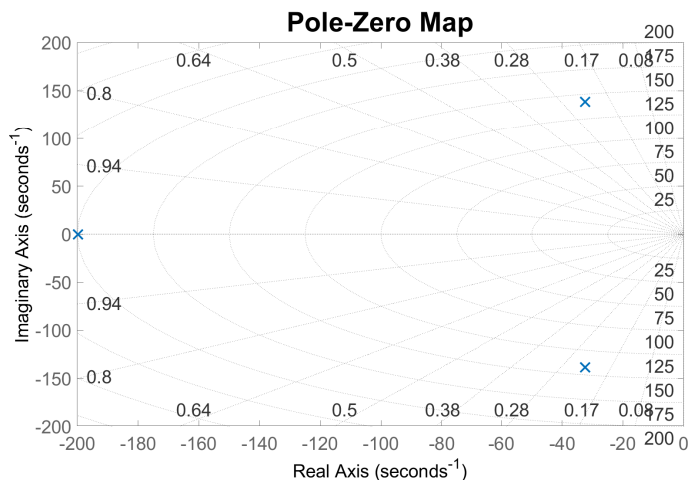


Figure C.1: Eigenvalues:  $-199.76, -32.44 \pm j138.59$ .

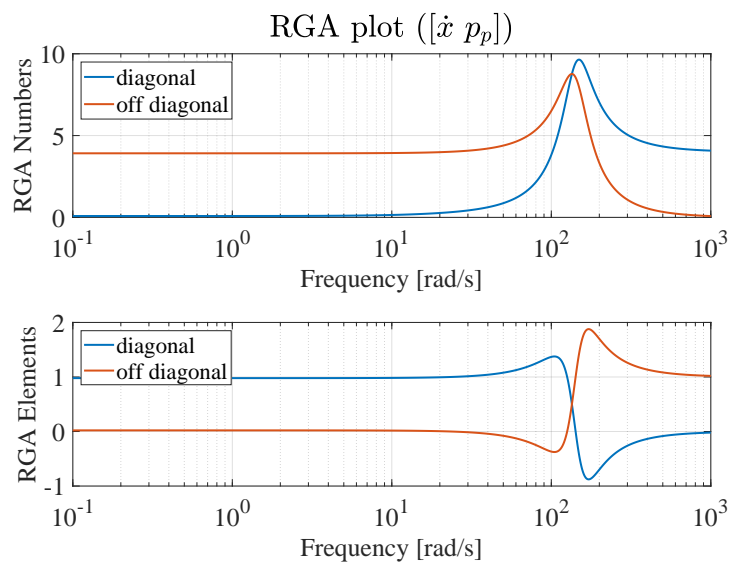
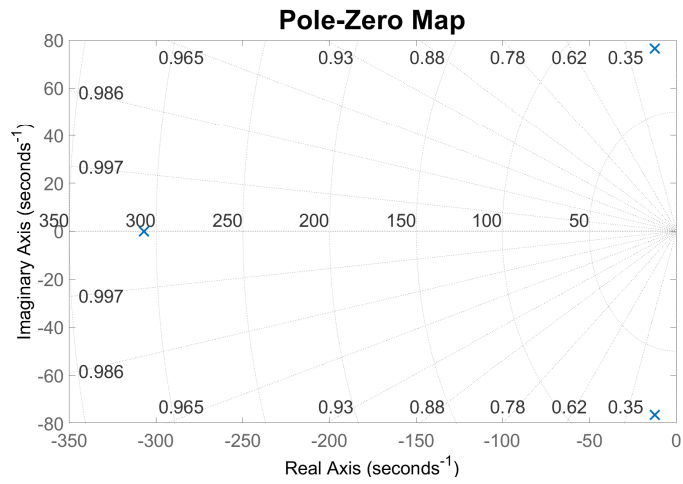
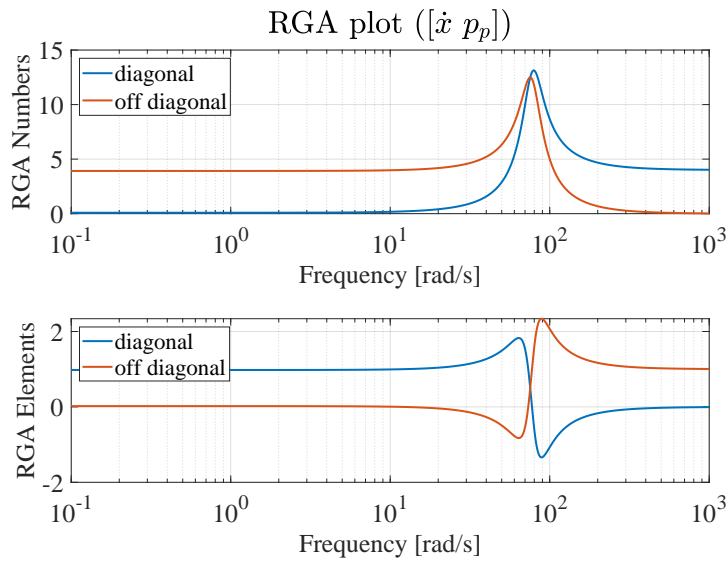


Figure C.2: RGA analysis.

$$\left. \begin{array}{l} \dot{x}_0 = 0.1 \text{ m/s} \\ F_{L,0} = 0 \text{ kN} \\ p_{r,0} = 10 \text{ bar} \\ x_0 = L_{stroke}/2 = 0.1525 \text{ m} \end{array} \right\} \begin{array}{l} p_{p,0} = 4.9 \text{ bar} \\ u_{p,0} = 0.1932 \\ u_{r,0} = 0.4517 \\ K_{qu_p} = 1.61 \cdot 10^{-3} \\ K_{qp_p} = 7.60 \cdot 10^{-12} \\ K_{qu_r} = 3.38 \cdot 10^{-4} \\ K_{qp_r} = 8.48 \cdot 10^{-11} \\ V_{p,0} = 0.67 \text{ l} \\ V_{r,0} = 0.43 \text{ l} \end{array} \quad (\text{C.6})$$



**Figure C.3:** Eigenvalues:  $-306.98, -12.28 \pm j76.50$ .



**Figure C.4:** RGA analysis.

$$\left. \begin{array}{l} \dot{x}_0 = 0.1 \text{ m/s} \\ F_{L,0} = 0 \text{ kN} \\ p_{r,0} = 10 \text{ bar} \\ x_0 = L_{stroke} = 0.305 \text{ m} \end{array} \right\} \begin{cases} p_{p,0} = 4.9 \text{ bar} \\ u_{p,0} = 0.1932 \\ u_{r,0} = 0.4517 \\ K_{qu_p} = 1.61 \cdot 10^{-3} \\ K_{qp_p} = 7.60 \cdot 10^{-12} \\ K_{qu_r} = 3.38 \cdot 10^{-4} \\ K_{qp_r} = 8.48 \cdot 10^{-11} \\ V_{p,0} = 1.15 \text{ l} \\ V_{r,0} = 0.2 \text{ l} \end{cases} \quad (C.7)$$

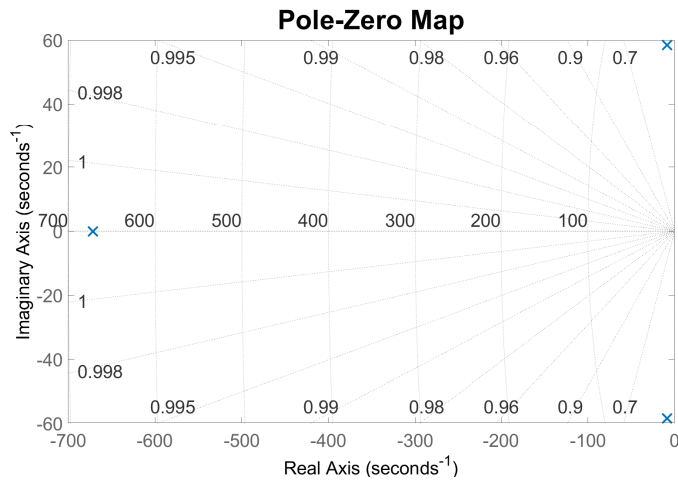


Figure C.5: Eigenvalues:  $-671.83, -8.71 \pm j58.39$ .

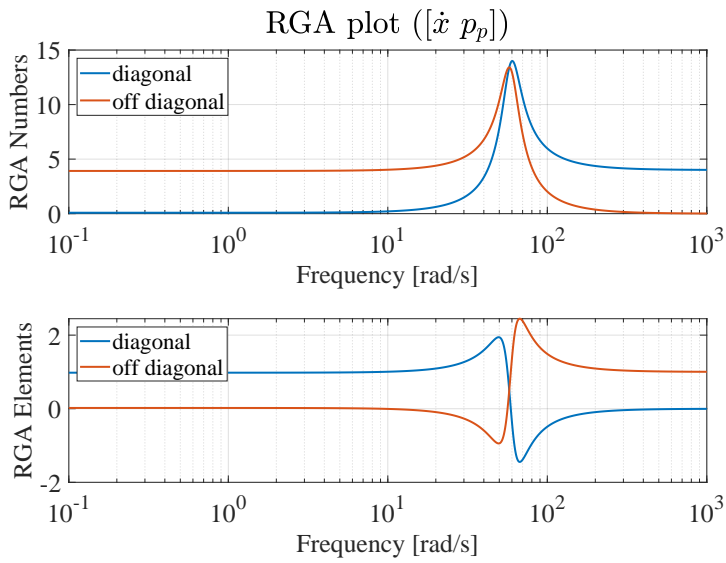
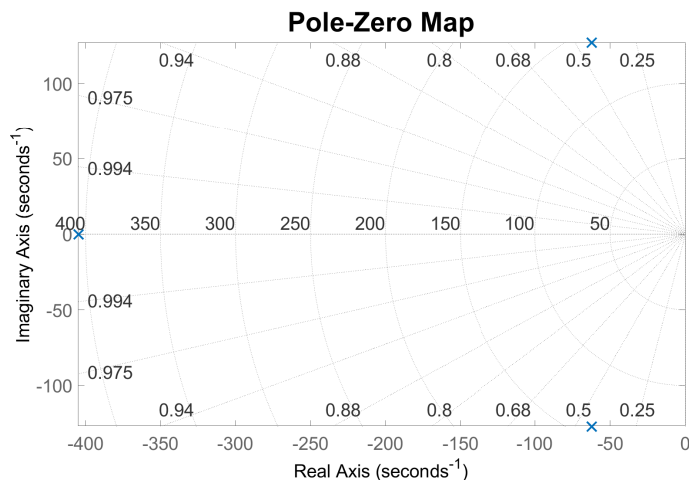


Figure C.6: RGA analysis.

## Initial Velocity Change

$$\left. \begin{array}{l} \dot{x}_0 = 0.2 \text{ m/s} \\ F_{L,0} = 0 \text{ kN} \\ p_{r,0} = 10 \text{ bar} \\ x_0 = 0 \text{ m} \end{array} \right\} \left\{ \begin{array}{l} p_{p,0} = 4.9 \text{ bar} \\ u_{p,0} = 0.3863 \\ u_{r,0} = 0.9035 \\ K_{qup} = 1.61 \cdot 10^{-3} \\ K_{qpp} = 1.52 \cdot 10^{-11} \\ K_{qu_r} = 3.38 \cdot 10^{-4} \\ K_{qpr} = 1.70 \cdot 10^{-10} \\ V_{p,0} = 0.2 \text{ l} \\ V_{r,0} = 0.67 \text{ l} \end{array} \right. \quad (\text{C.8})$$



**Figure C.7:** Eigenvalues:  $-404.82, -62.26 \pm j126.95$ .

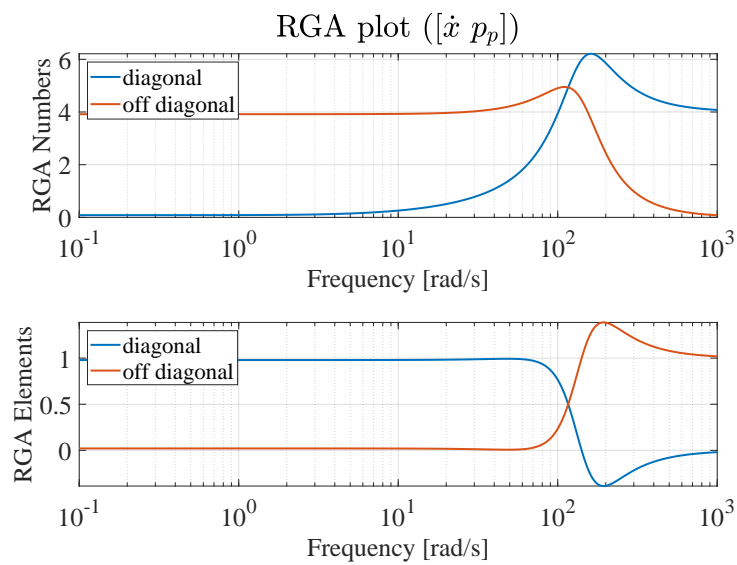


**Figure C.8:** RGA analysis.

$$\left. \begin{array}{l}
 \dot{x}_0 = 0.2 \text{ m/s} \\
 F_{L,0} = 0 \text{ kN} \\
 p_{r,0} = 10 \text{ bar} \\
 x_0 = L_{stroke}/2 = 0.1525 \text{ m}
 \end{array} \right\} \begin{array}{l}
 p_{p,0} = 4.9 \text{ bar} \\
 u_{p,0} = 0.3863 \\
 u_{r,0} = 0.9035 \\
 K_{qu_p} = 1.61 \cdot 10^{-3} \\
 K_{qp_p} = 1.52 \cdot 10^{-11} \\
 K_{qu_r} = 3.38 \cdot 10^{-4} \\
 K_{qp_r} = 1.70 \cdot 10^{-10} \\
 V_{p,0} = 0.67 \text{ l} \\
 V_{r,0} = 0.43 \text{ l}
 \end{array} \quad (C.9)$$

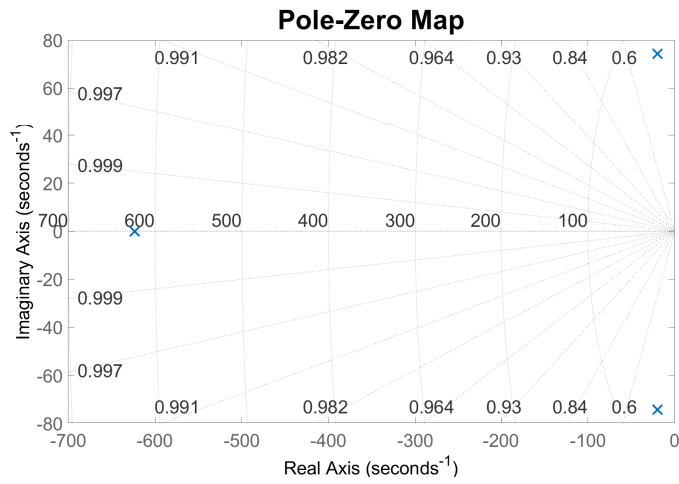


Figure C.9: Eigenvalues:  $-623.76, -19.69 \pm j74.31$ .

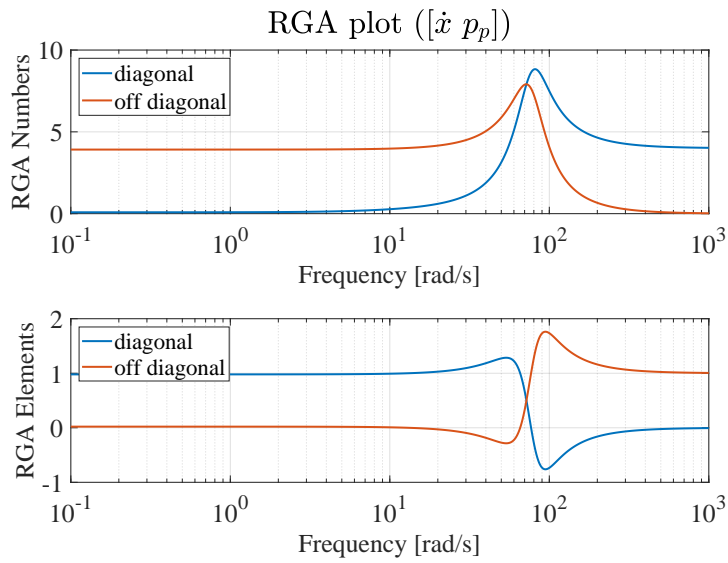


Figure C.10: RGA analysis.

$$\left. \begin{array}{l} \dot{x}_0 = 0.2 \text{ m/s} \\ F_{L,0} = 0 \text{ kN} \\ p_{r,0} = 10 \text{ bar} \\ x_0 = L_{stroke} = 0.305 \text{ m} \end{array} \right\} \left\{ \begin{array}{l} p_{p,0} = 4.9 \text{ bar} \\ u_{p,0} = 0.3863 \\ u_{r,0} = 0.9035 \\ K_{qup} = 1.61 \cdot 10^{-3} \\ K_{qp_p} = 1.52 \cdot 10^{-11} \\ K_{qu_r} = 3.38 \cdot 10^{-4} \\ K_{qp_r} = 1.70 \cdot 10^{-10} \\ V_{p,0} = 1.15 \text{ l} \\ V_{r,0} = 0.2 \text{ l} \end{array} \right. \quad (C.10)$$

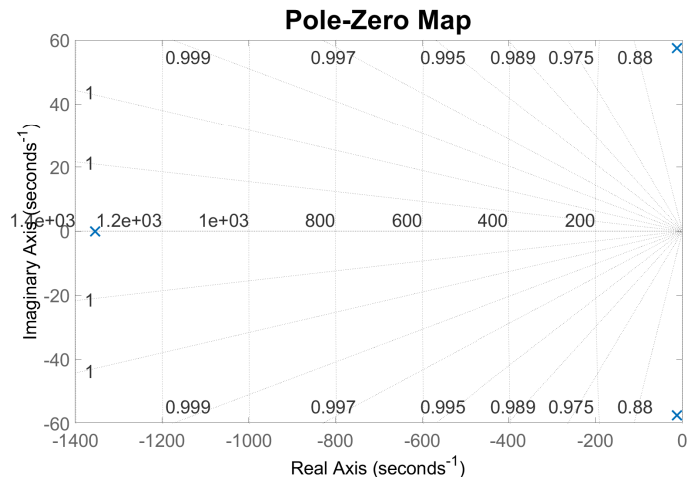


Figure C.11: Eigenvalues:  $-1354, -12.27 \pm j57.51$ .

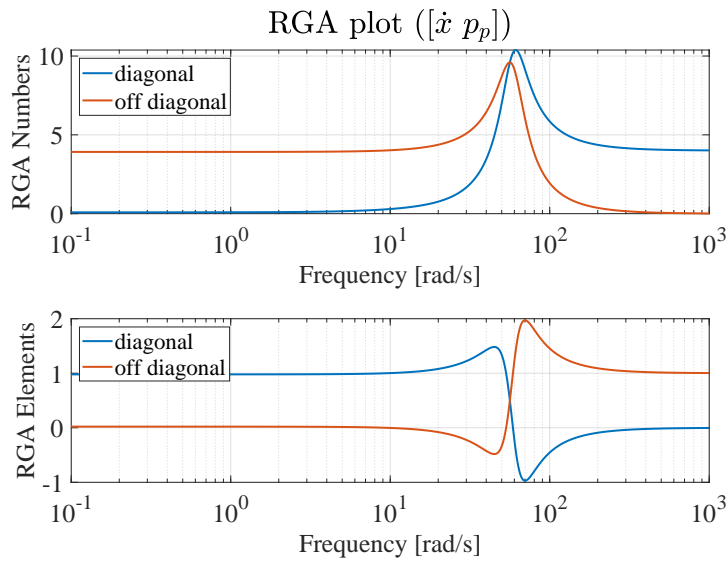
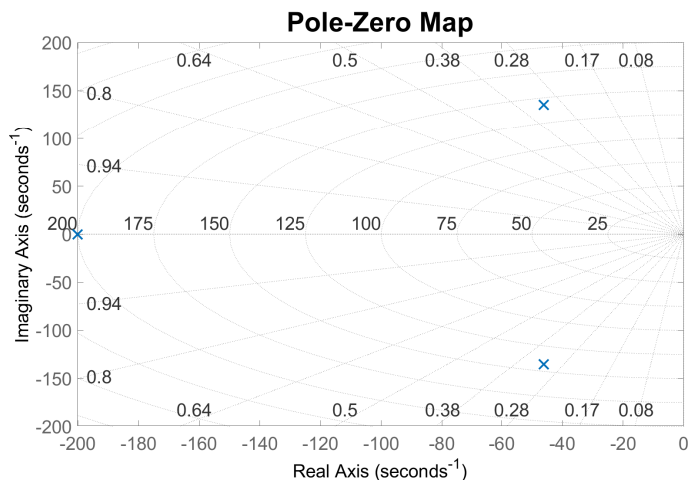


Figure C.12: RGA analysis.

## Load Force Change

$$\left. \begin{array}{l} \dot{x}_0 = 0.1 \text{ m/s} \\ F_{L,0} = 20 \text{ kN} \\ p_{r,0} = 10 \text{ bar} \\ x_0 = 0 \text{ m} \end{array} \right\} \begin{cases} p_{p,0} = 69 \text{ bar} \\ u_{p,0} = 0.2330 \\ u_{r,0} = 0.4517 \\ K_{qu_p} = 1.33 \cdot 10^{-3} \\ K_{qp_p} = 1.10 \cdot 10^{-11} \\ K_{qu_r} = 3.38 \cdot 10^{-4} \\ K_{qp_r} = 8.48 \cdot 10^{-11} \\ V_{p,0} = 0.2 \text{ l} \\ V_{r,0} = 0.67 \text{ l} \end{cases} \quad (\text{C.11})$$



**Figure C.13:** Eigenvalues:  $-200.14, -46.09 \pm j135.24$ .

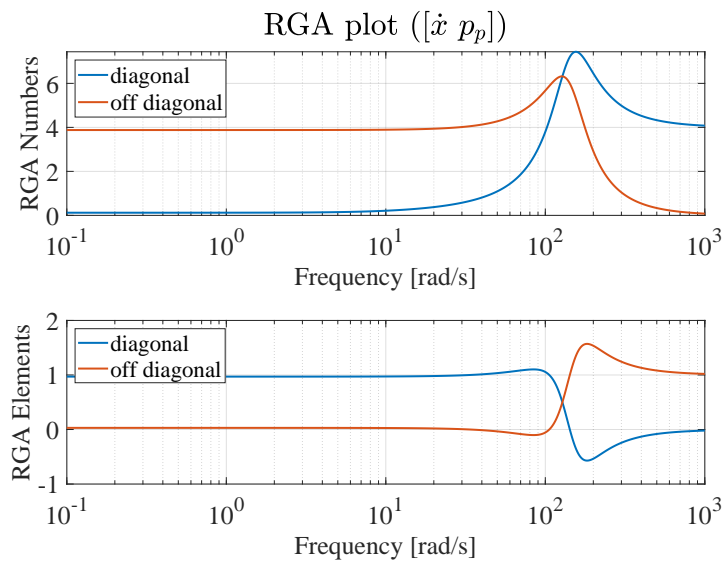


**Figure C.14:** RGA analysis.

$$\left. \begin{array}{l}
 \dot{x}_0 = 0.1 \text{ m/s} \\
 F_{L,0} = 20 \text{ kN} \\
 p_{r,0} = 10 \text{ bar} \\
 x_0 = L_{stroke}/2 = 0.1525 \text{ m}
 \end{array} \right\} \begin{array}{l}
 p_{p,0} = 69 \text{ bar} \\
 u_{p,0} = 0.2330 \\
 u_{r,0} = 0.4517 \\
 K_{qu_p} = 1.33 \cdot 10^{-3} \\
 K_{qp_p} = 1.10 \cdot 10^{-11} \\
 K_{qu_r} = 3.38 \cdot 10^{-4} \\
 K_{qp_r} = 8.48 \cdot 10^{-11} \\
 V_{p,0} = 0.67 \text{ l} \\
 V_{r,0} = 0.43 \text{ l}
 \end{array} \quad (C.12)$$

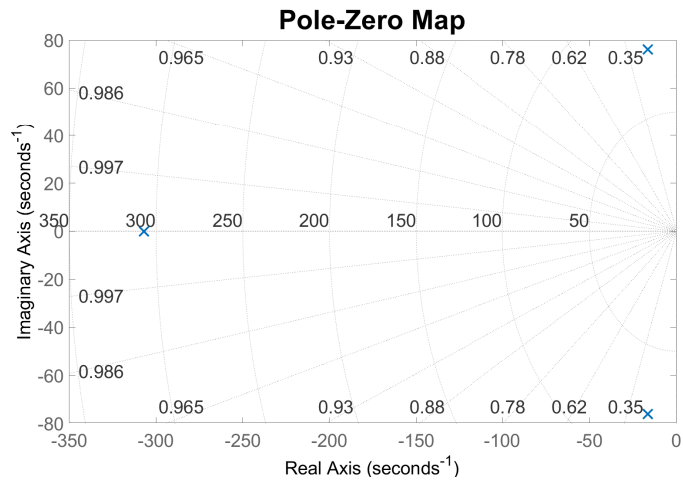


**Figure C.15:** Eigenvalues:  $-307.00, -16.37 \pm j76.11$ .

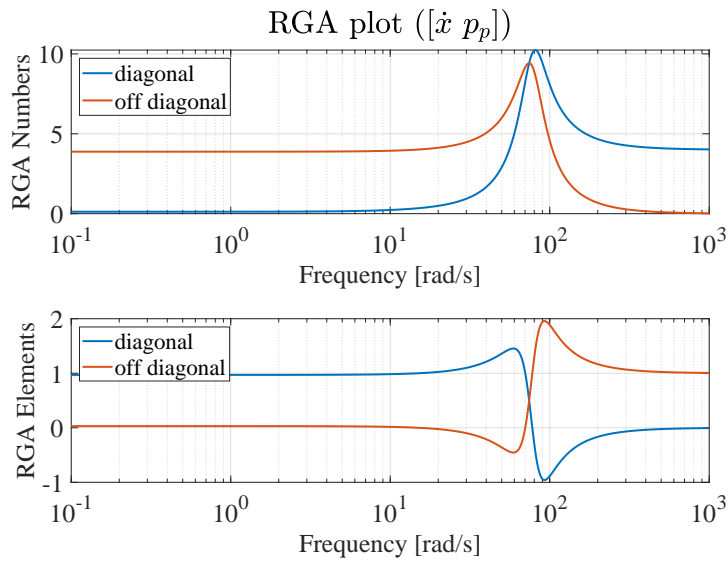


**Figure C.16:** RGA analysis.

$$\left. \begin{array}{l}
 \dot{x}_0 = 0.1 \text{ m/s} \\
 F_{L,0} = 20 \text{ kN} \\
 p_{r,0} = 10 \text{ bar} \\
 x_0 = L_{stroke} = 0.305 \text{ m}
 \end{array} \right\} \begin{cases}
 p_{p,0} = 69 \text{ bar} \\
 u_{p,0} = 0.2330 \\
 u_{r,0} = 0.4517 \\
 K_{qu_p} = 1.33 \cdot 10^{-3} \\
 K_{qp_p} = 1.10 \cdot 10^{-11} \\
 K_{qu_r} = 3.38 \cdot 10^{-4} \\
 K_{qp_r} = 8.48 \cdot 10^{-11} \\
 V_{p,0} = 1.15 \text{ l} \\
 V_{r,0} = 0.2 \text{ l}
 \end{cases} \quad (\text{C.13})$$

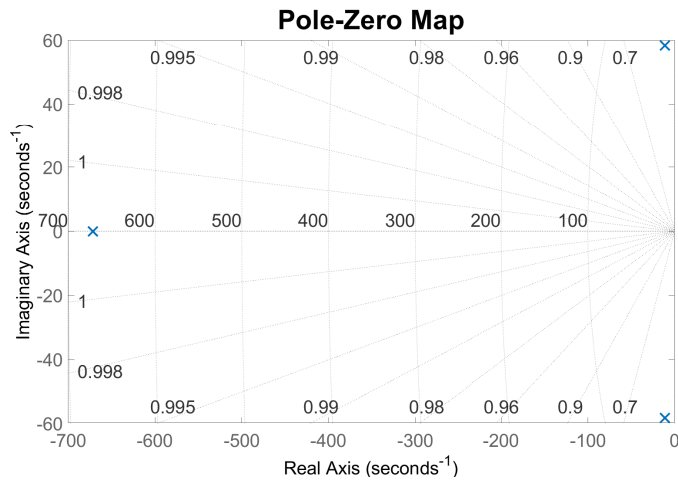


Figure C.17: Eigenvalues:  $-671.83, -11.12 \pm j58.26$ .

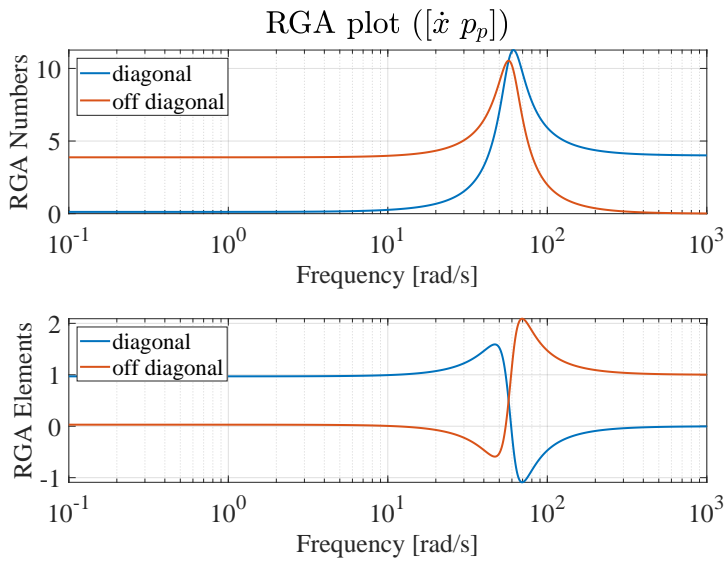


Figure C.18: RGA analysis.

No Load Force,  $p_r = 20$  bar

$$\left. \begin{array}{l} \dot{x}_0 = 0.1 \text{ m/s} \\ F_{L,0} = 0 \text{ kN} \\ p_{r,0} = 20 \text{ bar} \\ x_0 = 0 \text{ m} \end{array} \right\} \left\{ \begin{array}{l} p_{p,0} = 9.8 \text{ bar} \\ u_{p,0} = 0.1955 \\ u_{r,0} = 0.3109 \\ K_{qup} = 1.59 \cdot 10^{-3} \\ K_{qp_p} = 7.78 \cdot 10^{-12} \\ K_{qu_r} = 4.91 \cdot 10^{-4} \\ K_{qp_r} = 4.02 \cdot 10^{-11} \\ V_{p,0} = 0.2 \text{ l} \\ V_{r,0} = 0.67 \text{ l} \end{array} \right. \quad (\text{C.14})$$

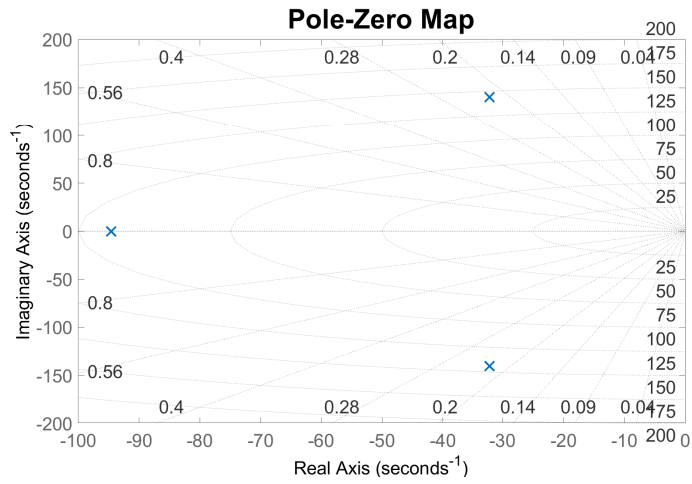


Figure C.19: Eigenvalues:  $-94.56, -32.13 \pm j140.48$ .

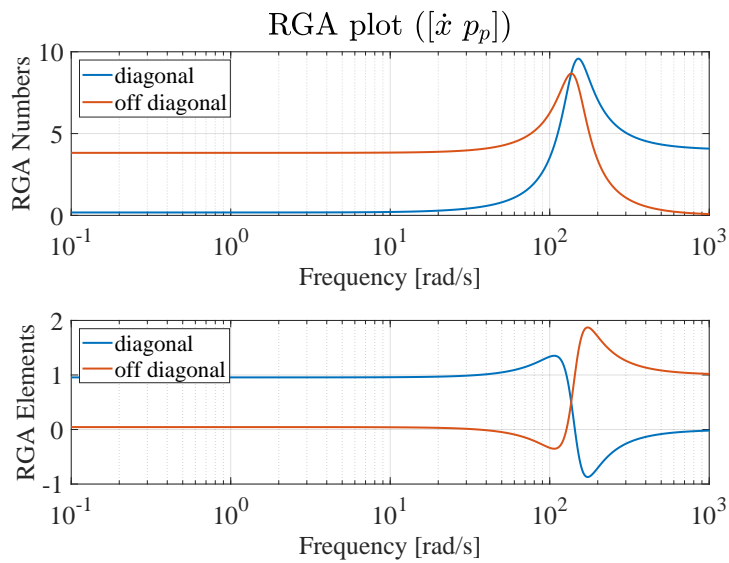


Figure C.20: RGA analysis.

$$\left. \begin{array}{l}
 \dot{x}_0 = 0.1 \text{ m/s} \\
 F_{L,0} = 0 \text{ kN} \\
 p_{r,0} = 20 \text{ bar} \\
 x_0 = L_{stroke}/2 = 0.1525 \text{ m}
 \end{array} \right\} \begin{array}{l}
 p_{p,0} = 9.8 \text{ bar} \\
 u_{p,0} = 0.1955 \\
 u_{r,0} = 0.3109 \\
 K_{qu_p} = 1.59 \cdot 10^{-3} \\
 K_{qp_p} = 7.78 \cdot 10^{-12} \\
 K_{qu_r} = 4.91 \cdot 10^{-4} \\
 K_{qp_r} = 4.02 \cdot 10^{-11} \\
 V_{p,0} = 0.67 \text{ l} \\
 V_{r,0} = 0.43 \text{ l}
 \end{array} \quad (C.15)$$

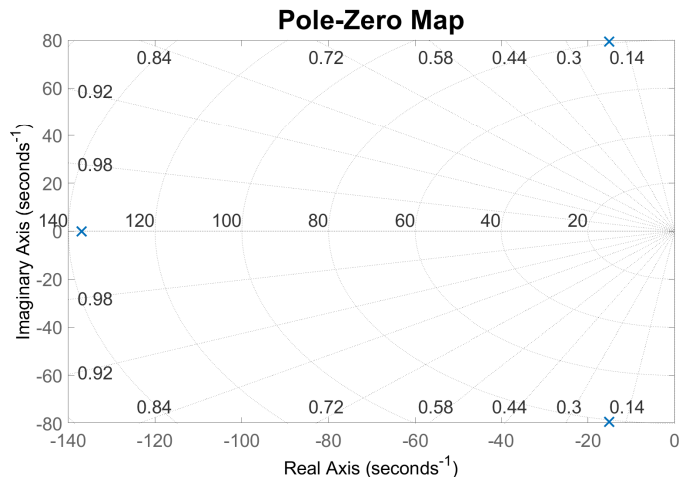


Figure C.21: Eigenvalues: -136.92, -15.01 ± j79.42.

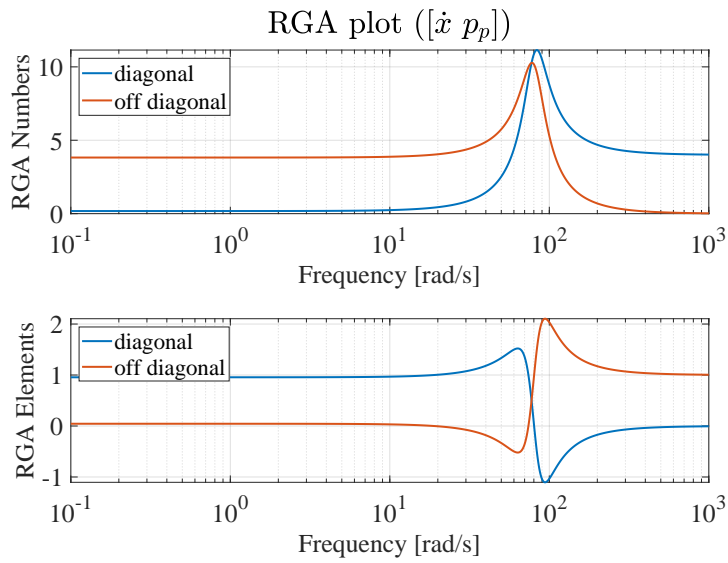
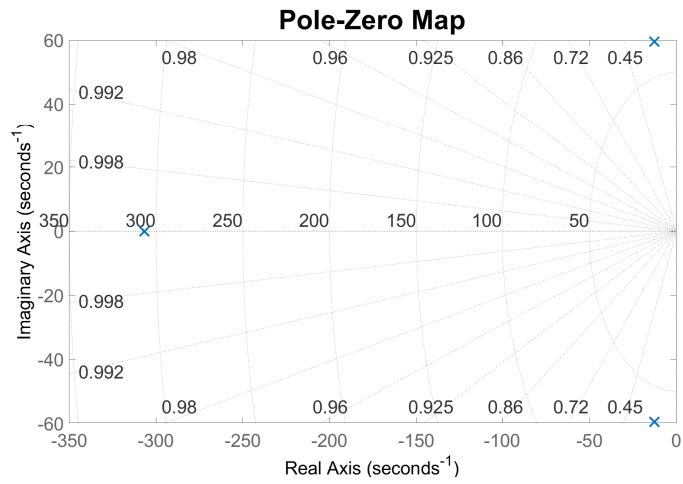
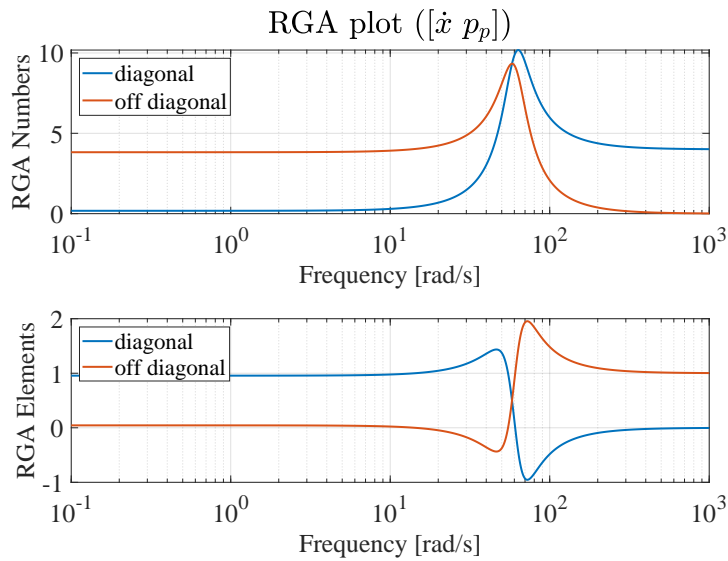


Figure C.22: RGA analysis.

$$\left. \begin{array}{l} \dot{x}_0 = 0.1 \text{ m/s} \\ F_{L,0} = 0 \text{ kN} \\ p_{r,0} = 20 \text{ bar} \\ x_0 = L_{stroke} = 0.305 \text{ m} \end{array} \right\} \left\{ \begin{array}{l} p_{p,0} = 9.8 \text{ bar} \\ u_{p,0} = 0.1955 \\ u_{r,0} = 0.3109 \\ K_{qup} = 1.59 \cdot 10^{-3} \\ K_{qp_p} = 7.78 \cdot 10^{-12} \\ K_{qu_r} = 4.91 \cdot 10^{-4} \\ K_{qp_r} = 4.02 \cdot 10^{-11} \\ V_{p,0} = 1.15 \text{ l} \\ V_{r,0} = 0.2 \text{ l} \end{array} \right. \quad (C.16)$$



**Figure C.23:** Eigenvalues: -306.84, -12.72 ± j59.50.



**Figure C.24:** RGA analysis.

No Load Force,  $p_r = 30$  bar

$$\left. \begin{array}{l} \dot{x}_0 = 0.1 \text{ m/s} \\ F_{L,0} = 0 \text{ kN} \\ p_{r,0} = 30 \text{ bar} \\ x_0 = 0 \text{ m} \end{array} \right\} \begin{cases} p_{p,0} = 14.7 \text{ bar} \\ u_{p,0} = 0.1979 \\ u_{r,0} = 0.2517 \\ K_{qu_p} = 1.57 \cdot 10^{-3} \\ K_{qp_p} = 7.98 \cdot 10^{-12} \\ K_{qu_r} = 6.07 \cdot 10^{-4} \\ K_{qp_r} = 2.63 \cdot 10^{-11} \\ V_{p,0} = 0.2 \text{ l} \\ V_{r,0} = 0.67 \text{ l} \end{cases} \quad (\text{C.17})$$

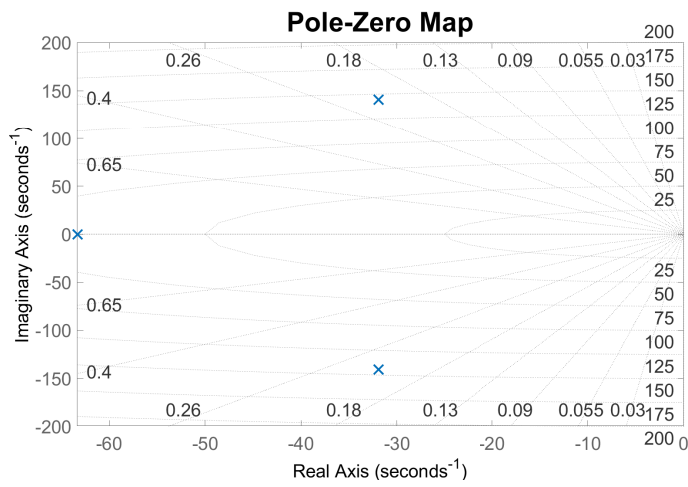


Figure C.25: Eigenvalues:  $-63.31, -31.89 \pm j140.77$ .

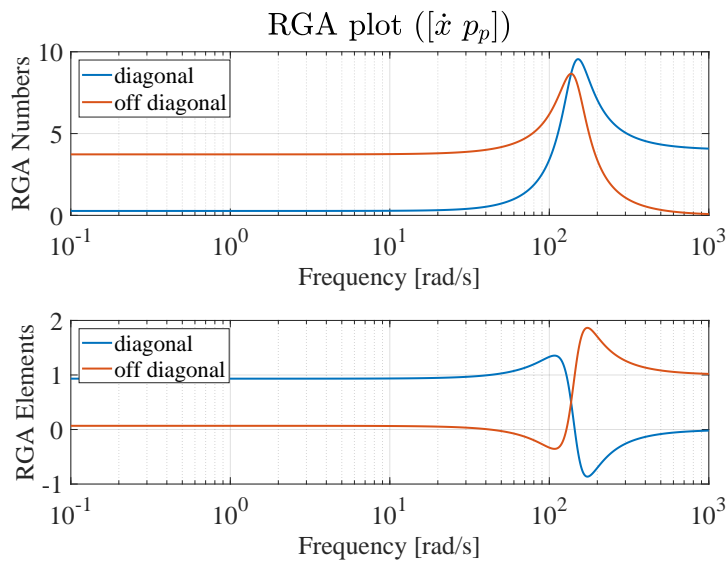
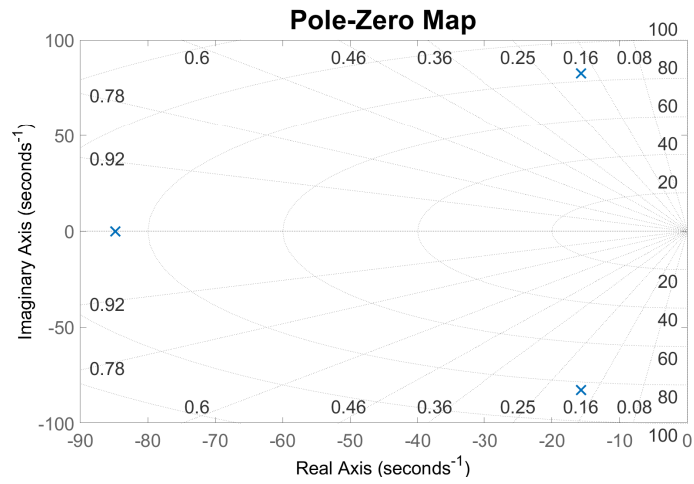
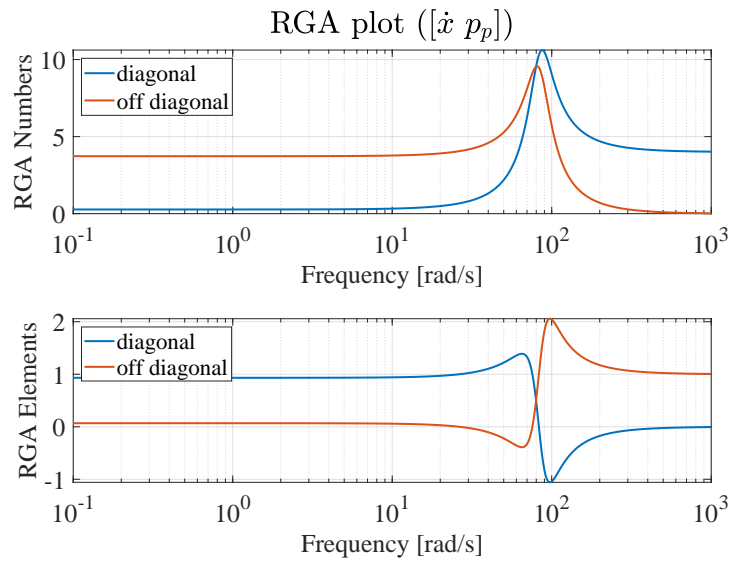


Figure C.26: RGA analysis.

$$\left. \begin{array}{l} \dot{x}_0 = 0.1 \text{ m/s} \\ F_{L,0} = 0 \text{ kN} \\ p_{r,0} = 30 \text{ bar} \\ x_0 = L_{stroke}/2 = 0.1525 \text{ m} \end{array} \right\} \begin{array}{l} p_{p,0} = 14.7 \text{ bar} \\ u_{p,0} = 0.1979 \\ u_{r,0} = 0.2517 \\ K_{qu_p} = 1.57 \cdot 10^{-3} \\ K_{qp_p} = 7.98 \cdot 10^{-12} \\ K_{qu_r} = 6.07 \cdot 10^{-4} \\ K_{qp_r} = 2.63 \cdot 10^{-11} \\ V_{p,0} = 0.67 \text{ l} \\ V_{r,0} = 0.43 \text{ l} \end{array} \quad (C.18)$$



**Figure C.27:** Eigenvalues:  $-84.80, -15.69 \pm j82.69$ .



**Figure C.28:** RGA analysis.

$$\left. \begin{array}{l}
 \dot{x}_0 = 0.1 \text{ m/s} \\
 F_{L,0} = 0 \text{ kN} \\
 p_{r,0} = 30 \text{ bar} \\
 x_0 = L_{stroke} = 0.305 \text{ m}
 \end{array} \right\} \begin{array}{l}
 p_{p,0} = 14.7 \text{ bar} \\
 u_{p,0} = 0.1979 \\
 u_{r,0} = 0.2517 \\
 K_{qu_p} = 1.57 \cdot 10^{-3} \\
 K_{qp_p} = 7.98 \cdot 10^{-12} \\
 K_{qu_r} = 6.07 \cdot 10^{-4} \\
 K_{qp_r} = 2.63 \cdot 10^{-11} \\
 V_{p,0} = 1.15 \text{ l} \\
 V_{r,0} = 0.2 \text{ l}
 \end{array} \quad (C.19)$$

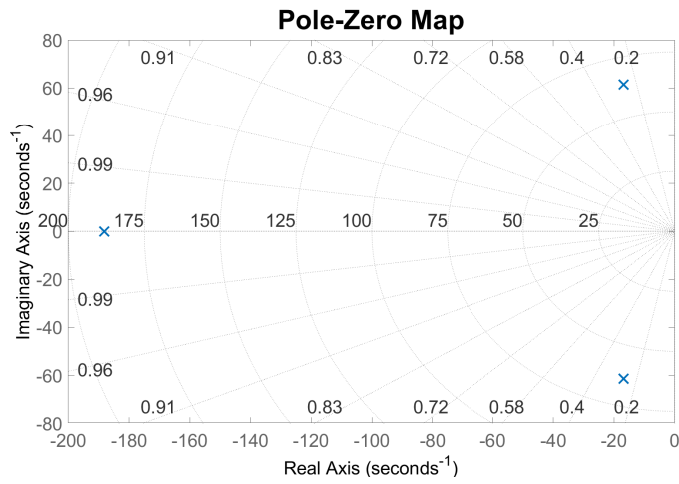


**Figure C.29:** Eigenvalues:  $-188.13, -16.78 \pm j61.43$ .

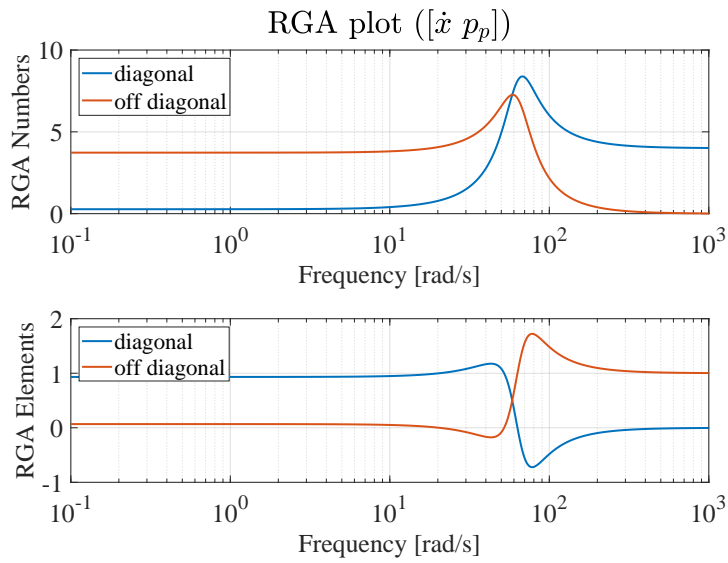


**Figure C.30:** RGA analysis.

Load Force 40 kN (  $p_p \approx 140\text{bar}$ ),  $p_r = 10\text{ bar}$

$$\left. \begin{array}{l} \dot{x}_0 = 0.1\text{ m/s} \\ F_{L,0} = 40\text{ kN} \\ p_{r,0} = 10\text{ bar} \\ x_0 = 0\text{ m} \end{array} \right\} \begin{cases} p_{p,0} = 133.2\text{ bar} \\ u_{p,0} = 0.3157 \\ u_{r,0} = 0.4517 \\ K_{qu_p} = 9.87 \cdot 10^{-4} \\ K_{qp_p} = 2.03 \cdot 10^{-11} \\ K_{qu_r} = 3.38 \cdot 10^{-4} \\ K_{qp_r} = 8.48 \cdot 10^{-11} \\ V_{p,0} = 0.2\text{ l} \\ V_{r,0} = 0.67\text{ l} \end{cases} \quad (\text{C.20})$$

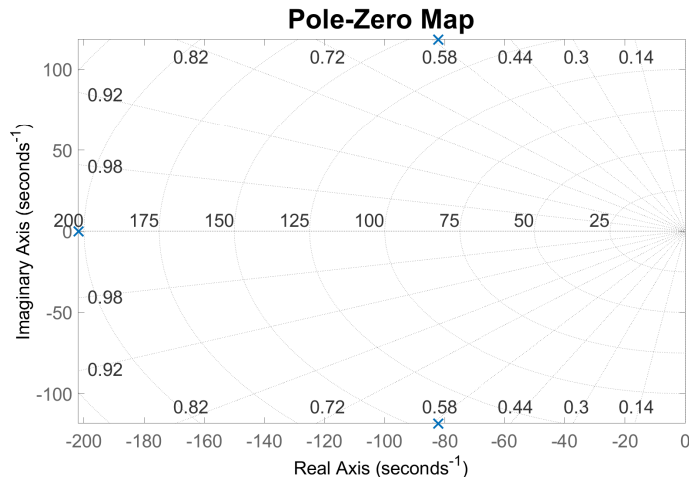


Figure C.31: Eigenvalues:  $-201.87, -82.19 \pm j118.30$ .

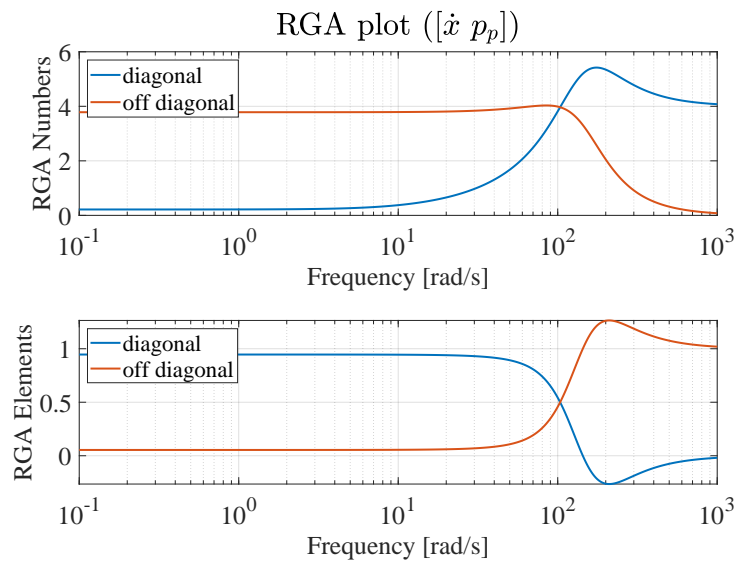
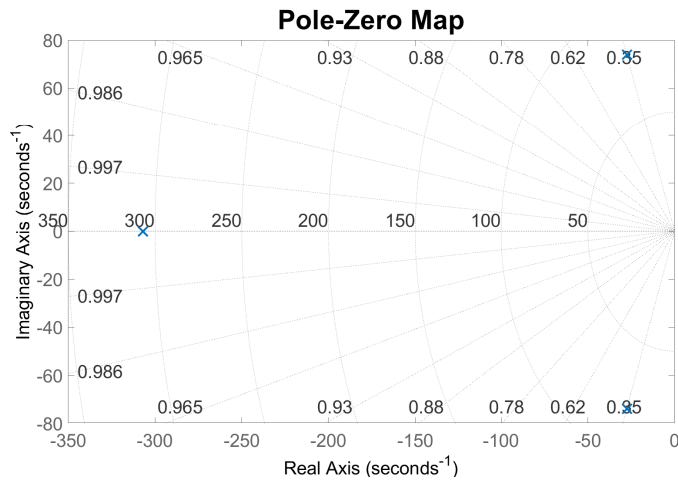
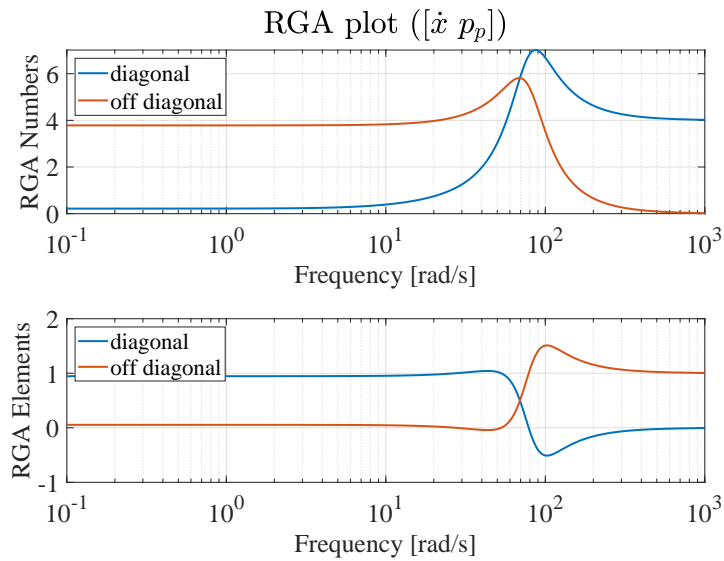


Figure C.32: RGA analysis.

$$\left. \begin{array}{l}
 \dot{x}_0 = 0.1 \text{ m/s} \\
 F_{L,0} = 40 \text{ kN} \\
 p_{r,0} = 10 \text{ bar} \\
 x_0 = L_{stroke}/2 = 0.1525 \text{ m}
 \end{array} \right\} \begin{array}{l}
 p_{p,0} = 133.2 \text{ bar} \\
 u_{p,0} = 0.3157 \\
 u_{r,0} = 0.4517 \\
 K_{qu_p} = 9.87 \cdot 10^{-4} \\
 K_{qp_p} = 2.03 \cdot 10^{-11} \\
 K_{qu_r} = 3.38 \cdot 10^{-4} \\
 K_{qp_r} = 8.48 \cdot 10^{-11} \\
 V_{p,0} = 0.67 \text{ l} \\
 V_{r,0} = 0.43 \text{ l}
 \end{array} \quad (C.21)$$



**Figure C.33:** Eigenvalues:  $-307.03, -27.30 \pm j73.94$ .



**Figure C.34:** RGA analysis.

$$\left. \begin{array}{l}
 \dot{x}_0 = 0.1 \text{ m/s} \\
 F_{L,0} = 40 \text{ kN} \\
 p_{r,0} = 10 \text{ bar} \\
 x_0 = L_{stroke} = 0.305 \text{ m}
 \end{array} \right\} \left\{ \begin{array}{l}
 p_{p,0} = 133.2 \text{ bar} \\
 u_{p,0} = 0.3157 \\
 u_{r,0} = 0.4517 \\
 K_{qup} = 9.87 \cdot 10^{-4} \\
 K_{qp_p} = 2.03 \cdot 10^{-11} \\
 K_{qu_r} = 3.38 \cdot 10^{-4} \\
 K_{qp_r} = 8.48 \cdot 10^{-11} \\
 V_{p,0} = 1.15 \text{ l} \\
 V_{r,0} = 0.2 \text{ l}
 \end{array} \right. \quad (C.22)$$

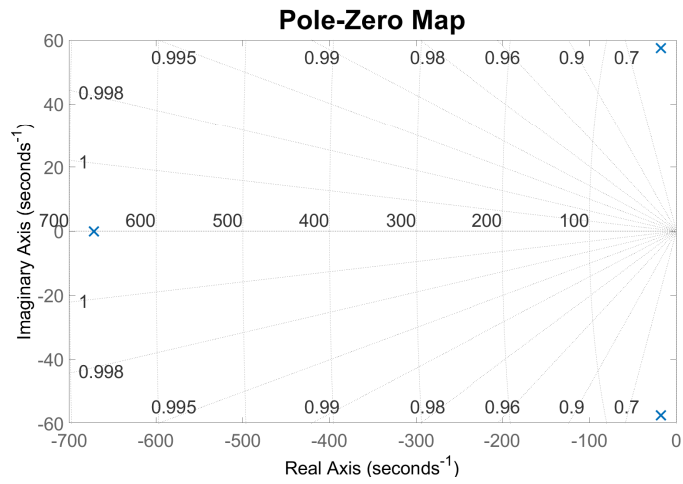


**Figure C.35:** Eigenvalues:  $-671.83, -17.54 \pm j57.44$ .

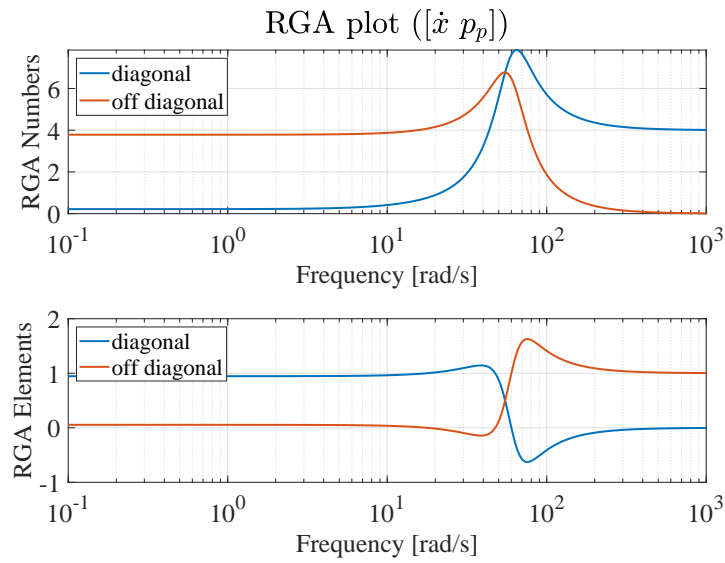


**Figure C.36:** RGA analysis.

## C Matrix Controlling $p_r$

$$\left. \begin{array}{l} \dot{x}_0 = 0.1 \text{ m/s} \\ F_{L,0} = 0 \text{ kN} \\ p_{r,0} = 10 \text{ bar} \\ x_0 = 0 \text{ m} \end{array} \right\} \begin{cases} p_{p,0} = 4.9 \text{ bar} \\ u_{p,0} = 0.1932 \\ u_{r,0} = 0.4517 \\ K_{qu_p} = 1.61 \cdot 10^{-3} \\ K_{qp_p} = 7.60 \cdot 10^{-12} \\ K_{qu_r} = 3.38 \cdot 10^{-4} \\ K_{qp_r} = 8.48 \cdot 10^{-11} \\ V_{p,0} = 0.2 \text{ l} \\ V_{r,0} = 0.67 \text{ l} \end{cases} \quad (\text{C.23})$$

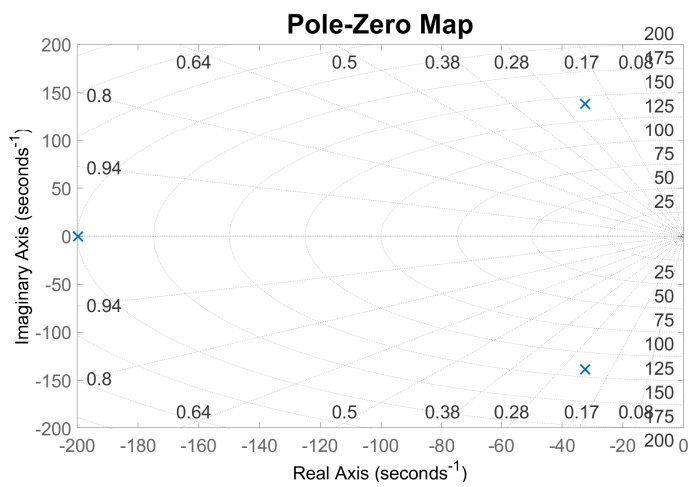


Figure C.37: Eigenvalues:  $-199.76, -32.44 \pm j138.59$ .

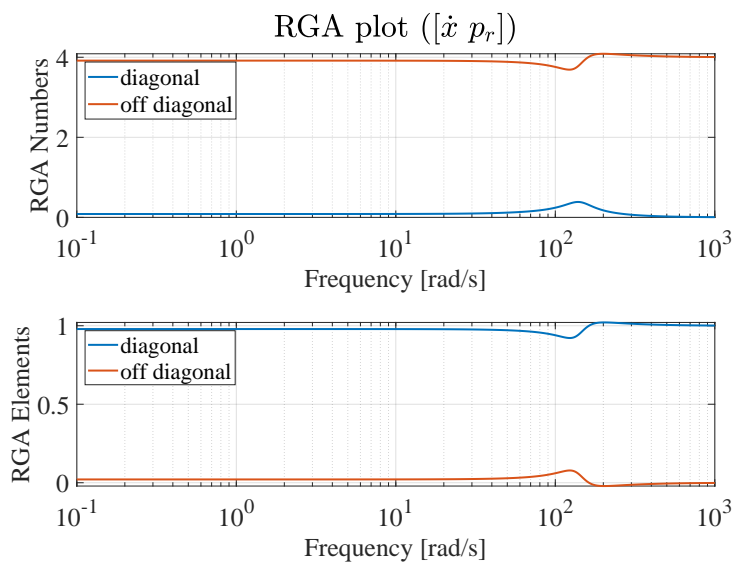
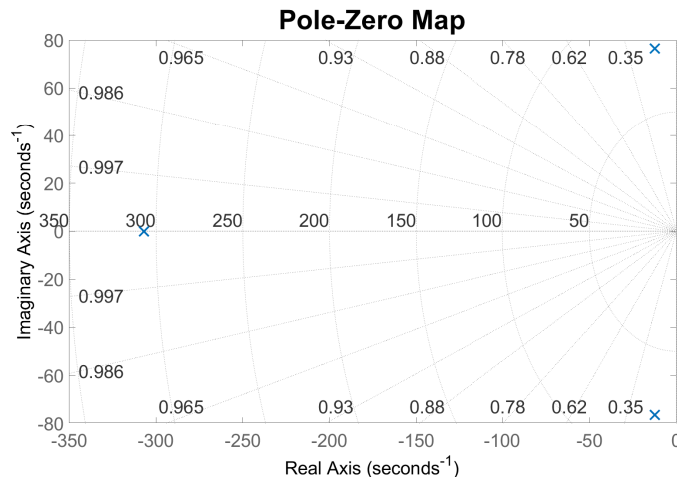
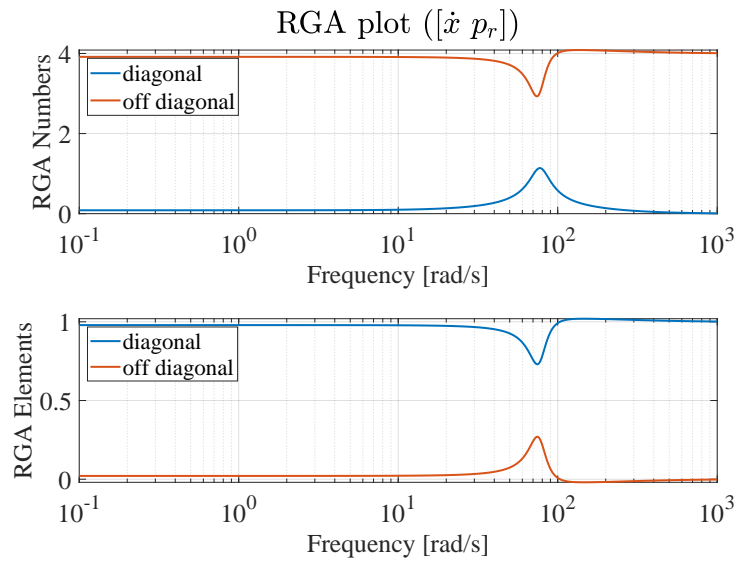


Figure C.38: RGA analysis.

$$\left. \begin{array}{l}
 \dot{x}_0 = 0.1 \text{ m/s} \\
 F_{L,0} = 0 \text{ kN} \\
 p_{r,0} = 10 \text{ bar} \\
 x_0 = L_{stroke}/2 = 0.1525 \text{ m}
 \end{array} \right\} \begin{array}{l}
 p_{p,0} = 4.9 \text{ bar} \\
 u_{p,0} = 0.1932 \\
 u_{r,0} = 0.4517 \\
 K_{qu_p} = 1.61 \cdot 10^{-3} \\
 K_{qp_p} = 7.60 \cdot 10^{-12} \\
 K_{qu_r} = 3.38 \cdot 10^{-4} \\
 K_{qp_r} = 8.48 \cdot 10^{-11} \\
 V_{p,0} = 0.67 \text{ l} \\
 V_{r,0} = 0.43 \text{ l}
 \end{array} \quad (C.24)$$



**Figure C.39:** Eigenvalues:  $-306.98, -12.28 \pm j76.50$ .



**Figure C.40:** RGA analysis.

$$\left. \begin{array}{l} \dot{x}_0 = 0.1 \text{ m/s} \\ F_{L,0} = 0 \text{ kN} \\ p_{r,0} = 10 \text{ bar} \\ x_0 = L_{stroke} = 0.305 \text{ m} \end{array} \right\} \begin{cases} p_{p,0} = 4.9 \text{ bar} \\ u_{p,0} = 0.1932 \\ u_{r,0} = 0.4517 \\ K_{qu_p} = 1.61 \cdot 10^{-3} \\ K_{qp_p} = 7.60 \cdot 10^{-12} \\ K_{qu_r} = 3.38 \cdot 10^{-4} \\ K_{qp_r} = 8.48 \cdot 10^{-11} \\ V_{p,0} = 1.15 \text{ l} \\ V_{r,0} = 0.2 \text{ l} \end{cases} \quad (C.25)$$

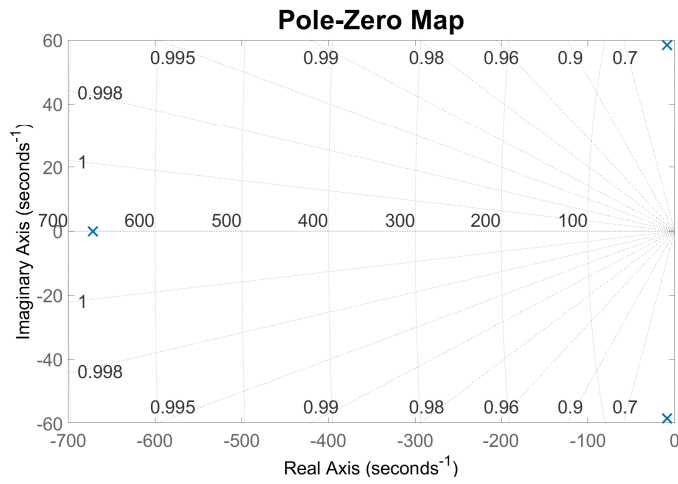


Figure C.41: Eigenvalues:  $-671.83, -8.71 \pm j58.39$ .

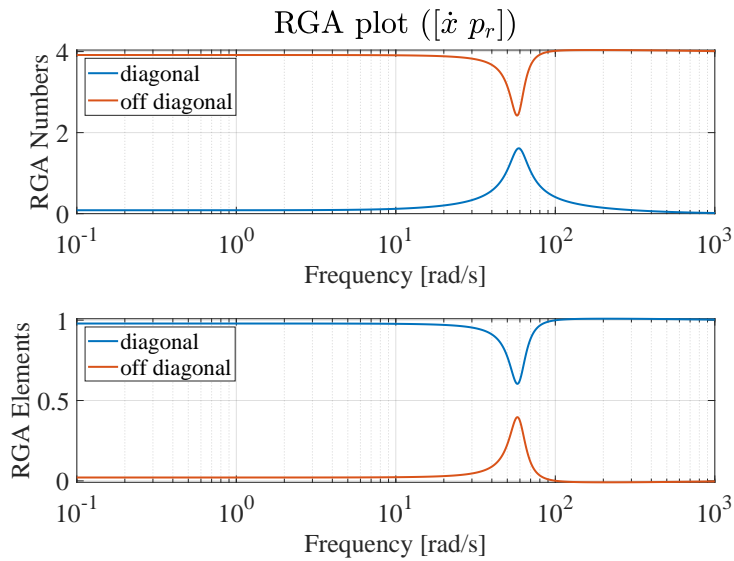
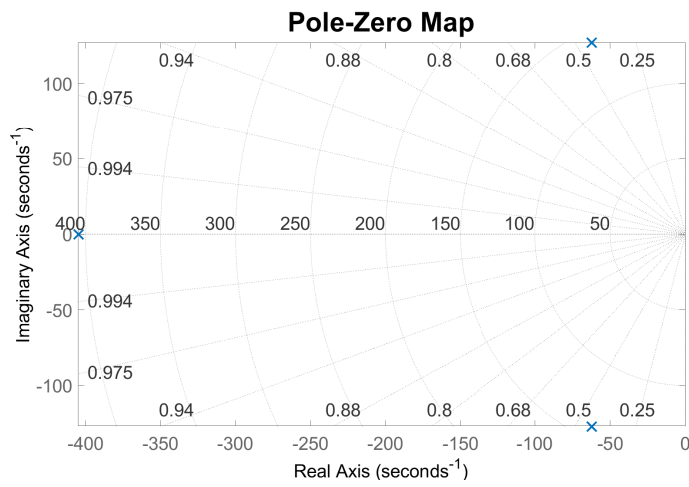


Figure C.42: RGA analysis.

## Initial Velocity Change

$$\left. \begin{array}{l} \dot{x}_0 = 0.2 \text{ m/s} \\ F_{L,0} = 0 \text{ kN} \\ p_{r,0} = 10 \text{ bar} \\ x_0 = 0 \text{ m} \end{array} \right\} \begin{cases} p_{p,0} = 4.9 \text{ bar} \\ u_{p,0} = 0.3863 \\ u_{r,0} = 0.9035 \\ K_{qup} = 1.61 \cdot 10^{-3} \\ K_{qpp} = 1.52 \cdot 10^{-11} \\ K_{qu_r} = 3.38 \cdot 10^{-4} \\ K_{qpr} = 1.69 \cdot 10^{-10} \\ V_{p,0} = 0.2 \text{ l} \\ V_{r,0} = 0.67 \text{ l} \end{cases} \quad (\text{C.26})$$



**Figure C.43:** Eigenvalues:  $-404.82, -62.26 \pm j126.95$ .

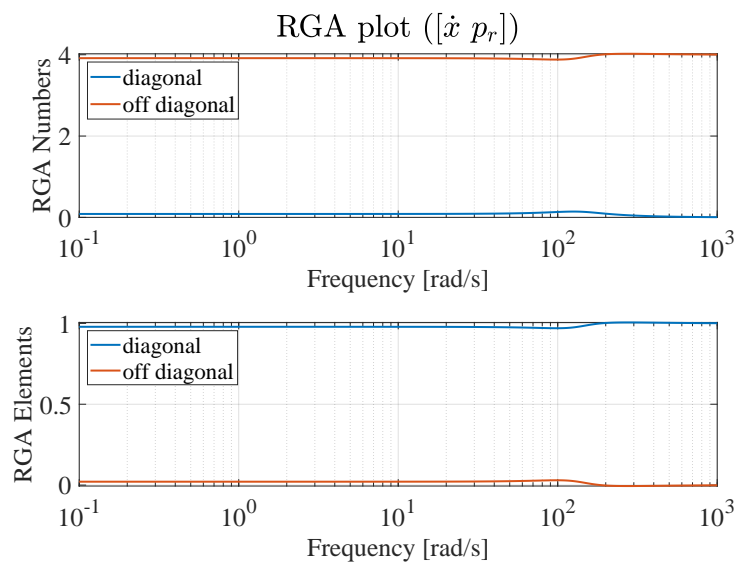


**Figure C.44:** RGA analysis.

$$\left. \begin{array}{l}
 \dot{x}_0 = 0.2 \text{ m/s} \\
 F_{L,0} = 0 \text{ kN} \\
 p_{r,0} = 10 \text{ bar} \\
 x_0 = L_{stroke}/2 = 0.1525 \text{ m}
 \end{array} \right\} \begin{array}{l}
 p_{p,0} = 4.9 \text{ bar} \\
 u_{p,0} = 0.3863 \\
 u_{r,0} = 0.9035 \\
 K_{qu_p} = 1.61 \cdot 10^{-3} \\
 K_{qp_p} = 1.52 \cdot 10^{-11} \\
 K_{qu_r} = 3.38 \cdot 10^{-4} \\
 K_{qp_r} = 1.69 \cdot 10^{-10} \\
 V_{p,0} = 0.67 \text{ l} \\
 V_{r,0} = 0.43 \text{ l}
 \end{array} \quad (C.27)$$

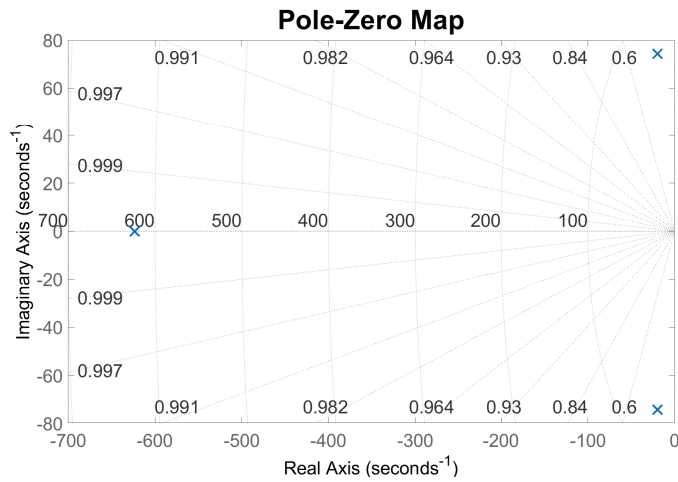


**Figure C.45:** Eigenvalues:  $-623.76, -19.69 \pm j74.31$ .

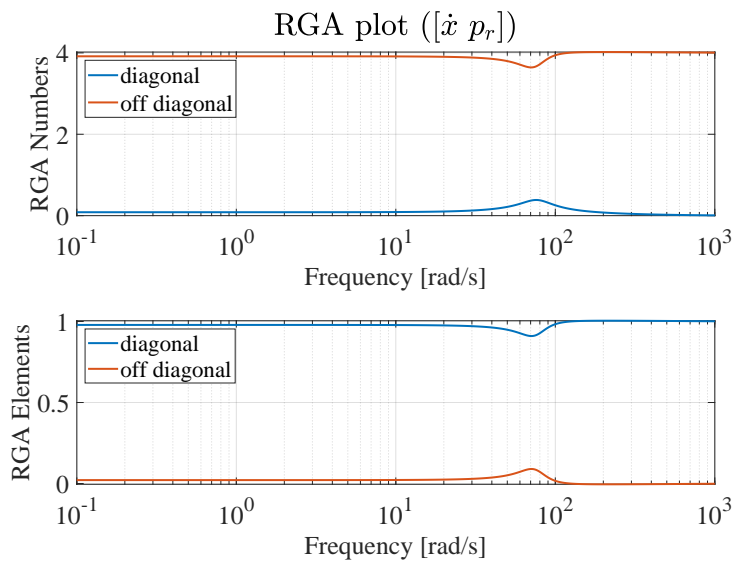


**Figure C.46:** RGA analysis.

$$\left. \begin{array}{l} \dot{x}_0 = 0.2 \text{ m/s} \\ F_{L,0} = 0 \text{ kN} \\ p_{r,0} = 10 \text{ bar} \\ x_0 = L_{stroke} = 0.305 \text{ m} \end{array} \right\} \begin{cases} p_{p,0} = 4.9 \text{ bar} \\ u_{p,0} = 0.3863 \\ u_{r,0} = 0.9035 \\ K_{qup} = 1.61 \cdot 10^{-3} \\ K_{qpp} = 1.52 \cdot 10^{-11} \\ K_{qu_r} = 3.38 \cdot 10^{-4} \\ K_{qpr} = 1.69 \cdot 10^{-10} \\ V_{p,0} = 1.15 \text{ l} \\ V_{r,0} = 0.2 \text{ l} \end{cases} \quad (\text{C.28})$$

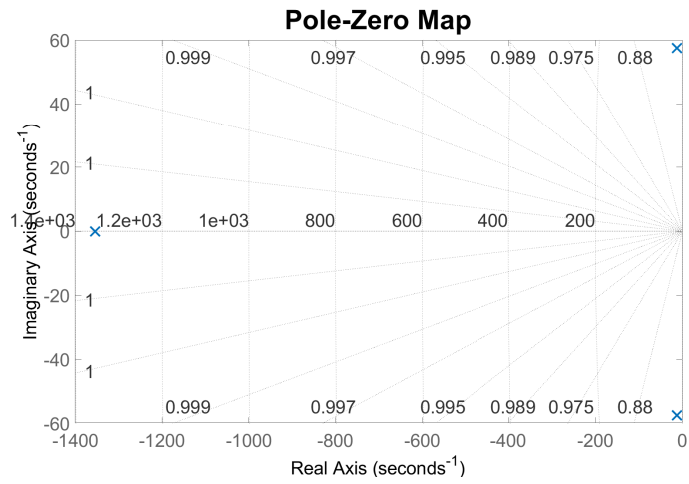


Figure C.47: Eigenvalues: -1354, -12.27 ± j57.51.

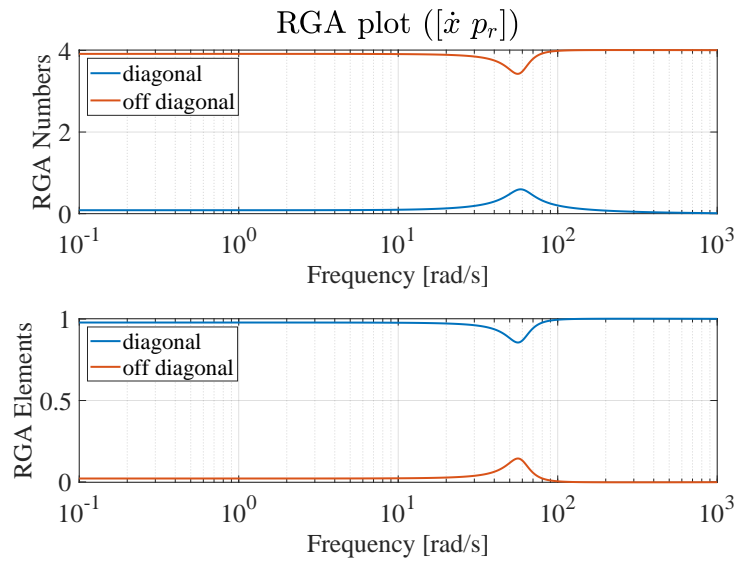
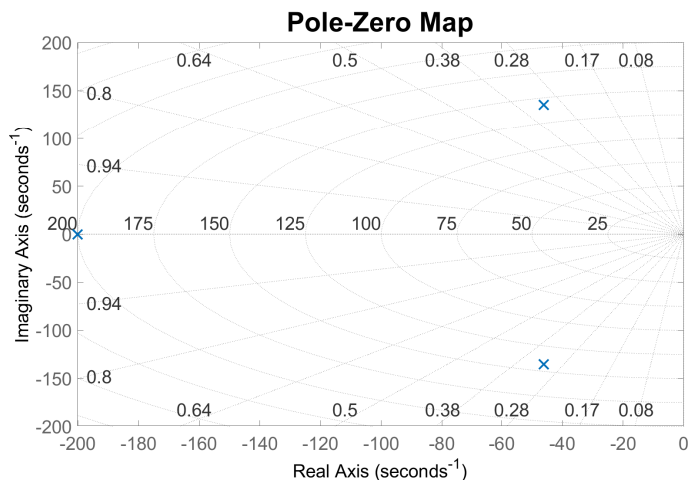


Figure C.48: RGA analysis.

## Load Force Change

$$\left. \begin{array}{l} \dot{x}_0 = 0.1 \text{ m/s} \\ F_{L,0} = 20 \text{ kN} \\ p_{r,0} = 10 \text{ bar} \\ x_0 = 0 \text{ m} \end{array} \right\} \begin{cases} p_{p,0} = 69 \text{ bar} \\ u_{p,0} = 0.2330 \\ u_{r,0} = 0.4517 \\ K_{qu_p} = 1.33 \cdot 10^{-3} \\ K_{qp_p} = 1.10 \cdot 10^{-11} \\ K_{qu_r} = 3.38 \cdot 10^{-4} \\ K_{qp_r} = 8.48 \cdot 10^{-11} \\ V_{p,0} = 0.2 \text{ l} \\ V_{r,0} = 0.67 \text{ l} \end{cases} \quad (\text{C.29})$$



**Figure C.49:** Eigenvalues:  $-200.14, -46.09 \pm j135.24$ .

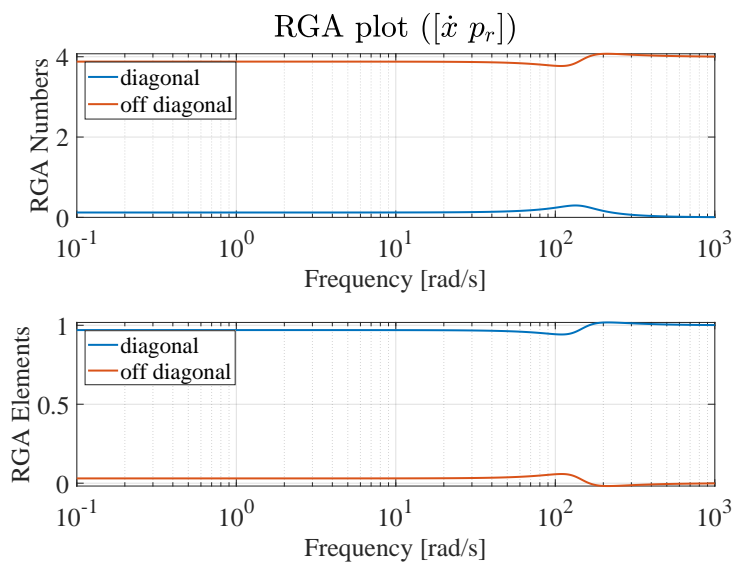


**Figure C.50:** RGA analysis.

$$\left. \begin{array}{l}
 \dot{x}_0 = 0.1 \text{ m/s} \\
 F_{L,0} = 20 \text{ kN} \\
 p_{r,0} = 10 \text{ bar} \\
 x_0 = L_{stroke}/2 = 0.1525 \text{ m}
 \end{array} \right\} \begin{array}{l}
 p_{p,0} = 69 \text{ bar} \\
 u_{p,0} = 0.2330 \\
 u_{r,0} = 0.4517 \\
 K_{qu_p} = 1.33 \cdot 10^{-3} \\
 K_{qp_p} = 1.10 \cdot 10^{-11} \\
 K_{qu_r} = 3.38 \cdot 10^{-4} \\
 K_{qp_r} = 8.48 \cdot 10^{-11} \\
 V_{p,0} = 0.67 \text{ l} \\
 V_{r,0} = 0.43 \text{ l}
 \end{array} \quad (C.30)$$

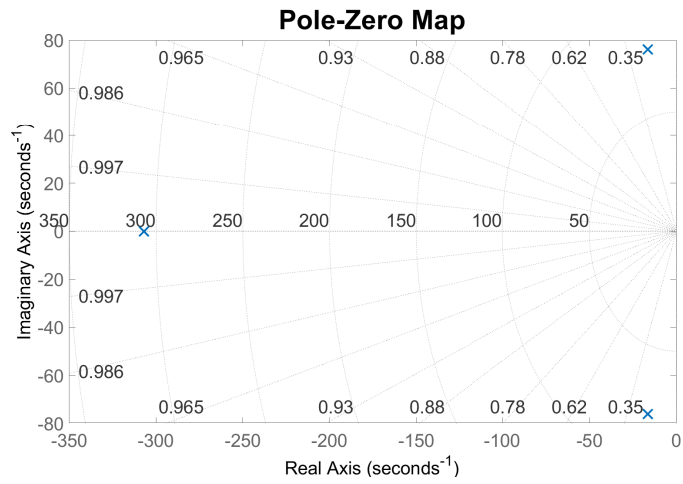


Figure C.51: Eigenvalues:  $-307, -16.37 \pm j76.11$ .

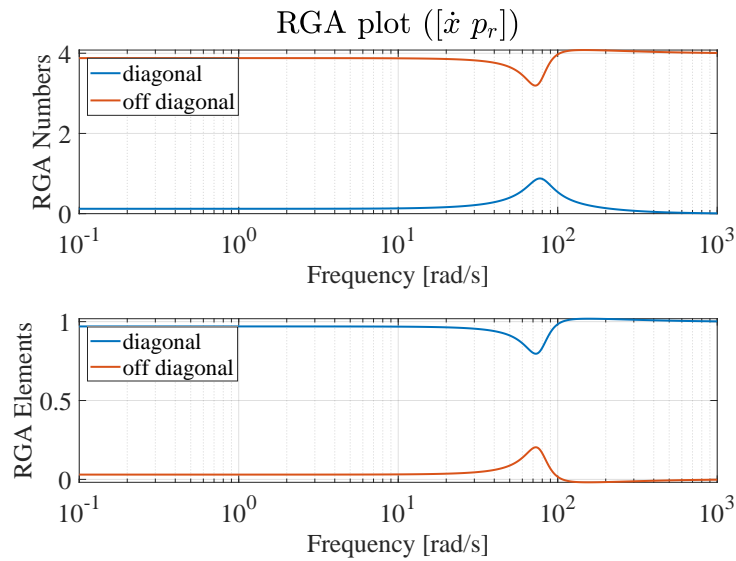
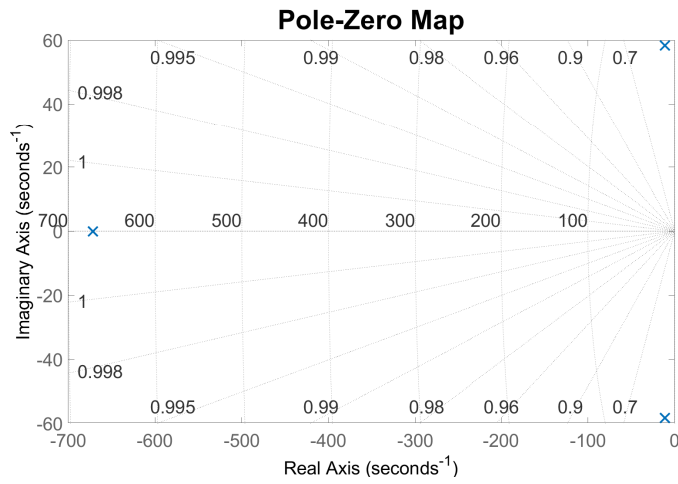
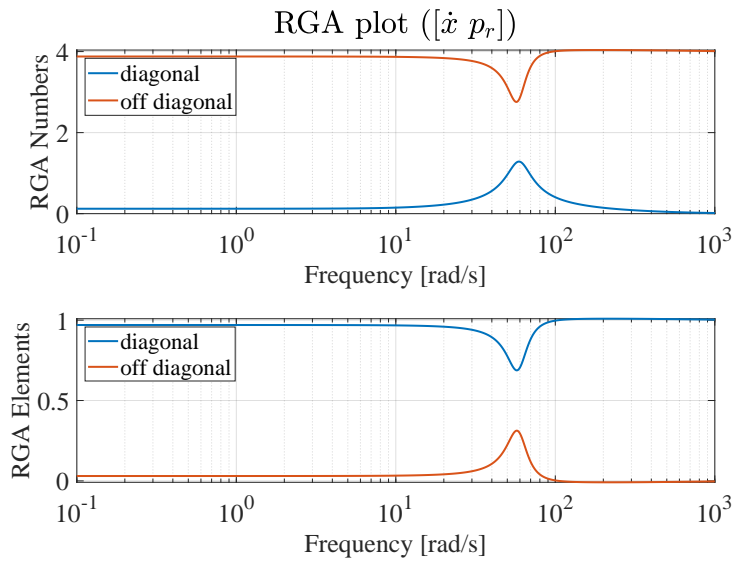


Figure C.52: RGA analysis.

$$\left. \begin{array}{l} \dot{x}_0 = 0.1 \text{ m/s} \\ F_{L,0} = 20 \text{ kN} \\ p_{r,0} = 10 \text{ bar} \\ x_0 = L_{stroke} = 0.305 \text{ m} \end{array} \right\} \begin{cases} p_{p,0} = 69 \text{ bar} \\ u_{p,0} = 0.2330 \\ u_{r,0} = 0.4517 \\ K_{qu_p} = 1.33 \cdot 10^{-3} \\ K_{qp_p} = 1.10 \cdot 10^{-11} \\ K_{qu_r} = 3.38 \cdot 10^{-4} \\ K_{qp_r} = 8.48 \cdot 10^{-11} \\ V_{p,0} = 1.15 \text{ l} \\ V_{r,0} = 0.2 \text{ l} \end{cases} \quad (\text{C.31})$$



**Figure C.53:** Eigenvalues:  $-671.83, -11.12 \pm j58.26$ .



**Figure C.54:** RGA analysis.

No Load Force,  $p_r = 20$  bar.

$$\left. \begin{array}{l} \dot{x}_0 = 0.1 \text{ m/s} \\ F_{L,0} = 0 \text{ kN} \\ p_{r,0} = 20 \text{ bar} \\ x_0 = 0 \text{ m} \end{array} \right\} \left\{ \begin{array}{l} p_{p,0} = 9.8 \text{ bar} \\ u_{p,0} = 0.1955 \\ u_{r,0} = 0.3109 \\ K_{qup} = 1.59 \cdot 10^{-3} \\ K_{qp_p} = 7.78 \cdot 10^{-12} \\ K_{qu_r} = 4.91 \cdot 10^{-4} \\ K_{qp_r} = 4.02 \cdot 10^{-11} \\ V_{p,0} = 0.2 \text{ l} \\ V_{r,0} = 0.67 \text{ l} \end{array} \right. \quad (\text{C.32})$$

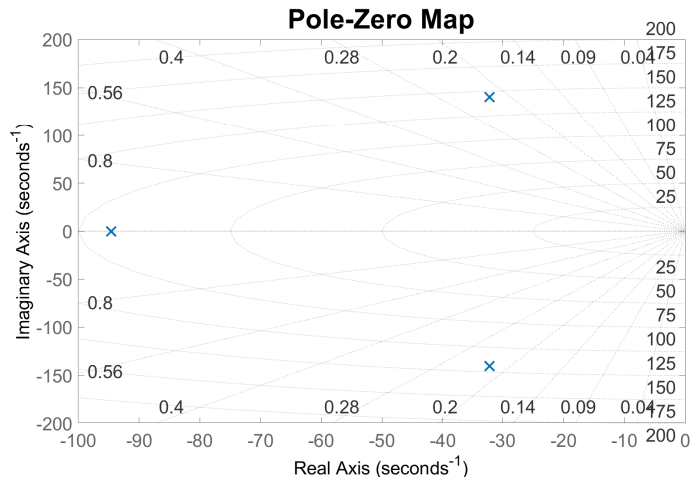


Figure C.55: Eigenvalues:  $-94.56, -32.13 \pm j140.48$ .

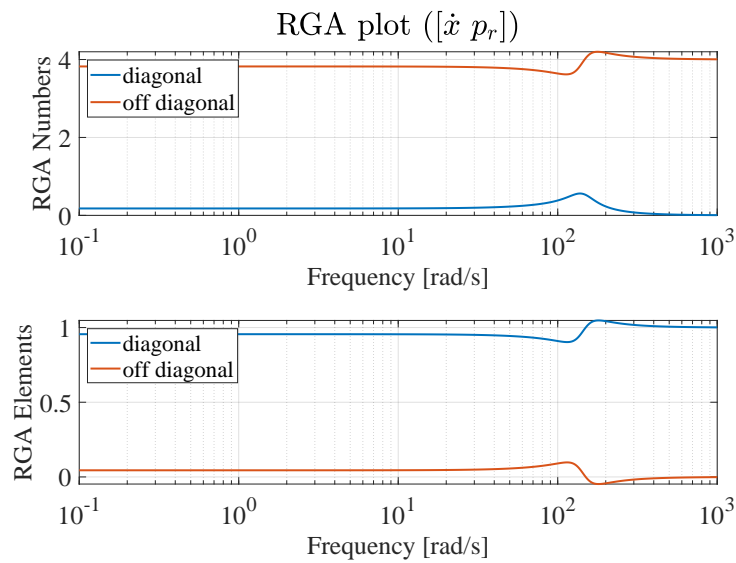
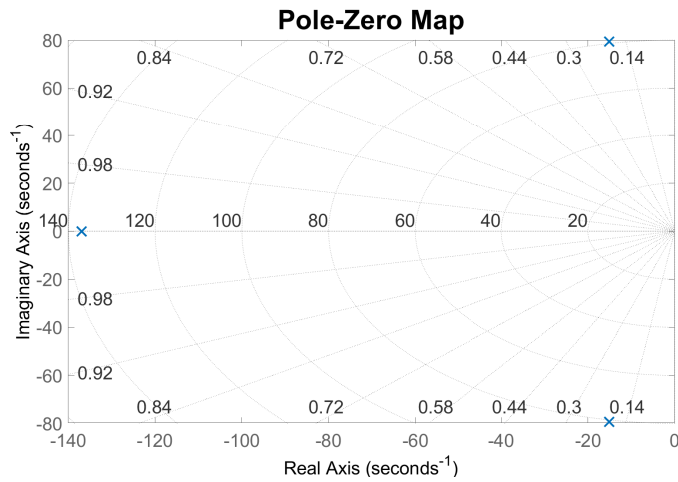
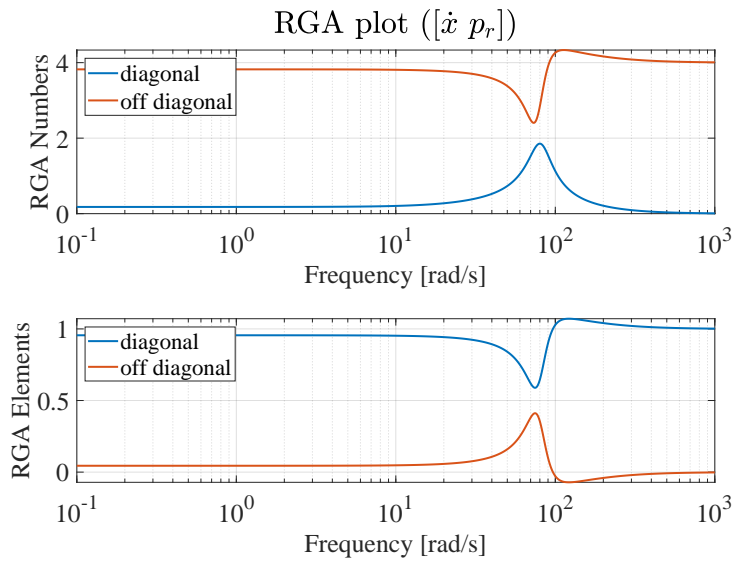


Figure C.56: RGA analysis.

$$\left. \begin{array}{l}
 \dot{x}_0 = 0.1 \text{ m/s} \\
 F_{L,0} = 0 \text{ kN} \\
 p_{r,0} = 20 \text{ bar} \\
 x_0 = L_{stroke}/2 = 0.1525 \text{ m}
 \end{array} \right\} \begin{array}{l}
 p_{p,0} = 9.8 \text{ bar} \\
 u_{p,0} = 0.1955 \\
 u_{r,0} = 0.3109 \\
 K_{qu_p} = 1.59 \cdot 10^{-3} \\
 K_{qp_p} = 7.78 \cdot 10^{-12} \\
 K_{qu_r} = 4.91 \cdot 10^{-4} \\
 K_{qp_r} = 4.02 \cdot 10^{-11} \\
 V_{p,0} = 0.67 \text{ l} \\
 V_{r,0} = 0.43 \text{ l}
 \end{array} \quad (\text{C.33})$$



**Figure C.57:** Eigenvalues:  $-136.92, -15.01 \pm j79.42$ .



**Figure C.58:** RGA analysis.

$$\left. \begin{array}{l} \dot{x}_0 = 0.1 \text{ m/s} \\ F_{L,0} = 0 \text{ kN} \\ p_{r,0} = 20 \text{ bar} \\ x_0 = L_{stroke} = 0.305 \text{ m} \end{array} \right\} \left\{ \begin{array}{l} p_{p,0} = 9.8 \text{ bar} \\ u_{p,0} = 0.1955 \\ u_{r,0} = 0.3109 \\ K_{qup} = 1.59 \cdot 10^{-3} \\ K_{qp_p} = 7.78 \cdot 10^{-12} \\ K_{qu_r} = 4.91 \cdot 10^{-4} \\ K_{qp_r} = 4.02 \cdot 10^{-11} \\ V_{p,0} = 1.15 \text{ l} \\ V_{r,0} = 0.2 \text{ l} \end{array} \right. \quad (C.34)$$

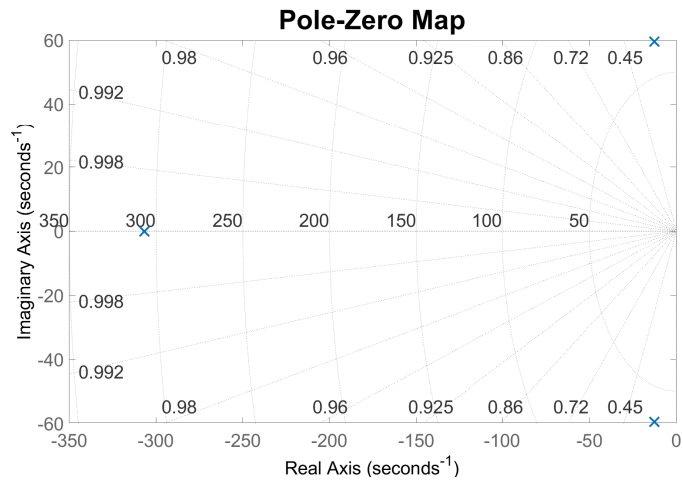


**Figure C.59:** Eigenvalues: -306.84, -12.72 ± j59.50.

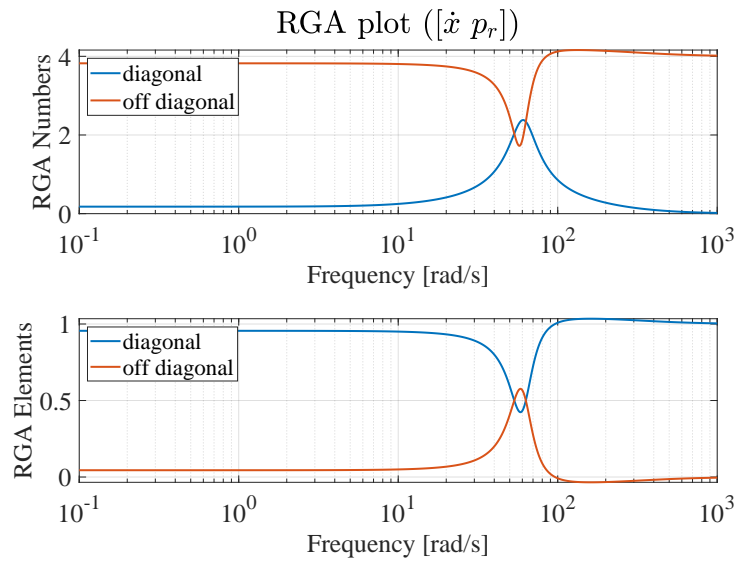


**Figure C.60:** RGA analysis.

No Load Force,  $p_r = 30$  bar.

$$\left. \begin{array}{l} \dot{x}_0 = 0.1 \text{ m/s} \\ F_{L,0} = 0 \text{ kN} \\ p_{r,0} = 30 \text{ bar} \\ x_0 = 0 \text{ m} \end{array} \right\} \begin{cases} p_{p,0} = 14.7 \text{ bar} \\ u_{p,0} = 0.1979 \\ u_{r,0} = 0.2517 \\ K_{qu_p} = 1.57 \cdot 10^{-3} \\ K_{qp_p} = 7.98 \cdot 10^{-12} \\ K_{qu_r} = 6.07 \cdot 10^{-4} \\ K_{qp_r} = 2.63 \cdot 10^{-11} \\ V_{p,0} = 0.2 \text{ l} \\ V_{r,0} = 0.67 \text{ l} \end{cases} \quad (\text{C.35})$$

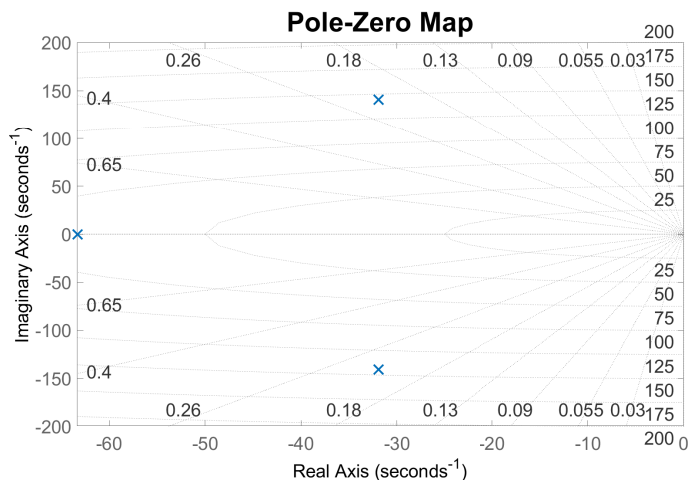


Figure C.61: Eigenvalues:  $-63.31, -31.89 \pm j140.77$ .

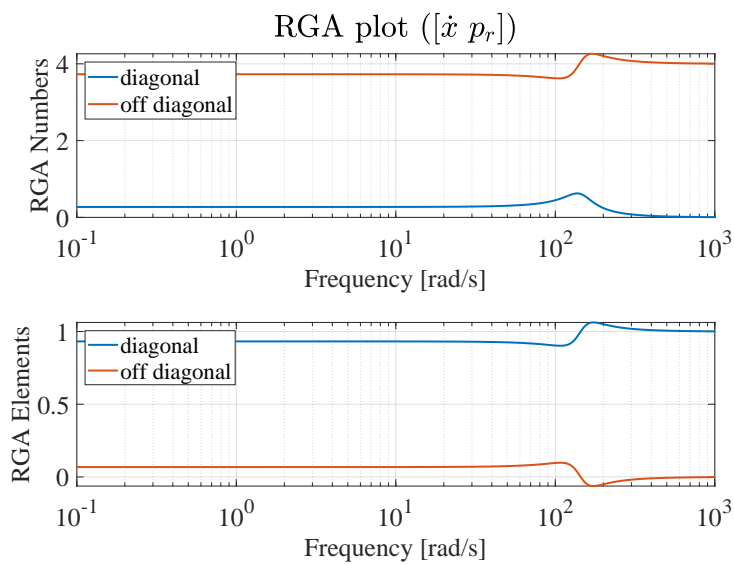
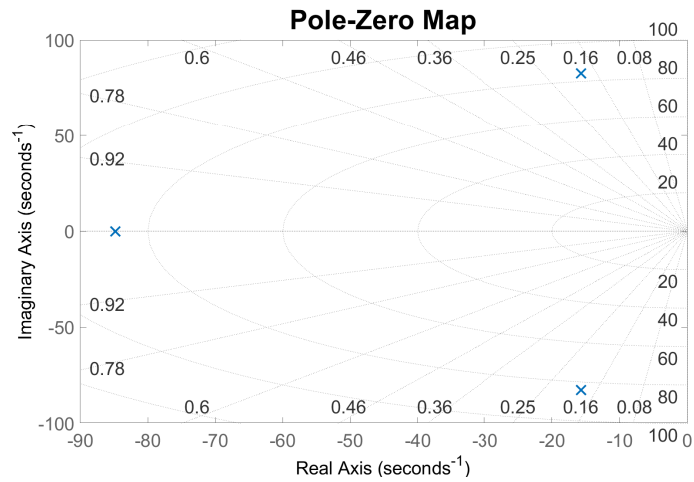
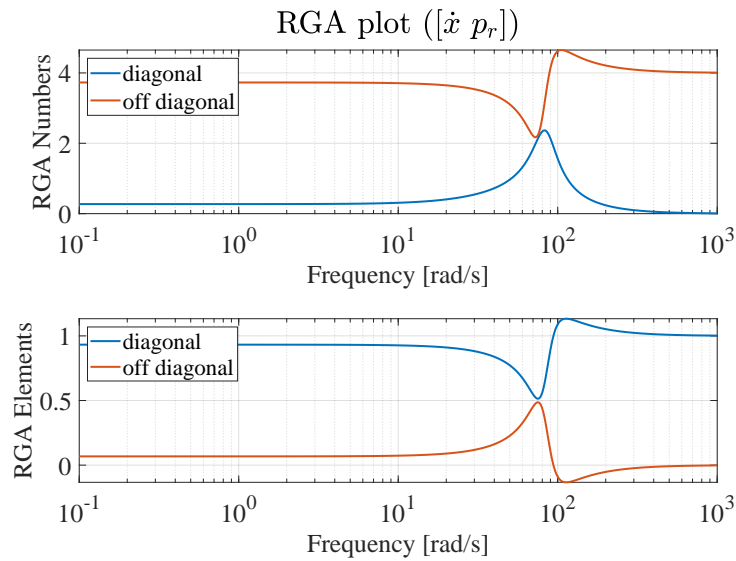


Figure C.62: RGA analysis.

$$\left. \begin{array}{l}
 \dot{x}_0 = 0.1 \text{ m/s} \\
 F_{L,0} = 0 \text{ kN} \\
 p_{r,0} = 30 \text{ bar} \\
 x_0 = L_{stroke}/2 = 0.1525 \text{ m}
 \end{array} \right\} \begin{array}{l}
 p_{p,0} = 14.7 \text{ bar} \\
 u_{p,0} = 0.1979 \\
 u_{r,0} = 0.2517 \\
 K_{qu_p} = 1.57 \cdot 10^{-3} \\
 K_{qp_p} = 7.98 \cdot 10^{-12} \\
 K_{qu_r} = 6.07 \cdot 10^{-4} \\
 K_{qp_r} = 2.63 \cdot 10^{-11} \\
 V_{p,0} = 0.67 \text{ l} \\
 V_{r,0} = 0.43 \text{ l}
 \end{array} \quad (\text{C.36})$$



**Figure C.63:** Eigenvalues:  $-84.80, -15.69 \pm j82.69$ .



**Figure C.64:** RGA analysis.

$$\left. \begin{array}{l} \dot{x}_0 = 0.1 \text{ m/s} \\ F_{L,0} = 0 \text{ kN} \\ p_{r,0} = 30 \text{ bar} \\ x_0 = L_{stroke} = 0.305 \text{ m} \end{array} \right\} \begin{cases} p_{p,0} = 14.7 \text{ bar} \\ u_{p,0} = 0.1979 \\ u_{r,0} = 0.2517 \\ K_{qu_p} = 1.57 \cdot 10^{-3} \\ K_{qp_p} = 7.98 \cdot 10^{-12} \\ K_{qu_r} = 6.07 \cdot 10^{-4} \\ K_{qp_r} = 2.63 \cdot 10^{-11} \\ V_{p,0} = 1.15 \text{ l} \\ V_{r,0} = 0.2 \text{ l} \end{cases} \quad (\text{C.37})$$

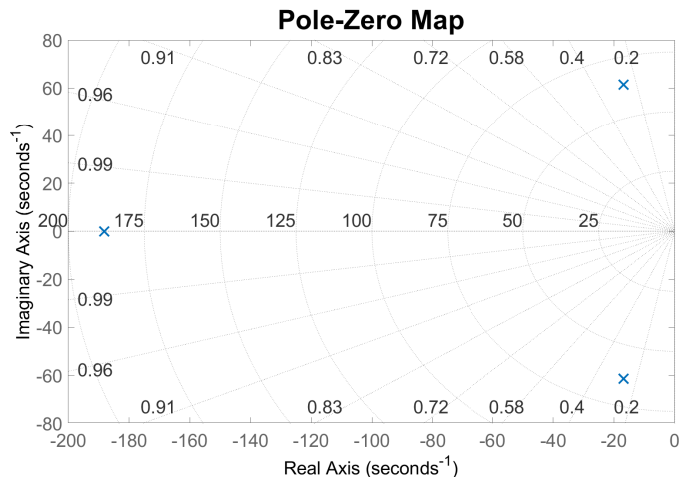


**Figure C.65:** Eigenvalues:  $-188.13, -16.78 \pm j61.43$ .

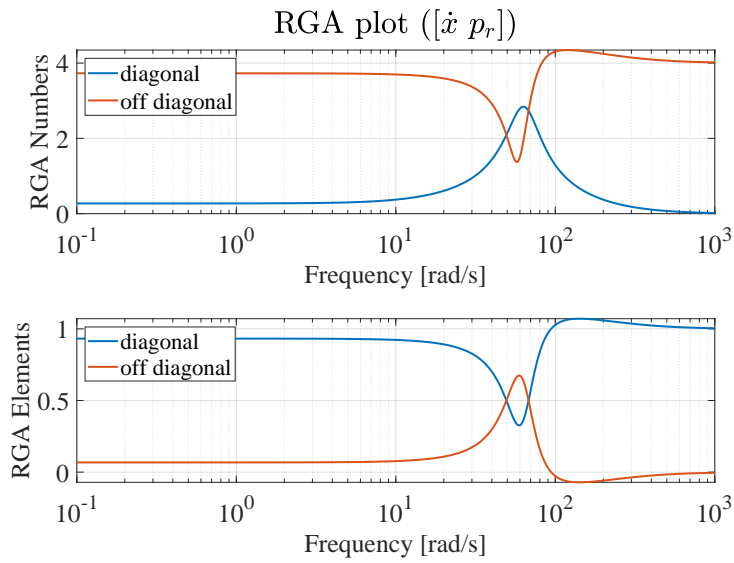


**Figure C.66:** RGA analysis.

Load Force 40 kN (  $p_p \approx 140\text{bar}$ ),  $p_r = 10\text{ bar}$

$$\left. \begin{array}{l} \dot{x}_0 = 0.1\text{ m/s} \\ F_{L,0} = 40\text{ kN} \\ p_{r,0} = 10\text{ bar} \\ x_0 = 0\text{ m} \end{array} \right\} \begin{cases} p_{p,0} = 133.2\text{ bar} \\ u_{p,0} = 0.3157 \\ u_{r,0} = 0.4517 \\ K_{qu_p} = 9.87 \cdot 10^{-4} \\ K_{qp_p} = 2.03 \cdot 10^{-11} \\ K_{qu_r} = 3.38 \cdot 10^{-4} \\ K_{qp_r} = 8.48 \cdot 10^{-11} \\ V_{p,0} = 0.2\text{ l} \\ V_{r,0} = 0.67\text{ l} \end{cases} \quad (\text{C.38})$$

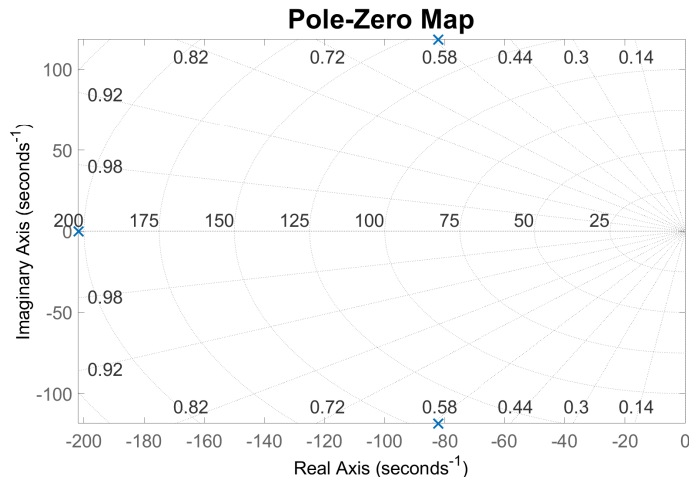


Figure C.67: Eigenvalues:  $-201.87, -82.19 \pm j118.30$ .

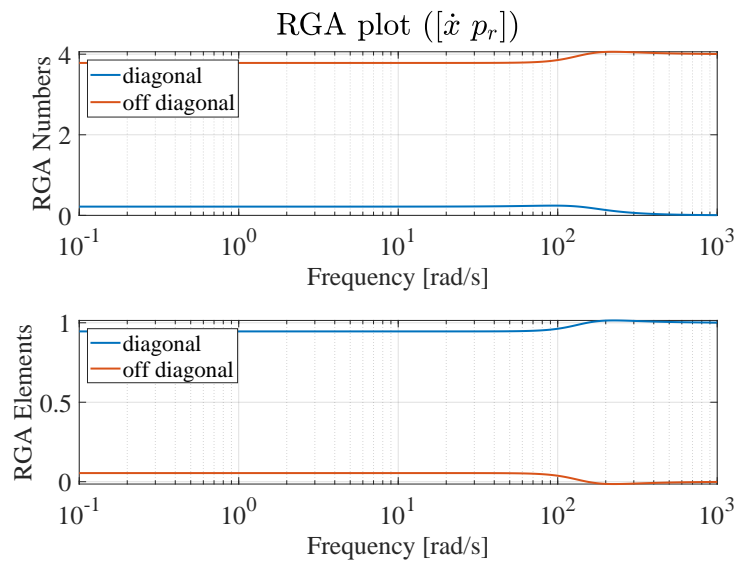
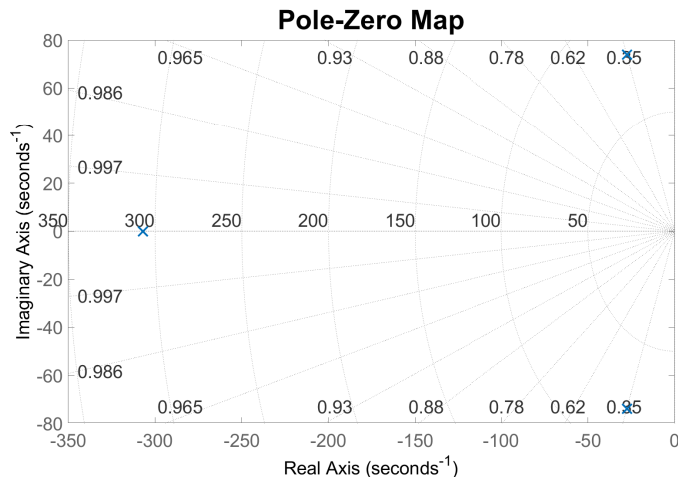
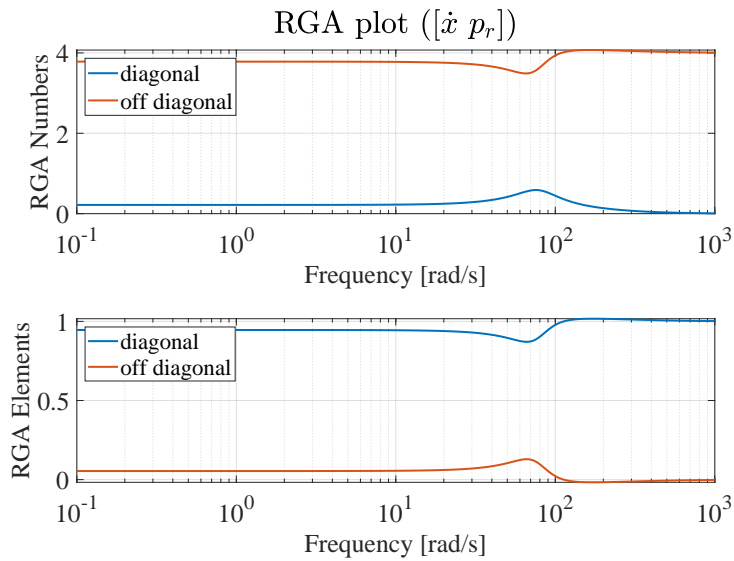


Figure C.68: RGA analysis.

$$\left. \begin{array}{l} \dot{x}_0 = 0.1 \text{ m/s} \\ F_{L,0} = 40 \text{ kN} \\ p_{r,0} = 10 \text{ bar} \\ x_0 = L_{stroke}/2 = 0.1525 \text{ m} \end{array} \right\} \begin{array}{l} p_{p,0} = 133.2 \text{ bar} \\ u_{p,0} = 0.3157 \\ u_{r,0} = 0.4517 \\ K_{qu_p} = 9.87 \cdot 10^{-4} \\ K_{qp_p} = 2.03 \cdot 10^{-11} \\ K_{qu_r} = 3.38 \cdot 10^{-4} \\ K_{qp_r} = 8.48 \cdot 10^{-11} \\ V_{p,0} = 0.67 \text{ l} \\ V_{r,0} = 0.43 \text{ l} \end{array} \quad (C.39)$$



**Figure C.69:** Eigenvalues:  $-307.03, -27.30 \pm j73.94$ .



**Figure C.70:** RGA analysis.

$$\left. \begin{array}{l}
 \dot{x}_0 = 0.1 \text{ m/s} \\
 F_{L,0} = 40 \text{ kN} \\
 p_{r,0} = 10 \text{ bar} \\
 x_0 = L_{stroke} = 0.305 \text{ m}
 \end{array} \right\} \left\{ \begin{array}{l}
 p_{p,0} = 133.2 \text{ bar} \\
 u_{p,0} = 0.3157 \\
 u_{r,0} = 0.4517 \\
 K_{qu_p} = 9.87 \cdot 10^{-4} \\
 K_{qp_p} = 2.03 \cdot 10^{-11} \\
 K_{qu_r} = 3.38 \cdot 10^{-4} \\
 K_{qp_r} = 8.48 \cdot 10^{-11} \\
 V_{p,0} = 1.15 \text{ l} \\
 V_{r,0} = 0.2 \text{ l}
 \end{array} \right. \quad (C.40)$$

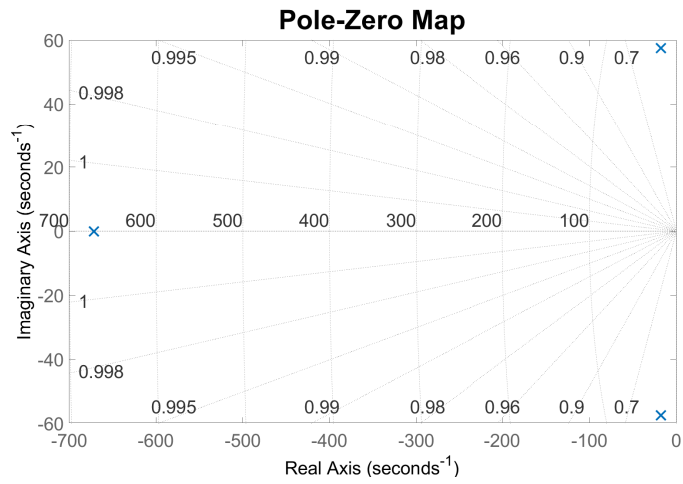


**Figure C.71:** Eigenvalues:  $-671.83, -17.54 \pm j57.44$ .

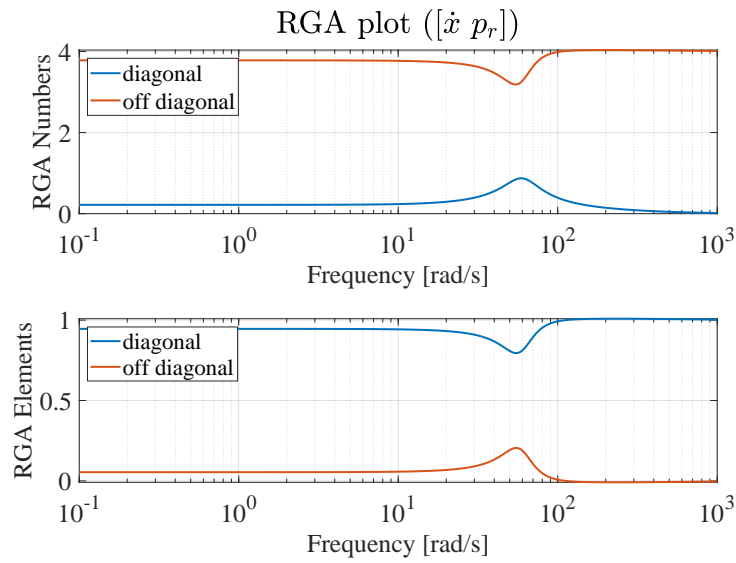


**Figure C.72:** RGA analysis.

## Negative velocity, $p_r = 20$ bar, $p_p$ control

$$\left. \begin{array}{l} \dot{x}_0 = -0.1 \text{ m/s} \\ F_{L,0} = 0 \text{ kN} \\ p_{r,0} = 20 \text{ bar} \\ x_0 = 0 \text{ m} \end{array} \right\} \begin{array}{l} p_{p,0} = 9.8 \text{ bar} \\ u_{p,0} = -0.9326 \\ u_{r,0} = -0.0983 \\ K_n q u_p = 3.34 \cdot 10^{-4} \\ K_n q p_p = -1.77 \cdot 10^{-10} \\ K_n q u_r = 1.55 \cdot 10^{-3} \\ K_n q p_r = -4.02 \cdot 10^{-12} \\ V_{p,0} = 0.2 \text{ l} \\ V_{r,0} = 0.67 \text{ l} \end{array} \quad (\text{C.41})$$

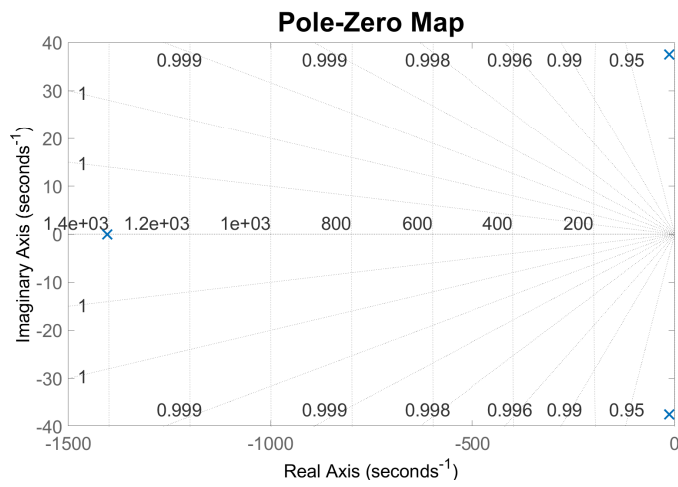


**Figure C.73:** Eigenvalues:  $-1403, -13.01 \pm j37.47$ .

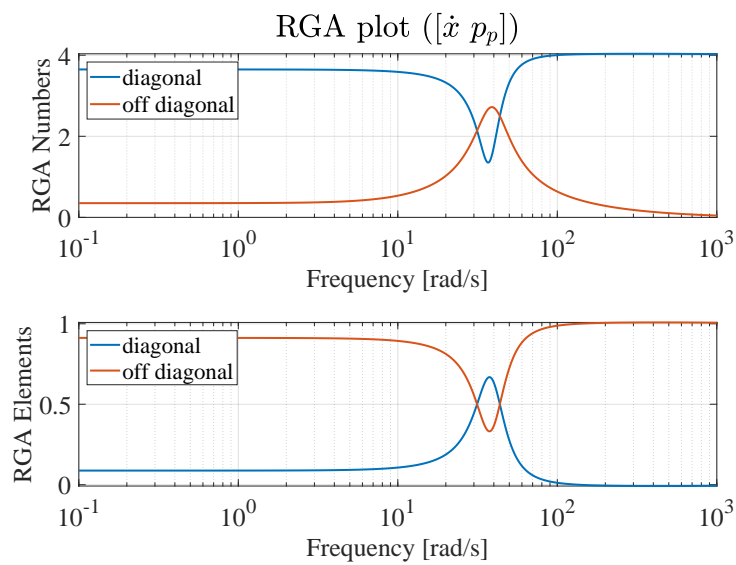


**Figure C.74:** RGA analysis.

$$\left. \begin{array}{l} \dot{x}_0 = -0.1 \text{ m/s} \\ F_{L,0} = 0 \text{ kN} \\ p_{r,0} = 20 \text{ bar} \\ x_0 = L_{stroke}/2 = 0.1525 \text{ m} \end{array} \right\} \begin{cases} p_{p,0} = 9.8 \text{ bar} \\ u_{p,0} = -0.9326 \\ u_{r,0} = -0.0983 \\ K_n q u_p = 3.34 \cdot 10^{-4} \\ K_n q p_p = -1.77 \cdot 10^{-10} \\ K_n q u_r = 1.55 \cdot 10^{-3} \\ K_n q p_r = -4.02 \cdot 10^{-12} \\ V_{p,0} = 0.67 \text{ l} \\ V_{r,0} = 0.43 \text{ l} \end{cases} \quad (\text{C.42})$$

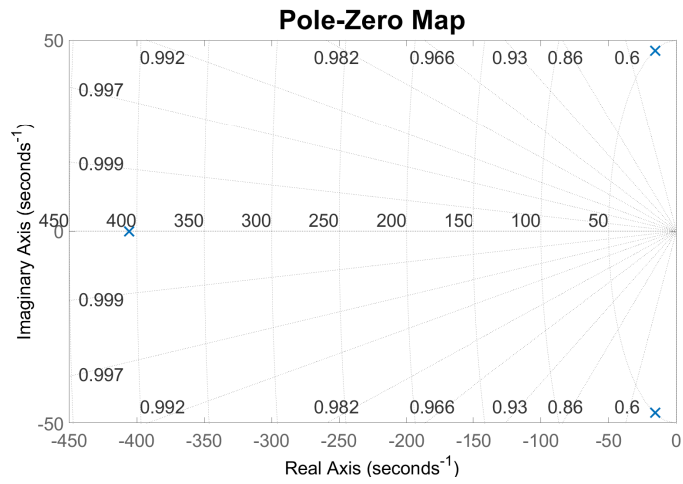


**Figure C.75:** Eigenvalues:  $-405.6, -15.71 \pm j47.24$ .

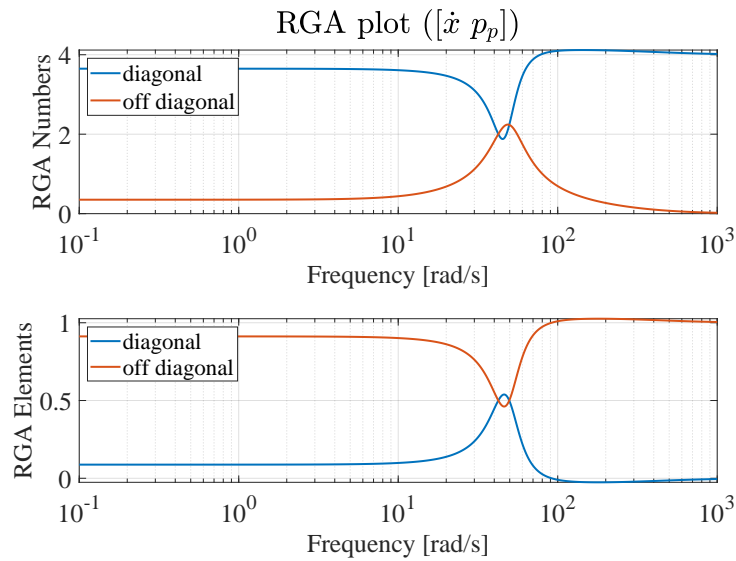


**Figure C.76:** RGA analysis.

$$\left. \begin{array}{l} \dot{x}_0 = -0.1 \text{ m/s} \\ F_{L,0} = 0 \text{ kN} \\ p_{r,0} = 20 \text{ bar} \\ x_0 = L_{stroke} = 0.305 \text{ m} \end{array} \right\} \left\{ \begin{array}{l} p_{p,0} = 9.8 \text{ bar} \\ u_{p,0} = -0.9326 \\ u_{r,0} = -0.0983 \\ K_n q u_p = 3.34 \cdot 10^{-4} \\ K_n q p_p = -1.77 \cdot 10^{-10} \\ K_n q u_r = 1.55 \cdot 10^{-3} \\ K_n q p_r = -4.02 \cdot 10^{-12} \\ V_{p,0} = 1.15 \text{ l} \\ V_{r,0} = 0.2 \text{ l} \end{array} \right. \quad (\text{C.43})$$

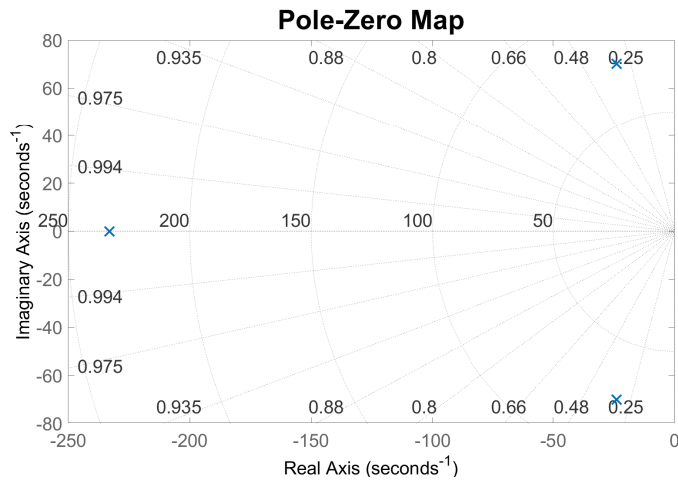


Figure C.77: Eigenvalues: -233, -23.98 ± j70.

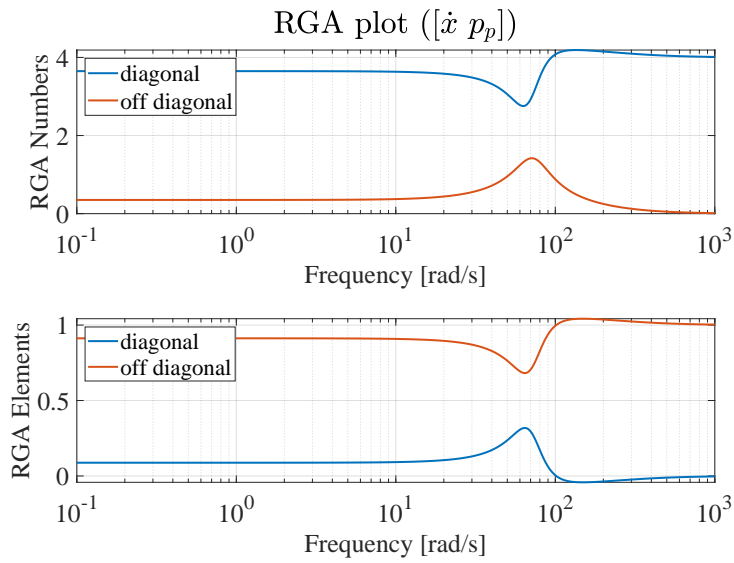


Figure C.78: RGA analysis.

## Negative velocity, $p_r = 20$ bar, $p_r$ control

$$\left. \begin{array}{l} \dot{x}_0 = -0.1 \text{ m/s} \\ F_{L,0} = 0 \text{ kN} \\ p_{r,0} = 20 \text{ bar} \\ x_0 = 0 \text{ m} \end{array} \right\} \begin{cases} p_{p,0} = 9.8 \text{ bar} \\ u_{p,0} = -0.9326 \\ u_{r,0} = -0.0983 \\ K_n q u_p = 3.34 \cdot 10^{-4} \\ K_n q p_p = -1.77 \cdot 10^{-10} \\ K_n q u_r = 1.55 \cdot 10^{-3} \\ K_n q p_r = -4.02 \cdot 10^{-12} \\ V_{p,0} = 0.2 \text{ l} \\ V_{r,0} = 0.67 \text{ l} \end{cases} \quad (\text{C.44})$$

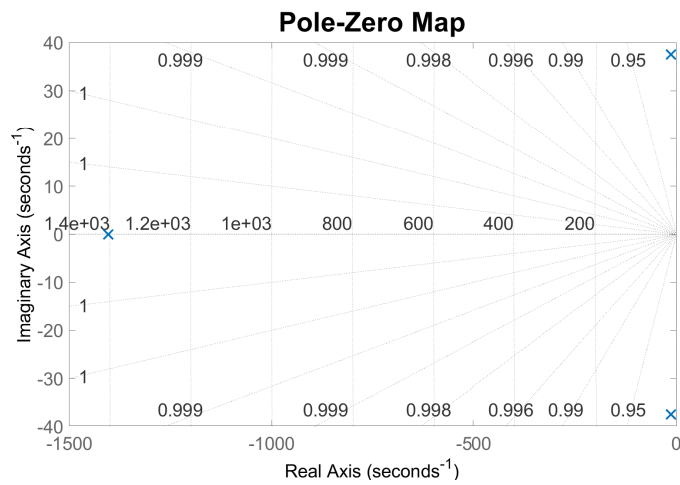


Figure C.79: Eigenvalues: -1403,  $-13.01 \pm j37.47$ .

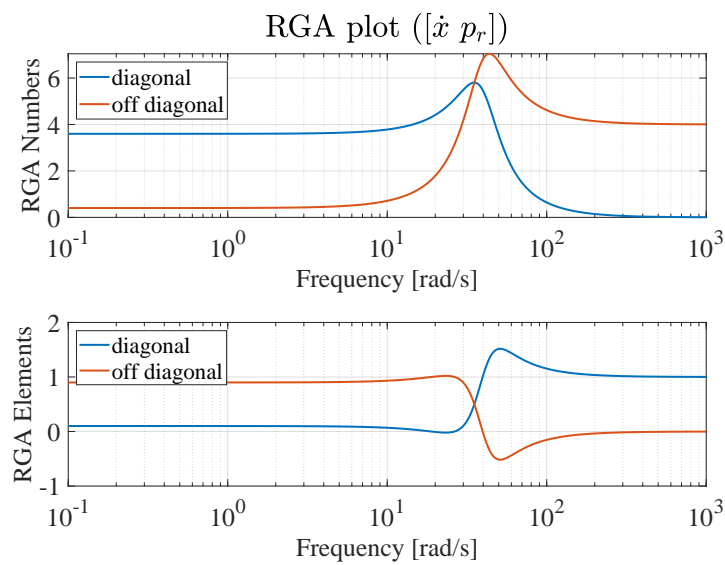
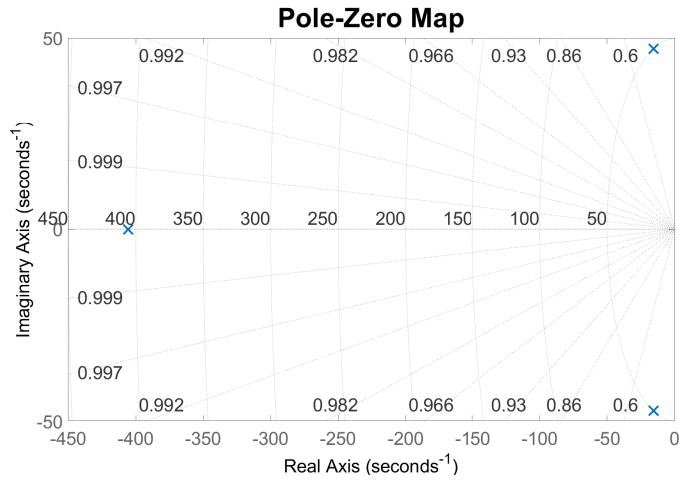
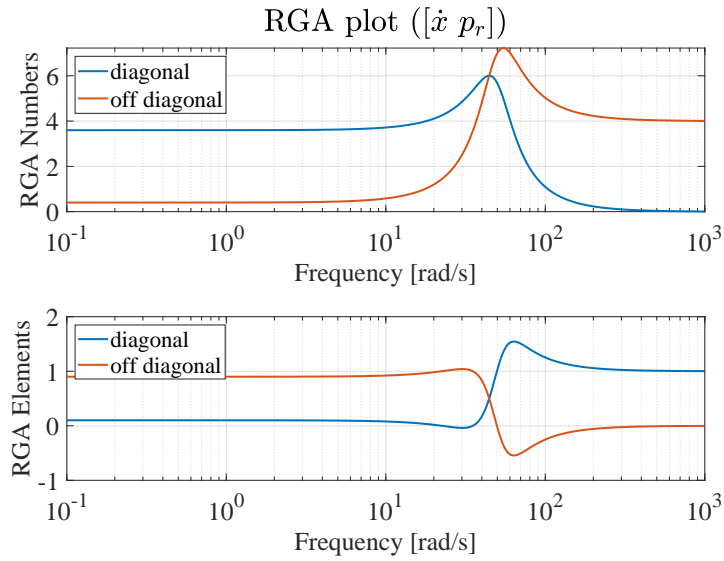


Figure C.80: RGA analysis.

$$\left. \begin{array}{l} \dot{x}_0 = -0.1 \text{ m/s} \\ F_{L,0} = 0 \text{ kN} \\ p_{r,0} = 20 \text{ bar} \\ x_0 = L_{stroke}/2 = 0.1525 \text{ m} \end{array} \right\} \begin{cases} p_{p,0} = 9.8 \text{ bar} \\ u_{p,0} = -0.9326 \\ u_{r,0} = -0.0983 \\ K_n q u_p = 3.34 \cdot 10^{-4} \\ K_n q p_p = -1.77 \cdot 10^{-10} \\ K_n q u_r = 1.55 \cdot 10^{-3} \\ K_n q p_r = -4.02 \cdot 10^{-12} \\ V_{p,0} = 0.67 \text{ l} \\ V_{r,0} = 0.43 \text{ l} \end{cases} \quad (\text{C.45})$$



**Figure C.81:** Eigenvalues:  $-405.6, -15.71 \pm j47.24$ .



**Figure C.82:** RGA analysis.

$$\left. \begin{array}{l} \dot{x}_0 = -0.1 \text{ m/s} \\ F_{L,0} = 0 \text{ kN} \\ p_{r,0} = 20 \text{ bar} \\ x_0 = L_{stroke} = 0.305 \text{ m} \end{array} \right\} \begin{cases} p_{p,0} = 9.8 \text{ bar} \\ u_{p,0} = -0.9326 \\ u_{r,0} = -0.0983 \\ K_n q u_p = 3.34 \cdot 10^{-4} \\ K_n q p_p = -1.77 \cdot 10^{-10} \\ K_n q u_r = 1.55 \cdot 10^{-3} \\ K_n q p_r = -4.02 \cdot 10^{-12} \\ V_{p,0} = 1.15 \text{ l} \\ V_{r,0} = 0.2 \text{ l} \end{cases} \quad (\text{C.46})$$

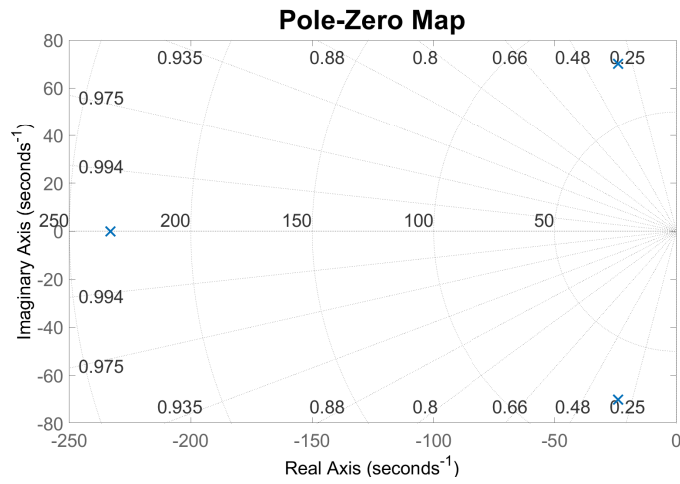


Figure C.83: Eigenvalues:  $-233, -23.98 \pm j70$ .

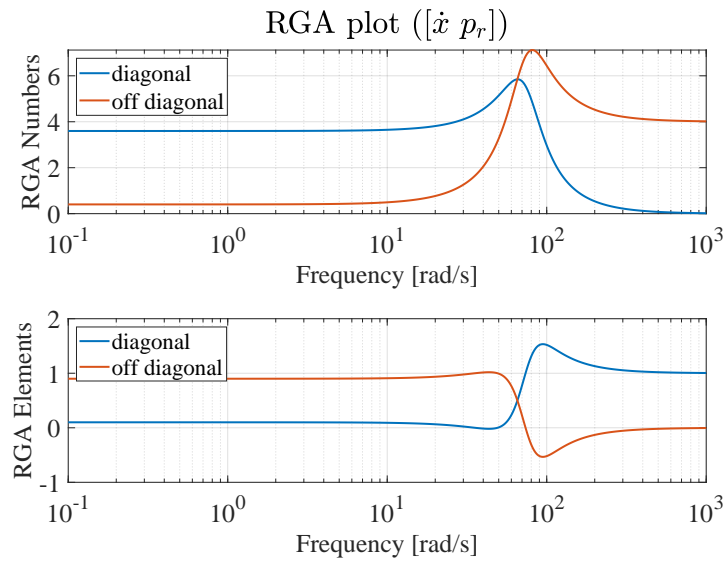


Figure C.84: RGA analysis.